

# Two-parton scattering in the high-energy limit



Prepared for submission to JHEP Edinburgh 2017/01

# Two-parton scattering in the high-energy limit

**Simon Caron-Huot,**[a] **Einan Gardi,**[b] **Leonardo Vernazza**[b]

[a] *Department of Physics, McGill University, 3600 rue University, Montréal, QC Canada H3A 2T8*
[b] *Higgs Centre for Theoretical Physics, School of Physics and Astronomy, The University of Edinburgh, Edinburgh EH9 3FD, Scotland, UK*

*E-mail:* schuot@physics.mcgill.ca, Einan.Gardi@ed.ac.uk, lvernazz@staffmail.ed.ac.uk

Abstract: Considering $2 \to 2$ gauge-theory scattering with general colour in the high-energy limit, we compute the Regge-cut contribution to three loops through next-to-next-to-leading high-energy logarithms (NNLL) in the signature-odd sector. Our formalism is based on using the non-linear Balitsky-JIMWLK rapidity evolution equation to derive an effective Hamiltonian acting on states with a fixed number of Reggeized gluons. A new effect occurring first at NNLL is mixing between states with $k$ and $k+2$ Reggeized gluons due non-diagonal terms in this Hamiltonian. Our results are consistent with a recent determination of the infrared structure of scattering amplitudes at three loops, as well as a computation of $2 \to 2$ gluon scattering in $\mathcal{N} = 4$ super Yang-Mills theory. Combining the latter with our Regge-cut calculation we extract the three-loop Regge trajectory in this theory. Our results open the way to predict high-energy logarithms through NNLL at higher-loop orders.

Keywords: scattering amplitudes, Regge, resummation, QCD, SYM

## Contents



## 1 Introduction

The high-energy limit of gauge-theory scattering amplitudes has long been understood to offer a unique insight into gauge dynamics. In this kinematic limit, amplitudes drastically simplify and factorise in rapidity, giving rise to new degrees of freedom in two dimensions. Within perturbative QCD, BFKL [1, 2] and related rapidity evolution equations allow

us to translate concepts from Regge theory [3] into calculation tools, leading to concrete predictions. The simplest example is that of the Reggeized gluon, the effective interaction which governs the behaviour of $2 \to 2$ scattering amplitudes in QCD in the limit where the energy $s$ is much larger than the momentum transfer $-t$. In the leading logarithmic approximation the exchange of a single Reggeized gluon leads to a trivial evolution equation in rapidity, which amounts to straightforward exponentiation of logarithms of $|s/t|$ to all orders in the coupling. At higher logarithmic accuracy more complex analytic structure emerges, which can be understood in QCD as compound states of two or more Reggeized gluons [4–6]. In contrast to the single Reggeon case, these are difficult to solve in general [7, 8]. Nevertheless, they can be integrated iteratively, thus generating perturbative high-energy amplitudes order-by-order in the coupling.

Taking the high-energy limit, $s \gg -t$, a fast moving projectile can be seen as a cloud of partons, each of which is dressed by a Wilson line, sourcing additional radiation. The high-energy limit corresponds to forward scattering, where recoil is neglected, hence the effective description is in terms of straight infinite lightlike Wilson lines [9, 10]. The number and transverse positions of these Wilson lines are not fixed, since the projectile can contain an arbitrary number of quantum fluctuations. The evolution of the system in rapidity is controlled by the Balitsky-JIMWLK equation [11–15]. In Ref. [16] it was shown how to translate the latter into evolution equations controlling a given number of Reggeized gluons. These equations are in general coupled, and in particular, the evolution of three Reggeized gluons involves mixing with a single Reggeized gluon. In the present paper we explore this mixing for the first time. We use the leading-order Balitsky-JIMWLK equation to derive the effective Hamiltonians governing the diagonal and next-to-diagonal evolution terms describing $k$ Reggeized gluon evolution into $k$ and $k+2$ ones, respectively, and use symmetry considerations to obtain the mixing into $k-2$ ones. We then use these evolution equations to explicitly compute three-loop corrections to the signature odd $2 \to 2$ amplitude in the high-energy limit, and compare them to other recent results.

It is well known that gauge-theory amplitudes have long-distance singularities, which cancel in physical observables such as sufficiently inclusive cross sections. Owing to the factorization properties of fixed-angle scattering amplitudes [17, 18] these singularities are largely process-independent. Furthermore, they admit evolution equations leading to exponentiation. Of special interest are soft singularities, which in contrast to collinear ones, are sensitive to the colour flow of the underlying hard process. Soft singularities can be computed by considering correlators of semi-infinite Wilson lines [19–27]. The corresponding *soft anomalous dimension* encodes the structure of these singularities to all orders in perturbation theory. In recent years there has been significant progress [28–36] in determining the precise structure of long-distance singularities to massless gauge theories. Through a recent explicit computation of the soft anomalous dimension, these are now known in full for amplitudes with any number of legs in general kinematics through three loops [35, 36].

While infrared factorization of fixed-angle scattering and high-energy factorization start from different kinematic set ups, and are based on different evolution equations, they lead to partially overlapping predictions for the structure of scattering amplitudes. In recent years the complementary nature of these two factorization pictures has been put to use [16, 37–40].

For example, Refs. [37, 38] showed that infrared factorization excludes the simplest form of Regge factorization where the amplitude in the high-energy limit is governed by a so-called Regge pole, and predicts that contributions associated with a Regge cut appear starting from the next-to-leading logarithmic (NLL) accuracy for the imaginary part of the amplitude and starting from the next-to-next-to-leading logarithmic (NNLL) accuracy for its real part. Conversely, it was shown how the Regge limit can constrain the (then unknown) three-loop soft anomalous dimension. Ref. [16] used the Balitsky-JIMWLK equation to computed the first few orders in the Regge cut of the signature even part of the amplitude at NLL accuracy, and predicted a corresponding correction to the soft anomalous dimension in the high-energy limit at four loops. In this paper we use a similar technique to predict the signature odd amplitude at NNLL accuracy. This requires us to address for the first time the effect of non-diagonal terms in the effective Hamiltonian. We are then able to compute three-loop corrections generated by the evolution of three Reggeized gluons and their mixing with a single Reggeized gluon. Finally, we contrast our result with other recent calculations at three loops. First, the infrared singularities are compared with predictions based on the soft anomalous dimension [35, 36], finding full consistency. Second, considering the case of gluon scattering in $\mathcal{N} = 4$ Supersymmetric Yang-Mills theory (SYM), we find full agreement with the results of Ref. [41], expanded in the high-energy limit. The latter, in combination with the Regge cut we computed, allows us to fix the three-loop gluon Regge trajectory in this theory.

The outline of the paper is as follows. Section 2 introduces the relevant aspects of Regge and BFKL theory. This includes, in section 2.1, a review and analysis of the relation between reality properties and signature within Regge theory. Section 2.2 then focuses on reviewing the perturbative description of gluon Reggeisation and the structure of $2 \to 2$ scattering amplitudes in the high-energy limit. We conclude the introduction in section 2.3 where we explain how we use the Balitsky-JIMWLK equation to obtain information on the (non-diagonal) evolution of states with a fixed number of Reggeized gluons. The computation itself is described in section 3, which starts with a derivation of the explicit form of the Hamiltonian for $k$ goes to $k$, $k+2$ and $k-2$ Reggeized gluons, and concludes with a calculation of all the relevant signature-odd matrix elements contributing through three loops. Finally, section 4 is dedicated to a detailed comparison between the results of section 3 with the theory of infrared factorization. We begin by reviewing the latter, specializing the results of [35, 36] to the high-energy limit. We then systematically determine the "infrared renormalized" hard function based on our results of section 3 for the amplitude in the high-energy limit, and verify that the result is indeed finite. Explicit expressions for the anomalous dimensions are quoted in Appendix A, while Appendices B and C collect the hard function in QCD gluon-gluon scattering in the $t$-channel colour flow basis and the "trace" basis, respectively. Finally Appendix D collects the results for high-energy factorization in $\mathcal{N} = 4$ SYM. Our conclusions and some open questions are discussed in section 5.

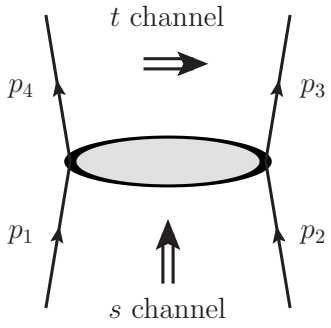


**Figure 1**. The $t$-channel exchange dominating the high-energy limit, $s \gg -t > 0$. The figure also defined our conventions for momenta assignment and Mandelstam invariants. We shall assume that particles 2 and 3 are of the same type, and similarly for particles 1 and 4.

## 2 Aspects of $2 \to 2$ scattering amplitudes in the high-energy limit

In this paper we explore properties of $2 \to 2$ QCD scattering amplitudes in the high-energy limit. This kinematical configuration is interesting because of the appearance of large logarithms of the centre of mass energy $s$ over the momentum transfer $t$, $\log|s/t|$. It is a well-known fact that these logarithms exponentiate at leading logarithmic (LL) accuracy, and also at the next-to-leading logarithmic (NLL) order, for some parts of the amplitude. A deeper understanding of their factorisation and exponentiation relies however on non-trivial properties of scattering amplitudes, that we discuss in this section.

Our starting point is the study of analytic properties of scattering amplitudes. This is historically one of the first approaches to the study of amplitudes, which leads to the concepts of signature and of Regge poles, Regge cuts and Regge trajectories, that we briefly review below. Next, we explain how these concepts relate to the standard calculation of QCD scattering amplitudes as a perturbative expansion in the strong coupling constant. We introduce then the modern framework in which the factorisation of amplitudes in the the high-energy limit needs to be discussed, namely, the treatment of QCD radiation as originating from Wilson lines associated to the direction of the incoming and outgoing quarks and gluons. This framework allows one to link the origin of high-energy logarithms to the renormalisation-group evolution of amplitudes with respect to the rapidity, which is governed by BFKL theory, more specifically by the Balitsky-JIMWLK equation.

### 2.1 Signature and the high-energy limit of $2 \to 2$ amplitudes

We consider $2 \to 2$ scattering amplitudes, $\mathcal{M}_{ij\to ij}$, where $i$, $j$ can be a quark or a gluon. In the following we will suppress these indices $i$, $j$, unless explicitly needed. In the high-energy limit the Mandelstam variables satisfy $s \gg -t > 0$. The various terms of the amplitude will have definite reality properties, which are related to the properties of the amplitude under crossing. This is a consequence of the analytic structure, which is conveniently summarised

via dispersion relations:

$$\mathcal{M}(s,t) = \frac{1}{\pi}\int_0^\infty \frac{d\hat{s}}{\hat{s}-s-i0}\, D_s(\hat{s},t) + \frac{1}{\pi}\int_0^\infty \frac{d\hat{u}}{\hat{u}+s+t-i0}\, D_u(\hat{u},t) \tag{2.1}$$

where $D_s$ and $D_u$ are the discontinuities of $\mathcal{M}(s,t)$ in the $s$- and $u$-channels, respectively. In general the lower limit of integration should of course be a positive threshold, and there could be subtraction terms, but this would not matter for our discussion. The important fact is that the discontinuities $D_s$ and $D_u$ are real, having a physical interpretation as spectral density of positive energy states propagating in the $s$ and $u$ channel respectively. To see the consequence on the amplitude, let us parametrize the discontinuities as a sum of power laws by means of a Mellin transformation:

$$a_j^s(t) = \frac{1}{\pi}\int_0^\infty \frac{d\hat{s}}{\hat{s}}\, D_s(\hat{s},t)\, \left(\frac{\hat{s}}{-t}\right)^{-j}, \tag{2.2a}$$

$$D_s(s,t) = \frac{1}{2i}\int_{\gamma-i\infty}^{\gamma+i\infty} dj\, a_j^s(t)\, \left(\frac{s}{-t}\right)^{j}, \tag{2.2b}$$

and similarly for $a^u$ and $D_u$. Note that the reality condition of $D_s(s,t)$ implies that the Fourier coefficients admit

$$\big(a^s_{j^*}(t)\big)^* = a_j^s(t), \tag{2.3}$$

and similarly for $a_j^u(t)$. Substituting the inverse transform eq. (2.2b) into the dispersive representation eq. (2.1), swapping the order of integration and performing the $\hat{s}$ and $\hat{u}$ integrals, one obtains a Mellin representation of the amplitude:

$$\mathcal{M}(s,t) = \frac{-1}{2i}\int_{\gamma-i\infty}^{\gamma+i\infty} \frac{dj}{\sin(\pi j)} \left( a_j^s(t)\, \left(\frac{-s-i0}{-t}\right)^{j} + a_j^u(t)\, \left(\frac{s+t-i0}{-t}\right)^{j}\right). \tag{2.4}$$

Since the coefficients $a_j^{s,u}$ are real (for real $j$), and $(-s-i0)^j = e^{-i\pi j}|s|^j$ for $s>0$, we see that the phase of each power law contribution is related to its exponent. The statement simplifies when one projects the amplitude onto eigenstates of *signature*, that is crossing symmetry $s \leftrightarrow u$:

$$\mathcal{M}^{(\pm)}(s,t) = \tfrac{1}{2}\Big(\mathcal{M}(s,t) \pm \mathcal{M}(-s-t,t)\Big), \tag{2.5}$$

where $\mathcal{M}^{(+)}$, $\mathcal{M}^{(-)}$ are refered respectively to as the *even* and *odd* amplitudes. Restricting to the region $s>0$ and working to leading power as $s \gg |t|$, the formula then evaluates to

$$\mathcal{M}^{(+)}(s,t) = i\int_{\gamma-i\infty}^{\gamma+i\infty} \frac{dj}{\sin(\pi j)} \cos\left(\tfrac{\pi j}{2}\right) a_j^{(+)}(t)\, e^{jL}, \tag{2.6a}$$

$$\mathcal{M}^{(-)}(s,t) = \int_{\gamma-i\infty}^{\gamma+i\infty} \frac{dj}{\sin(\pi j)} \sin\left(\tfrac{\pi j}{2}\right) a_j^{(-)}(t)\, e^{jL}, \tag{2.6b}$$

where we have defined $a_j^{(\pm)}(t) \equiv \frac{1}{2}(a_j^s(t) \pm a_j^u(t))$ and $L$ is the natural signature-even combination of logarithms:

$$\begin{aligned} L &\equiv \log\left|\frac{s}{t}\right| - i\frac{\pi}{2} \\ &= \frac{1}{2}\left(\log\frac{-s-i0}{-t} + \log\frac{-u-i0}{-t}\right). \end{aligned} \tag{2.7}$$

Let us interpret eq. (2.6). First of all, we notice that the reality properties of $a_j^s(t)$, $a_j^u(t)$ stated in eq. (2.3) implies that the coefficients of powers of $L$ in $\mathcal{M}^{(+)}$ and $\mathcal{M}^{(-)}$ are imaginary and real, respectively. Note, however, that it is important for these reality properties to express results in terms of $L$ defined in eq. (2.7), which has an extra imaginary part, rather than in terms of the large logarithm $\log|s/t|$ itself. This simple observation will remove many explicit $i\pi$'s from expressions in this paper, and facilitate non-trivial checks of the results. Moreover, for gluon scattering, invoking Bose symmetry we deduce that $\mathcal{M}^{(+)}$, which is symmetric under permutation of the kinematic variables $s$ and $u$, picks out the colour component which are symmetric under permutation of the indices of particles 2 and 3, and $\mathcal{M}^{(-)}$, which is antisymmetric upon swapping $s$ and $u$, picks out the colour-antisymmetric part.

In this paper we focus on the leading power in $t/s$, and in this limit the Mellin variable $j$ used above is identical to the spin $j$ which enters conventional partial wave functions[1]. This explains our notation. One could easily extend the above discussion to subleading powers, but one would have to replace the Mellin transform by the partial wave expansion. For example, $(s/t)^{-j-1}$ and $(s/t)^j$ in eqs. (2.2a) and (2.4) would be replaced respectively by the associated Legendre function $Q_j(1+2s/t)$ and Legendre polynomials $P_j(1+2s/t)$, see [3].

The simplest conceivable asymptotic behaviour would be a pure power law, whose Mellin transform is a simple Regge pole, namely

$$a_j^{(-)}(t) \simeq \frac{1}{j-1-\alpha(t)}. \tag{2.10}$$

The leading perturbative behaviour is obtained upon taking the residue of eq. (2.6b) about the Regge pole, getting

$$\mathcal{M}^{(-)}(s,t)|_{\text{Regge pole}} \simeq \frac{\pi}{\sin\frac{\pi\,\alpha(t)}{2}}\frac{s}{t}\,e^{L\,\alpha(t)} + \dots, \tag{2.11}$$

where the ellipsis indicated subleading contributions. Regge poles give the correct behaviour of the $2 \to 2$ amplitude at leading logarithm accuracy in perturbation theory, where $\alpha(t)$

[1] The standard partial wave decomposition of a $2 \to 2$ scattering amplitude is given by (see e.g. [3])

$$\mathcal{M}_j(t) = \frac{1}{16\pi}\frac{1}{2}\int_{-1}^{1} dz_t P_j(z_t)\mathcal{M}(s(z_t,t),t), \qquad j = 0,1,2,\dots \tag{2.8a}$$

$$\mathcal{M}(s,t) = 16\pi\sum_{j=0}^{\infty}(2j+1)\mathcal{M}_j(t)P_j(z_t), \tag{2.8b}$$

where $P_j(z_t)$ are Lagendre polynomials obeying $P_j(-z) = (-1)^j P_j(z)$, and $z_t = \cos(\theta_t)$ where $\theta_t$ is the $t$-channel scattering angle (namely, using the conventions of Fig. 1, it is the angle between the $p_1$ and $p_2$ in the centre-of-mass frame of $p_1$ and $p_4$). For massless scattering considered here, where $s+t+u=0$,

$$z_t = 1 + \frac{2s}{t} = -1 - \frac{2u}{t}\,. \tag{2.9}$$

The symmetry $z_t \to -z_t$ relates scattering with angle $\theta_t$ to scattering with angle $\pi - \theta_t$; in terms of the Mandelstam invariants, it corresponds to $s \leftrightarrow u$. We see that under an $s \leftrightarrow u$ interchange $\mathcal{M}_j(t)$ of eq. (2.8a) is even for even $j$ and odd for odd $j$.

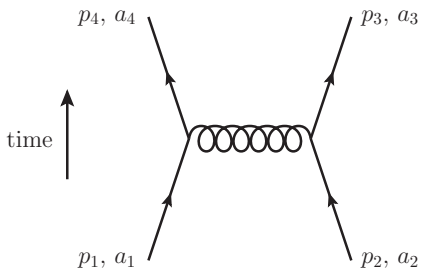


**Figure 2**. Tree-level t-channel exchange contributing in the high-energy limit to quark-quark, quark-gluon or gluon-gluon scattering. The solid external lines represent either quarks or gluons, depending on the process considered.

is interpreted as the gluon Regge trajectory, $\alpha(t) \equiv \alpha_g(t) \sim \mathcal{O}(\alpha_s(t))$. In order to get the precise behavior at higher orders in perturbation theory one needs to take into account the contribution of Regge cuts, which arises from $a_j^{(-)}(t)$ of the form

$$a_j^{(-)}(t) \simeq \frac{1}{(j-1-\alpha(t))^{1+\beta(t)}}, \tag{2.12}$$

which has a branch point from $1+\alpha(t)$ to $-\infty$, or a multiple pole if $\beta(t)$ is a positive integer. Integrating along the discontinuity one gets

$$\mathcal{M}^{(-)}(s,t)|_{\text{Regge cut}} \simeq \frac{\pi}{\sin\frac{\pi\,\alpha(t)}{2}}\frac{s}{t}\frac{1}{\Gamma\left(1+\beta(t)\right)}L^{\beta(t)}\,e^{L\,\alpha(t)} + \text{subleading logs}. \tag{2.13}$$

While Regge poles contribute to LL accuracy, therefore to the odd amplitude, Regge cuts start contributing at the NLL order, to the even amplitude. A complete treatment of scattering amplitudes up to NNLL accuracy requires to take into account the contribution of Regge cuts both to the odd and the even amplitude. In order to clarify this structure, we are now going to explore the implications of Regge poles and cuts in perturbation theory.

### 2.2 The Regge limit in perturbation theory

We write the perturbative expansion of a $2 \to 2$ scattering amplitude in the high-energy limit as

$$\mathcal{M}(s,t) = 4\pi\alpha_s \sum_{n=0}^{\infty}\left(\frac{\alpha_s}{\pi}\right)^n \mathcal{M}^{(n)}(s,t), \tag{2.14}$$

where we systematically neglect any powers suppressed terms in $t/s$. This perturbative expansion correspond to the ultraviolet-renormalised scattering amplitude, with the strong coupling $\alpha_s$ renormalized for convenience at the momentum-transfer scale, $\mu^2 = -t$. Infrared divergences are regulated in $d = 4-2\epsilon$ dimensions.

In the previous section we have shown that an amplitude can always be written as the sum of its signature odd and even component,

$$\mathcal{M}(s,t) = \mathcal{M}^{(-)}(s,t) + \mathcal{M}^{(+)}(s,t), \tag{2.15}$$

as defined in eq. (2.5). Moreover, the reality condition in eq. (2.3) guarantees that, upon expressing the amplitude in terms of the variable $L$ defined in eq. (2.7), its real and imaginary parts are separately fixed by its odd and even components, respectively, see eq. (2.6). As a consequence, the perturbative expansion of $\mathcal{M}^{(-)}$ and $\mathcal{M}^{(+)}$ is of the form

$$\mathcal{M}^{(\pm)}(s,t) = 4\pi\alpha_s \sum_{l,m} \left(\frac{\alpha_s}{\pi}\right)^l L^m \, \mathcal{M}^{(\pm,l,m)}\,, \tag{2.16}$$

where the coefficients $\mathcal{M}^{(-,l,m)}$ and $\mathcal{M}^{(+,l,m)}$ are purely real and imaginary, respectively.

At tree level, in the high-energy limit, the amplitude reduces to the $t$-channel exchange represented in figure 2. Moreover, only helicity conserving scattering processes are leading in the high energy limit. This gives

$$\mathcal{M}^{(0)}_{ij\to ij} = \mathcal{M}^{(-,0)}_{ij\to ij} = \frac{2s}{t}\,(T_i^b)_{a_1a_4}(T_j^b)_{a_2a_3}\,\delta_{\lambda_1\lambda_4}\delta_{\lambda_2\lambda_3}, \qquad \mathcal{M}^{(+,0)}_{ij\to ij} = 0, \tag{2.17}$$

where $T_i$, $T_i$ are color generators in the representation of the corresponding particle: $(T_i^b)_{a_1a_4} = t^b_{a_1a_4}$ for quarks, $(T_i^b)_{a_1a_4} = -t^b_{a_4a_1}$ for antiquarks, and $(T_i^b)_{a_1a_4} = if^{a_1ba_4}$ for gluons, and the factor $\delta_{\lambda_1\lambda_4}\delta_{\lambda_2\lambda_3}$ represents helicity conservation. It is a well-known fact that, at higher orders, the leading logaritmic (LL) contribution is due to a Regge pole term of the type in eq. (2.10). Such term contributes to the odd part of the amplitude, and one has

$$\mathcal{M}_{ij\to ij}|_{\rm LL} = \mathcal{M}^{(-)}_{ij\to ij}|_{\rm LL} = \left(\frac{s}{-t}\right)^{\frac{\alpha_s}{\pi}\,C_A\,\alpha_g^{(1)}(t)}\, 4\pi\alpha_s\,\mathcal{M}^{(0)}_{ij\to ij}, \tag{2.18}$$

which is interpreted as the exchange of a Reggeized gluon, or "Reggeon", as represented by the double wavy line in diagram (a) of figure 4. The function $\alpha_g^{(1)}(t)$ in eq. (2.18) represents the leading order contribution to the gluon Regge trajectory[2]

$$\alpha_g(t) \,=\, \sum_{n=1}^{\infty}\left(\frac{\alpha_s}{\pi}\right)^n \alpha_g^{(n)}(t), \qquad \alpha_g^{(1)}(t) \,=\, \frac{r_\Gamma}{2\epsilon}\left(\frac{-t}{\mu^2}\right)^{-\epsilon} \overset{\mu^2\to -t}{=} \frac{r_\Gamma}{2\epsilon}, \tag{2.19}$$

where $r_\Gamma$ is a ubiquitous loop factor

$$r_\Gamma = e^{\epsilon\gamma_{\rm E}}\,\frac{\Gamma(1-\epsilon)^2\Gamma(1+\epsilon)}{\Gamma(1-2\epsilon)} \approx 1 - \frac{1}{2}\zeta_2\,\epsilon^2 - \frac{7}{3}\zeta_3\,\epsilon^3 + \ldots \tag{2.20}$$

At next to leading logarithmic (NLL) accuracy the single Reggeon exchange described by eq. (2.18) receives corrections, which, based on our discussion in section 2.1, are expected to be of the form

$$\mathcal{M}^{(-)}_{ij\to ij} \sim e^{C_A\,\alpha_g(t)\,L}\,Z_i(t)D_i(t)\,Z_j(t)D_j(t)\,4\pi\alpha_s\,\mathcal{M}^{(0)}_{ij\to ij}, \tag{2.21}$$

where $\alpha_g(t)$ is the Regge trajectory defined in eq. (2.19), and the factors $Z_{i/j}(t)D_{i/j}(t)$ represent corrections to the scattering amplitude independent of the centre of mass energy $s$.

[2]Compared to the standard definition in literature, we single out a factor $C_A$ from the definition of the Regge trajectory, see eq. (2.18), in order to simplify comparison with the infrared factorisation formula in section 4.

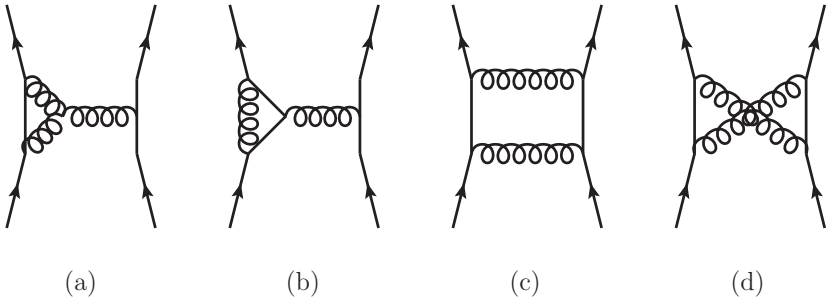


**Figure 3**. A few sample of one-loop diagram contributing to quark and gluon scattering at next-to-leading order, in the high-energy limit. Diagrams such as (a) and (b) have the same color structure of the tree-level diagram, and contribute to the one-Reggeon impact factor. Diagrams such as (c) and (d) introduce color structures different from the color structure of the tree-level amplitude, and contribute to the two-Reggeon exchange.

These corrections contain in general collinear divergences, which factorise according to the infrared factorisation formula, [30–32], to be introduced in section 4.1, see in particular eq. (4.14). Anticipating our analysis below, it proves useful to make the form of this factorisation manifest, such that the factors $Z_{i/j}(t)$ contain the collinear singularities, while the terms $D_{i/j}(t)$, to which we will refer in the following as "impact factors", represent the finite correction. In perturbation theory these objects are calculated as an expansion in the strong coupling constant, according to

$$Z_i(t) = \sum_{n=0}^{\infty} \left(\frac{\alpha_s}{\pi}\right)^n Z_i^{(n)}(t), \qquad D_i(t) = \sum_{n=0}^{\infty} \left(\frac{\alpha_s}{\pi}\right)^n D_i^{(n)}(t). \tag{2.22}$$

A graphical representation of these corrections is given in diagram (a) of figure 4. More in details, Eq. (2.21) involves three types of subleading corrections to eq. (2.18): first of all, there is a NLL contribution which arises because of the exponentiation pattern, which involve $L = \log|s/t| - i\pi/2$ instead of just $\log|s/t|$, as a consequence of symmetry with respect to the signature, discussed in section 2.1. Next, there are contributions arising from higher-order corrections to the *gluon Regge trajectory*, indicated as a shaded blob denoted by $\alpha_g$ in diagram (a) of figure 4. At NLL, such a correction arises from the next-to-leading order (NLO) contribution $\mathcal{O}(\alpha_s^2)$ to the Regge trajectory, i.e. $\alpha_g^{(2)}(t)$ in eq. (2.19). As we will discuss below, beyond NLO the Regge trajectory corresponding to a single Reggeon exchange is not uniquely defined; clarifying this issue is one of the goals of this papers. For now, it suffices to say that eq. (2.21) can be interpreted consistently only up to NLL accuracy. The third type of subleading corrections is due to the impact factor $D_i(t)$, which can be seen as an "effective vertex" associated to the emission (or absorption) of a single Reggeon, indicated by the shaded blobs in diagram (a) of figure 4. These type of corrections, which depend only on the momentum transfer $t$ (and not on the energy $s$), arise in perturbation theory for instance from diagrams like (a) and (b) in figure 3.

Starting at NLL accuracy there are new corrections, which cannot be interpreted as the exchange of a single-Reggeized gluon, and originate instead from Regge cuts as in eq. (2.13)

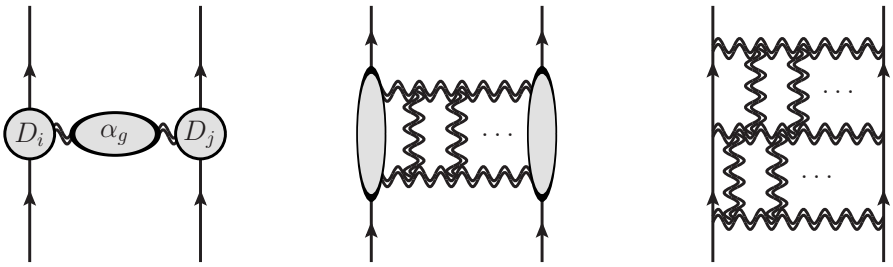


**Figure 4**. From left to right, exchange of one, two and three Reggeized gluons, respectively. We draw the Reggeized gluons as double wavy lines, in order to distinguish them from standard gluon exchange in perturbation theory. Single Reggeon exchange in the first diagram contribute at LL accuracy, while two-Reggeon exchange in the second diagram contribute at NLL accuracy. Last, three Reggeons exchange start contributing at NNLL accuracy. The shaded blobs in the first and second diagram account for single- and two-Reggeon impact factors, which give additional contributions at subleading logaritmic accuracy to these diagrams.

corresponding to the exchange of two or more Reggeized gluons, as indicated by diagrams (b) and (c) in figure 4. This paper focuses on the determination of these corrections.

Restricting for now to NLL accuracy, the Regge cut contribution involves the exchange of two Reggeized gluons, and the symmetry properties of this state dictate that it contributes to the even amplitude, i.e. to $\mathcal{M}^{(+)}_{ij\to ij}$. From the point of view of perturbation theory this can be understood by inspecting diagrams (c) and (d) in figure 3. These diagrams introduce new color structures compared to the tree-level color factor $(T^b_i)_{a_1a_4}(T^b_j)_{a_2a_3}$ in eq. (2.17). To proceed and characterise these corrections, let us briefly review some aspects of color decomposition of scattering amplitudes.

Scattering amplitudes can be seen as vectors in color-flow space,

$$\mathcal{M}(s,t) = \sum_i c^{[i]}\, \mathcal{M}^{[i]}(s,t), \tag{2.23}$$

where $c^{[i]}$ represent the elements of a color basis, and $\mathcal{M}^{[i]}(s,t)$ are the corresponding amplitude coefficients. Examples of color bases are the $t$-channel exchange orthonormal basis provided in appendix B, or the "trace" basis provided in appendix C. From the point of view of Regge theory it is convenient to focus on the former, in which the color operator (defined in (2.30)) in the $t$ channel, $\mathbf{T}^2_t$, is diagonal (see in (B.3)), hence providing insight into the factorisation structure of the amplitude in the high-energy limit.

An orthonormal color basis in the $t$-channel can be obtained by decomposing the direct product of the color representations associated to the incoming and outgoing particle 1 and 4 (see Figure 2) into a direct sum. For instance, in case of gluon-gluon scattering the amplitude lives in the space of the $8\otimes 8$ color representation. An orthonormal color basis is obtained decomposing it into a direct sum, i.e. $8\otimes 8 = 1\oplus 8_s\oplus 8_a\oplus 10\oplus\overline{10}\oplus 27\oplus 0$. At this point it is useful to make contact with the discussion following eq. (2.7): because of Bose

symmetry, the symmetry of the color structure mirrors the signature of the corresponding amplitude coefficients, which can thus be separated into signature odd and even:

$$\text{odd: } \mathcal{M}^{[8_a]}, \mathcal{M}^{[10+\overline{10}]}, \qquad \text{even: } \mathcal{M}^{[1]}, \mathcal{M}^{[8s]}, \mathcal{M}^{[27]}, \mathcal{M}^{[0]} \qquad (gg \text{ scattering}) \,. \tag{2.24}$$

Here $8_s$ and $8_a$ represent respectively a symmetric and antisymmetric octet representation, and 0 is a "null" representation, which is present in general for SU(N), and vanishes for N = 3. A more exhaustive discussion on how to decompose the amplitude into orthonormal color basis, together with explicit expressions for the orthonormal color basis of quark-quark, quark-gluon and gluon-gluon scattering have been given in [40, 42, 43], to which we refer for further details, as well as appendix B.

For our discussion, it suffices to note that the exchange of one Reggeized gluon contributes only to the antisymmetric octet, so that at leading-log order only this structure is nonzero:

$$\mathcal{M}_{gg\to gg}(s,t)\big|_{LL} = c_{[8_a]}\, \mathcal{M}^{[8_a]}(s,t)\big|_{LL} = \frac{2s}{t}\,(T_i^b)_{a_1a_4}(T_j^b)_{a_2a_3}\,\delta_{\lambda_1\lambda_4}\delta_{\lambda_2\lambda_3}\,. \tag{2.25}$$

At NLL order, certain diagrams like (a) and (b) in figure 3 contribute only to the $8_a$ color structure also, but others like (c) and (d) contribute in addition to the even structures listed in eq. (2.24). These signature-even contributions represent the exchange of a pair of Reggeized gluons and do not exponentiate in a simple way. Rather they contribute a Regge cut which can be calculated order by order in perturbation theory within a framework developed in [16], based on BFKL theory, and reviewed shortly.

This paper will focus on the three-Reggeon exchange at the NNLL order, which contributes to both the $8_a$ and $10 + \overline{10}$ color structures. At NNLL order, presently unknown corrections to single-Reggeon exchange also enter but they only contribute to the $8_a$ color structure. We will therefore unambiguously predict the $10 + \overline{10}$ amplitude. Furthermore, the relationship between the $8_a$ contributions to gluon-gluon, quark-gluon and quark-quark amplitudes will be unambiguously predicted.

In order to display the Regge-cut contributions in the most transparent way, it proves useful to define a "reduced" amplitude by removing from it the Reggeized gluon and collinear divergences as follows:

$$\hat{\mathcal{M}}_{ij\to ij} \equiv (Z_i Z_j)^{-1}\; e^{-\mathbf{T}_t^2\,\alpha_g(t)\,L}\,\mathcal{M}_{ij\to ij}\,, \tag{2.26}$$

where $\mathbf{T}_t^2$ represents the colour charge of a Reggeized gluon exchanged in the $t$ channel (see eq. (2.30) below) and $Z_i$ and $Z_j$ stand for collinear divergences, defined in (4.14) below. At tree-level one obviously has $\hat{\mathcal{M}}^{(0)} = \mathcal{M}^{(0)}$, and based on our discussion so far the odd component of the reduced amplitude up to NLL reads [16, 44]

$$\hat{\mathcal{M}}^{(-)}_{ij\to ij} = \left[1 + \frac{\alpha_s}{\pi}\left(D_i^{(1)}(t) + D_j^{(1)}(t)\right)\right] 4\pi\alpha_s\,\hat{\mathcal{M}}^{(0)}_{ij\to ij}\,, \tag{2.27}$$

where $D^{(1)}_{i/j}(t)$ are the finite single-Reggeon impact factors evaluated at one loop. In turn, the even reduced amplitude at NLL accuracy is given by [16]

$$\hat{\mathcal{M}}^{(+)}_{ij\to ij}|_{\text{NLL}} = i\pi \sum_{\ell=1}^{\infty} \frac{1}{\ell!}\left(\frac{\alpha_s}{\pi}\right)^{\ell} L^{\ell-1} \times d_\ell \times 4\pi\alpha_s\,\hat{\mathcal{M}}^{(0)}_{ij\to ij}, \tag{2.28}$$

where the coefficients $d_\ell$ contain non-diagonal color operators. These coefficients are infrared divergent and have been calculated in [16] up to the fourth order. One has, for instance,

$$\begin{aligned} d_1 &= \mathbb{d}_1 \mathbf{T}^2_{s-u}, & \mathbb{d}_1 &= r_\Gamma \frac{1}{2\epsilon}, \\ d_2 &= \mathbb{d}_2 [\mathbf{T}^2_t, \mathbf{T}^2_{s-u}], & \mathbb{d}_2 &= (r_\Gamma)^2 \left( -\frac{1}{4\epsilon^2} - \frac{9}{2}\epsilon\zeta_3 - \frac{27}{4}\epsilon^2\zeta_4 + \mathcal{O}(\epsilon^3) \right), \\ d_3 &= \mathbb{d}_3 [\mathbf{T}^2_t, [\mathbf{T}^2_t, \mathbf{T}^2_{s-u}]], & \mathbb{d}_3 &= (r_\Gamma)^3 \left( \frac{1}{8\epsilon^3} - \frac{11}{4}\zeta_3 - \frac{33}{8}\epsilon\zeta_4 - \frac{357}{4}\epsilon^2\zeta_5 + \mathcal{O}(\epsilon^3) \right). \end{aligned} \tag{2.29}$$

$\mathbf{T}^2_{s-u}$ in eq. (2.29) represents a color operator acting on the tree-level vector of amplitudes in eq. (2.24), according to the color-space formalism introduced in [28, 45, 46]. With this notation, a color operator $\mathbf{T}_i$ corresponds to the color generator associated with the $i$-th parton in the scattering amplitude, which acts as an $\mathrm{SU}(N_c)$ matrix on the color indices of that parton. More in details, one assigns $(\mathbf{T}^a_i)_{\alpha\beta} = t^a_{\alpha\beta}$ for a final-state quark or initial-state anti-quark, $(\mathbf{T}^a_i)_{\alpha\beta} = -t^a_{\beta\alpha}$ for a final-state anti-quark or initial-state quark, and $(\mathbf{T}^a_i)_{bc} = -if^{abc}$ for a gluon. We also use the notation $\mathbf{T}_i \cdot \mathbf{T}_j \equiv \mathbf{T}^a_i \mathbf{T}^a_j$ summed over $a$. Generators associated with different particles trivially commute, $\mathbf{T}_i \cdot \mathbf{T}_j = \mathbf{T}_j \cdot \mathbf{T}_i$ for $i \neq j$, while $\mathbf{T}^2_i = C_i$ is given in terms of the quadratic Casimir operator of the corresponding color representation, i.e $C_g = C_A$ for gluons. In the high-energy limit the color factors can be simplified considerably, by using the basis of Casimirs corresponding to color flow through the three channels [38, 47]:

$$\begin{aligned} \mathbf{T}_s &= \mathbf{T}_1 + \mathbf{T}_2 = -\mathbf{T}_3 - \mathbf{T}_4 \\ \mathbf{T}_u &= \mathbf{T}_1 + \mathbf{T}_3 = -\mathbf{T}_2 - \mathbf{T}_4 \\ \mathbf{T}_t &= \mathbf{T}_1 + \mathbf{T}_4 = -\mathbf{T}_2 - \mathbf{T}_3 \end{aligned} \tag{2.30}$$

and using the color conservation identity $(\mathbf{T}_1 + \mathbf{T}_2 + \mathbf{T}_3 + \mathbf{T}_4)\,\mathcal{M} = 0$ to rewrite in terms of signature eigenstates. One obtains $\mathbf{T}^2_s + \mathbf{T}^2_u + \mathbf{T}^2_t = \sum_{i=1}^4 C_i \equiv C_{\mathrm{tot}}$. One may then define a color operator that is *odd* under $s \leftrightarrow u$ crossing:

$$\mathbf{T}^2_{s-u} \equiv \tfrac{1}{2}\left(\mathbf{T}^2_s - \mathbf{T}^2_u\right), \tag{2.31}$$

which is the operator used to describe the NLL even amplitude in eq. (2.29). Useful relations are given by

$$\begin{aligned} \mathbf{T}_1 \cdot \mathbf{T}_2 + \mathbf{T}_3 \cdot \mathbf{T}_4 &= \mathbf{T}^2_s - \tfrac{1}{2} C_{\mathrm{tot}} = \mathbf{T}^2_{s-u} - \tfrac{1}{2}\mathbf{T}^2_t, \\ \mathbf{T}_1 \cdot \mathbf{T}_3 + \mathbf{T}_2 \cdot \mathbf{T}_4 &= -\mathbf{T}^2_{s-u} - \tfrac{1}{2}\mathbf{T}^2_t, \\ \mathbf{T}_1 \cdot \mathbf{T}_4 + \mathbf{T}_2 \cdot \mathbf{T}_3 &= \mathbf{T}^2_t - \tfrac{1}{2} C_{\mathrm{tot}}. \end{aligned} \tag{2.32}$$

The goal of this paper is to provide for the first time a systematic derivation of the contributions arising at the NNLL accuracy. Based on our discussion so far, we can anticipate that one has to consider the following contributions: on the one hand, there will be a contribution to the even amplitude, in the form of corrections to the two-Reggeon

exchange. These corrections are expected to be of similar origin as the ones arising for the single-Reggeon exchange at NLL. Namely, there will be a next-to-leading order correction to the exchange of two Reggeons; there will be a correction accounted for by the $i\pi/2$ factor included in the expansion parameter $L$; and there will be a correction in the form of impact factors for the two-Reggeon exchange, as indicated by the shaded blobs in the diagram at the centre of figure 4.

More interesting, however, are the corrections concerning the odd amplitude at NNLL accuracy, which, for this reason, are the focus of this paper. In this case one has to take into account for the first time the exchange of three Reggeized gluons, as indicated by the right diagram in figure 4. This implies that, starting at NNLL, one has mixing between one- and three-Reggeons exchange. Schematically, this can be encoded by writing the full amplitude as

$$\hat{\mathcal{M}}_{ij\to ij}|_{\text{NNLL}} = \hat{\mathcal{M}}^{(-)}_{ij\to ij}|_{\text{1-Reggeon + 3-Reggeon}} + \hat{\mathcal{M}}^{(+)}_{ij\to ij}|_{\text{2-Reggeon}}. \tag{2.33}$$

The mixing between one- and three-Reggeons exchange has significant consequences. First of all, it is at the origin of the breaking of the simple power law one finds at NLL accuracy in eq. (2.27). Such a breaking appears for the first time at two loops, and has been singled out for the first time in a perturbative calculation in [44], and investigated further from the point of view of the infrared factorisation formula in [39, 40]. Second, it implies that, starting at three loops, there will be a single-logarithmic contribution originating from the three-Reggeon exchange, and from the interference of the one- and three-Reggeon exchange as well. As a consequence, the interpretation of the Regge trajectory at three loops, i.e. the coefficient $\alpha_g^{(3)}$, needs to be clarified. Understanding these issues requires to investigate the structure of the amplitude in the context of the BFKL theory, which we are going to introduce in the next section.

### 2.3 BFKL theory abridged

The modern approach to high-energy scattering can be formulated in terms of Wilson lines:

$$U(z_\perp) = \mathcal{P}\exp\left[ig_s\int_{-\infty}^{+\infty} A_+^a(x^+, x^-{=}0, z_\perp)dx^+T^a\right]. \tag{2.34}$$

The Wilson lines follow the paths of color charges inside the projectile, and are thus null and labelled by transverse coordinates $z_\perp$. The idea is to approximate, to leading power, the fast projectile and target by Wilson lines and then compute the scattering amplitude between Wilson lines. An important feature of this limit is that the full transverse structure needs to be retained, because the high-energy limit is taken with fixed momentum transfer. This has nontrivial implications since, due to quantum fluctuations, a projectile necessarily contains multiple color charges at different transverse positions: the number of Wilson lines cannot be held fixed. However, in perturbation theory, the unitary matrices $U(z)$ will be close to identity and so can be usefully parametrized by a field $W$ (from now on we drop the $\perp$ subscript):

$$U(z) = e^{ig_s\,T^aW^a(z)}\,. \tag{2.35}$$

The color-adjoint field $W^a$ sources a BFKL Reggeized gluon. A generic projectile, created with four-momentum $p_1$ and absorbed with $p_4$, can thus be expanded at weak coupling as

$$|\psi_i\rangle \equiv \frac{Z_i^{-1}}{2p_1^+} a_i(p_4) a_i^\dagger(p_1)|0\rangle \sim g_s\, D_{i,1}(t)\,|W\rangle + g_s^2\, D_{i,2}(t)\,|WW\rangle + g_s^3\, D_{i,3}(t)\,|WWW\rangle + \dots$$
$$\equiv |\psi_{i,1}\rangle + |\psi_{i,2}\rangle + |\psi_{i,3}\rangle + \dots, \tag{2.36}$$

where the factor $Z_i^{-1}$ removes collinear divergences from the wavefunction $|\psi_i\rangle$, and is related to our definition of the reduced amplitude in eq. (2.26). The factors $D_{i,j}$ depend on the transverse coordinates of the $W$ fields, suppressed here, but not on the center of mass energy. They correspond to the impact factors for the exchange of one-, two- and three-Reggeons discussed in section 2.2 and represented in figure 4. A more precise definition with exact momentum dependence will be given in section 3. The energy dependence enters from the fact that the Wilson lines have rapidity divergences which must be regulated, which leads to a rapidity evolution equation:

$$-\frac{d}{d\eta}\,|\psi_i\rangle = H\,|\psi_i\rangle. \tag{2.37}$$

The Hamiltonian, known as the Balitsky-JIMWLK equation, is given in the next section. A key feature for our perturbative purposes is that it is diagonal in the leading approximation:

$$H \begin{pmatrix} W \\ WW \\ WWW \\ \dots \end{pmatrix} \equiv \begin{pmatrix} H_{1\to1} & 0 & H_{3\to1} & \dots \\ 0 & H_{2\to2} & 0 & \dots \\ H_{1\to3} & 0 & H_{3\to3} & \dots \\ \dots & \dots & \dots & \dots \end{pmatrix} \begin{pmatrix} W \\ WW \\ WWW \\ \dots \end{pmatrix}$$
$$\sim \begin{pmatrix} g_s^2 & 0 & g_s^4 & \dots \\ 0 & g_s^2 & 0 & \dots \\ g_s^4 & 0 & g_s^2 & \dots \\ \dots & \dots & \dots & \dots \end{pmatrix} \begin{pmatrix} W \\ WW \\ WWW \\ \dots \end{pmatrix}. \tag{2.38}$$

Notice, moreover, that only even transition $n \to n \pm 2$ are allowed: odd transition of the type $n \to n \pm 1$ are forbidden by the signature symmetry, because they would originate transitions between even and odd parts of the amplitude.

After using the rapidity evolution equation eq. (2.37) to resum all logarithms of the energy, the amplitude is obtained from the scattering amplitude between equal-rapidity Wilson lines, which depends only on the transverse scale $t$:

$$\frac{i(Z_iZ_j)^{-1}}{2s}\mathcal{M}_{ij\to ij} = \langle\psi_j|e^{-HL}|\psi_i\rangle. \tag{2.39}$$

The prefactor on the left comes simply from the terms like $Z_i^{-1}/(2p_1^+)$ in eq. (2.36), which we have included in order to remove trivial tree-level factors and factorized collinear divergences. In fact, we can go further and make contact with the reduced amplitude $\hat{\mathcal{M}}$ of

eq. (2.26), by removing the Regge trajectory from the evolution:

$$\frac{i}{2s}\hat{\mathcal{M}}_{ij\to ij} = \langle\psi_j|e^{-\hat{H}L}|\psi_i\rangle, \qquad \hat{H} \equiv H + \mathbf{T}_t^2\,\alpha_g(t). \tag{2.40}$$

In these expressions we have identified the evolution variable, the rapidity $\eta$, with the signature-even logarithm appearing in eq. (2.7):

$$\eta = L \equiv \log\left|\frac{s}{t}\right| - i\frac{\pi}{2}. \tag{2.41}$$

The essential requirement is that $\eta$ increases by one unit under boost of the projectile by one e-fold compared to the target, which $L$ can be verified to do due to the $\log s$. The $t$ in the denominator is arbitrary and could be replaced by any other boost-invariant scale, for example $\mu^2$, since different choices represent simply different conventions for the impact factors $|\psi_i\rangle$. Choosing $t$ however avoids introducing much artificial infrared dependence. The $-i\pi/2$ term is a similarly arbitrary choice, but it ensures that the coefficients of powers of $L$ have simple reality properties, as discussed previously, which greatly minimize the number of $i\pi$'s appearing in equations. All these conventions, embodied in eq. (2.40), will go a long way toward simplifying the higher-loop BFKL calculations.

The inner product in eq. (2.40) is by definition the scattering amplitude of Wilson lines renormalized to equal rapidity. It must be calculated within the full QCD theory and therefore cannot be predicted within the effective theory of Wilson lines that we are working in. For our purposes of this paper, however, it will suffice to know that it is Gaussian to leading-order:

$$G_{11'} \equiv \langle W_1|W_{1'}\rangle = i\,\frac{\delta^{a_1a_1'}}{p_1^2}\,\delta^{(2-2\epsilon)}(p_1 - p_1') + \mathcal{O}(g_s^2). \tag{2.42}$$

Multi-Reggeon correlators are obtained by Wick contractions, e.g.

$$\begin{aligned}\langle W_1W_2|W_{1'}W_{2'}\rangle &= G_{11'}G_{22'} + G_{12'}G_{21'} + \mathcal{O}(g_s^2),\\ \langle W_1W_2W_3|W_{1'}W_{2'}W_{3'}\rangle &= G_{11'}G_{22'}G_{33'} + (5\text{ permutations}) + \mathcal{O}(g_s^2),\\ &\quad\text{etc.}\end{aligned} \tag{2.43}$$

We believe that the $\mathcal{O}(g_s^2)$ corrections could be extracted, if needed, from the results of [48]. There are also off-diagonal elements, which can be *defined* to have zero overlap:

$$\langle W_1W_2W_3|W_4\rangle = \langle W_4|W_1W_2W_3\rangle = 0; \tag{2.44}$$

in other words, we assume the Reggeons to be free fields. This is an implicit assumption in the classic BFKL literature. In the Wilson line approach it can be justified by noticing that, starting from a scheme in which the inner products in eq. (2.44) is different from zero, it is always possible to perform a scheme transformations (redefinition of the $W$ field, for instance $WWW \mapsto WWW - g_s^2 G\,W$) such as to reduce to eq. (2.44). It is possible to derive the transformation $G$ only by calculating the inner product in eq. (2.44) in full QCD in a given scheme. While we leave this calculation to be investigated in future work, we notice that the precise form of $G$ is not needed in order to obtain quantitative predictions for

NNLL amplitudes. Indeed, choosing the 1-$W$ and 3-$W$ states to be orthogonal, combined with symmetry of the Hamiltonian, which in turn is a consequence of boost invariance:

$$\frac{d}{d\eta}\langle\mathcal{O}_1|\mathcal{O}_2\rangle = 0 \quad \Leftrightarrow \quad \langle H\mathcal{O}_1|\mathcal{O}_2\rangle = \langle\mathcal{O}_1|H\mathcal{O}_2\rangle \equiv \langle\mathcal{O}_1|H|\mathcal{O}_2\rangle, \tag{2.45}$$

where $\mathcal{O}_1$, $\mathcal{O}_2$ represent an arbitrary number of $W$ fields, implies that in this scheme one has $H_{1\to3} = H_{3\to1}$, and more in general $H_{k\to k+2} = H_{k+2\to k}$. This relation is known as projectile-target duality. As we will see in the next section, it is actually essential in order to obtain predictions at NNLL accuracy based only on the leading order BFKL hamiltonian. As an additional comment, we note that in principle one could diagonalize the Hamiltonian in eq. (2.38), given the fact that it is symmetrical with respect to the inner product, so there is no invariant meaning to its "off-diagonal elements being nonzero". In practice, however, this would require inverting its (complicated) diagonal terms, and for this reason we work with the undiagonalized Hamiltonian.

We can finally list the ingredients which build up the amplitude up to three loops. Since the odd and even sectors are orthogonal and closed under the action of $\hat{H}$ (as a consequence of signature symmetry), we have

$$\frac{i}{2s}\hat{\mathcal{M}}_{ij\to ij} \xrightarrow{\text{Regge}} \frac{i}{2s}\left(\hat{\mathcal{M}}^{(+)}_{ij\to ij} + \hat{\mathcal{M}}^{(-)}_{ij\to ij}\right) \equiv \langle\psi^{(+)}_j|e^{-\hat{H}L}|\psi^{(+)}_i\rangle + \langle\psi^{(-)}_j|e^{-\hat{H}L}|\psi^{(-)}_i\rangle. \tag{2.46}$$

Using that multi-Reggeon impact factors are coupling-suppressed, $|\psi_{i_k}\rangle \sim g^k$, and using the suppression eq. (2.38) of off-diagonal elements in the Hamiltonian, the signature even amplitude becomes to three loops:

$$\frac{i}{2s}\hat{\mathcal{M}}^{(+)\,\text{1-loop}}_{ij\to ij} = \langle\psi_{j,2}|\psi_{i,2}\rangle^{(\text{LO})}, \tag{2.47a}$$

$$\frac{i}{2s}\hat{\mathcal{M}}^{(+)\,\text{2-loops}}_{ij\to ij} = -L\langle\psi_{j,2}|\hat{H}_{2\to2}|\psi_{i,2}\rangle^{(\text{LO})} + \langle\psi_{j,2}|\psi_{i,2}\rangle^{(\text{NLO})}, \tag{2.47b}$$

$$\begin{aligned}\frac{i}{2s}\hat{\mathcal{M}}^{(+)\,\text{3-loops}}_{ij\to ij} = {}& \frac{L^2}{2}\langle\psi_{j,2}|(\hat{H}_{2\to2})^2|\psi_{i,2}\rangle^{(\text{LO})} - L\langle\psi_{j,2}|\hat{H}_{2\to2}|\psi_{i,2}\rangle^{(\text{NLO})} \\ & + \langle\psi_{j,4}|\psi_{i,4}\rangle^{(\text{LO})} + \langle\psi_{j,2}|\psi_{i,2}\rangle^{(\text{NNLO})}.\end{aligned} \tag{2.47c}$$

Here "LO" means that all ingredients are needed only to leading nonvanishing order. The first term was analyzed in ref. [16] and found to be quite powerful: it predicted that there should be no $\sim \alpha_s^3 L^2$ corrections to the dipole formula. At four loops, a similar leading-logarithmic computation predicted a non-vanishing $\Gamma \sim \alpha_s^4 L^3$ correction to the dipole formula, which hopefully will be tested in the future.

In this paper we analyze the similar expansion for the signature odd sector: $H_{1\to1} = -C_A\,\alpha_g(t)$

$$\frac{i}{2s}\hat{\mathcal{M}}^{(-)\,\text{tree}}_{ij\to ij} = \langle\psi_{j,1}|\psi_{i,1}\rangle^{(\text{LO})}, \tag{2.48a}$$

$$\frac{i}{2s}\hat{\mathcal{M}}^{(-)\,\text{1-loop}}_{ij\to ij} = -L\langle\psi_{j,1}|\hat{H}_{1\to1}|\psi_{i,1}\rangle^{(\text{LO})} + \langle\psi_{j,1}|\psi_{i,1}\rangle^{(\text{NLO})}, \tag{2.48b}$$

$$\frac{i}{2s}\hat{\mathcal{M}}^{(-)\,\text{2-loops}}_{ij\to ij} = +\frac{1}{2}L^2\langle\psi_{j,1}|(\hat{H}_{1\to1})^2|\psi_{i,1}\rangle^{(\text{LO})} - L\langle\psi_{j,1}|\hat{H}_{1\to1}|\psi_{i,1}\rangle^{(\text{NLO})} + \langle\psi_{j,3}|\psi_{i,3}\rangle^{(\text{LO})} + \langle\psi_{j,1}|\psi_{i,1}\rangle^{(\text{NNLO})}, \tag{2.48c}$$

$$\frac{i}{2s}\hat{\mathcal{M}}^{(-)\,\text{3-loops}}_{ij\to ij} = -\frac{1}{6}L^3\langle\psi_{j,1}|(\hat{H}_{1\to1})^3|\psi_{i,1}\rangle^{(\text{LO})} + \frac{1}{2}L^2\langle\psi_{j,1}|(\hat{H}_{1\to1})^2|\psi_{i,1}\rangle^{(\text{NLO})} - L\Big\{\langle\psi_{j,1}|\hat{H}_{1\to1}|\psi_{i,1}\rangle^{(\text{NNLO})} + \Big[\langle\psi_{j,3}|\hat{H}_{3\to3}|\psi_{i,3}\rangle + \langle\psi_{j,3}|\hat{H}_{1\to3}|\psi_{i,1}\rangle + \langle\psi_{j,1}|\hat{H}_{3\to1}|\psi_{i,3}\rangle\Big]^{(\text{LO})}\Big\} + \langle\psi_{j,3}|\psi_{i,3}\rangle^{(\text{NLO})} + \langle\psi_{j,1}|\psi_{i,1}\rangle^{(\text{N}^3\text{LO})}, \tag{2.48d}$$

where, for illustrative purposes, we have listed all terms that need to be considered by taking into account eq. (2.44), but without any specific assumption about the form of $\hat{H}$. Inspecting eq. (2.40), we notice now that the $1 \to 1$ transition is given, according to eq. (2.21), by the Regge trajectory $H_{1\to1} = -C_A\,\alpha_g(t)$. As a consequence one has $\hat{H}_{1\to1} = 0$, and this set to zero all terms of the type

$$\langle\psi_{j,1}|(\hat{H}_{1\to1})^n|\psi_{i,1}\rangle^{(\dots)} = 0, \tag{2.49}$$

in eq. (2.48). Starting from NNLL order, the "gluon Regge trajectory" is scheme-dependent. In this paper we *define* it to be $-H_{1\to1}/C_A$ in the scheme defined below eq. (2.44), so that $\hat{H}_{1\to1}$ identically vanishes. Excluding these terms, subleading logarithms in the reduced amplitude arise from roughly two mechanisms: corrections to the single-Reggeon exchange in the form of impact factors, such as for instance the term $\langle\psi_{j,1}|\psi_{i,1}\rangle^{(\text{NNLO})}$ in eq. (2.48), and exchanges of multiple Reggeized gluons, such as terms like $\langle\psi_{j,3}|\psi_{i,3}\rangle^{(\text{LO})}$ and $\langle\psi_{j,3}|\hat{H}_{1\to3}|\psi_{i,1}\rangle^{(\text{LO})}$.

The key observation for us will be that the NLO and NNLO effects are strongly constrained by factorization: for example, since the elementary Reggeon is color-adjoint, any term in the (full) amplitude related to the exchange of a single Reggeon vanishes upon projecting the amplitude onto other color structures. Due to this, as noted below eq. (2.25), many formally NNLL ($\sim L^1$) terms in the three-loop amplitude can be predicted using only the LO BFKL theory! In the next section we quantitatively work out these predictions.

## 3 The Balitsky-JIMWLK equation and the three-loop amplitude

The BFKL prediction eq. (2.48) for the three-loop amplitude involves the rapidity evolution $H$ and impact factors $|\psi\rangle$. We now describe both to the relevant order in perturbation theory.

The evolution equation takes a simple and compact form in the planar limit, known as the Balitsky-Kovchegov equation [11, 12, 49–51]:

$$H\,U_{ij} = \frac{\alpha_s C_A}{2\pi^2}\int\frac{d^2z_0\,z_{ij}^2}{z_{i0}^2 z_{0j}^2}\,[U_{ij} - U_{i0}U_{0j}] + \mathcal{O}(\alpha_s^2), \tag{3.1}$$

where $U_{ij} = \frac{1}{N_c}\text{Tr}[U(z_i)U(z_j)^\dagger]$ is the trace of a color dipole and $z_{ij} = z_i - z_j$ is a transverse distance. Physically, this accounts for radiation of a gluon at the impact parameter $z_0$ and its effect on the perceived color charge density of a projectile.

This form holds for a color singlet projectile, but a similar equation can also be derived for scattering of colored partons. However, since $U_{ij} = 1 + O(1/N_c^2)$ in the planar limit, the equation turns out to linearize and its solution for $2 \to 2$ scattering is essentially trivial: a pure Regge pole $\mathcal{M} \propto s^{C_A\,\alpha_g(t)}$ to any order in the 't Hooft coupling $g_s^2 N_c$. We refer to section 3 of [16] for more details.

The effects we focus on in this paper are fundamentally non-planar. To describe them we will need the finite $N_c$ generalization of eq. (3.1), known as the Balitsky-JIMWLK equation, which involves a sum over all possible color attachments of the radiated gluon:

$$H = \frac{\alpha_s}{2\pi^2} \int [dz_i][dz_j][dz_0] K_{ij;0} \Big[ T^a_{i,L} T^a_{j,L} + T^a_{i,R} T^a_{j,R} - U^{ab}_{\rm ad}(z_0) \left( T^a_{i,L} T^b_{j,R} + T^a_{j,L} T^b_{i,R} \right) \Big] + \mathcal{O}(\alpha_s^2). \tag{3.2}$$

Anticipating infrared divergences, here we have switched to dimensional regularization: $[dz] \equiv d^{2-2\epsilon}z$, where we recall that $z$ parametrizes the transverse impact parameter plane. $U^{ab}_{\rm ad}$ is the adjoint Wilson line associated with the radiated gluon, and the $T_{L/R}$'s are generators for left and right color rotations:

$$T^a_{i,L} = [T^a U(z_i)] \frac{\delta}{\delta U(z_i)}, \qquad T^a_{i,R}(z) = [U(z_i) T^a] \frac{\delta}{\delta U(z_i)}. \tag{3.3}$$

These act on the projectile and target impact factors $|\psi\rangle$, which are represented as functionals of Wilson lines $U(z)$. (In perturbation theory these are just polynomials, so the $i$ and $j$ integrals effectively represent discrete sums.) The $\mathcal{O}(\alpha_s^2)$ correction in eq. (3.2) has been recently determined by three groups [52–57]. In the following, however, we will need only the leading-order dimensionally-regulated kernel $K_{ij;0}$, which turns out to admit a simple, dimension-independent expression in momentum space (see ref. [16]):

$$R(q,p) = \frac{(q+p)^2}{q^2 p^2}. \tag{3.4}$$

The corresponding coordinate space expression is then

$$K_{ij;0} \equiv S_\epsilon(\mu^2) \int [đq][đp]\, e^{iq\cdot(z_i - z_0)} e^{ip\cdot(z_j - z_0)} (-2\pi^2) R(q,p) = S_\epsilon(\mu^2) \frac{\Gamma(1-\epsilon)^2}{\pi^{-2\epsilon}} \frac{z_{0i}\cdot z_{0j}}{(z_{0i}^2 z_{0j}^2)^{1-\epsilon}}, \tag{3.5}$$

where we have defined the integration measure $[đq] \equiv \frac{d^{2-2\epsilon}q}{(2\pi)^{2-2\epsilon}}$, and $S_\epsilon(\mu^2) = \left(\frac{\mu^2}{4\pi e^{-\gamma_E}}\right)^\epsilon$ is the usual $\overline{\rm MS}$ loop factor. As $\epsilon \to 0$ this reduces indeed to the well-known four-dimensional formula (compare for instance with eq. (2.7) of [16]). We note that in computing this Fourier transform we have dropped contact terms $\delta^{2-2\epsilon}(z_0 - z_i)$, which vanish in eq. (3.2) as a result of the color identities $U^{ab}(z_i) T^b_{i,R} = T^a_{i,L}$ and $U^{ab}(z_i) T^a_{i,L} = T^b_{i,R}$, see [16].

The corrections to the Balitsky-JIMWLK Hamiltonian eq. (3.2) are suppressed by $\alpha_s$ in a power-counting where the Wilson lines are generic, $U \sim 1$. This is more general than the perturbative counting of the preceding section, where $1 - U \sim g_s W \sim g_s$, implying that the equation resums infinite towers of Reggeon iterations. The relationship will be clarified shortly. First of all, one expands the Wilson line $U$ in terms of the Reggeon field $W$:

$$U = e^{ig_s\, W^a T^a} = 1 + ig_s\, W^a\, T^a - \frac{g_s^2}{2} W^a W^b\, T^a T^b - i\frac{g_s^3}{6} W^a W^b W^c\, T^a T^b T^c$$

$$+\frac{g_s^4}{24}W^aW^bW^cW^d\,T^aT^bT^cT^d+\mathcal{O}(g_s^5\,W^5). \tag{3.6}$$

Then, to extract the interactions efficiently, we simply use the Campbell-Baker-Hausdorf formula to convert the rotations defined by eq. (3.3) to derivatives with respect to $W$:

$$\begin{aligned} iT^a_{j,L/R} = {} & \frac{1}{g_s}\frac{\delta}{\delta W_j^a} \pm \frac{1}{2}f^{abx}W_j^x\frac{\delta}{\delta W_j^b} - \frac{g_s}{12}W_j^xW_j^y(F^xF^y)^a{}_b\frac{\delta}{\delta W_j^b} \\ & - \frac{g_s^3}{720}W_j^xW_j^yW_j^zW_j^t(F^xF^yF^zF^t)^a{}_b\frac{\delta}{\delta W_j^b}+\ldots, \end{aligned} \tag{3.7}$$

where we have introduced the Hermitian color matrix $(F^x)^a{}_b \equiv if^{axb}$. It is then a straightforward, if lengthy, exercise in algebra to expand the Hamiltonian eq. (3.2) in powers of $g_s$:

$$H = H_{k\to k} + H_{k\to k+2} + \ldots \tag{3.8}$$

For the diagonal terms, commuting $\delta/\delta W$'s to the right of $W$'s by using

$$\frac{\delta W^b(z')}{\delta W^a(z)} \equiv \delta^{ab}\delta^{2-2\epsilon}(z-z'), \tag{3.9}$$

one finds [16]:

$$\begin{aligned} H_{k\to k} = {} & \frac{\alpha_s C_A}{2\pi^2}\int [dz_i][dz_0]K_{ii;0}\,(W_i-W_0)^a\frac{\delta}{\delta W_i^a} \\ & -\frac{\alpha_s}{2\pi^2}\int [dz_i][dz_j][dz_0]K_{ij;0}(W_i-W_0)^x(W_j-W_0)^y(F^xF^y)^{ab}\frac{\delta^2}{\delta W_i^a\delta W_j^b}. \end{aligned} \tag{3.10}$$

For the first nonlinear corrections, not previously written in the literature, we find:

$$\begin{aligned} H_{k\to k+2} = {} & \frac{\alpha_s^2}{3\pi}\int [dz_i][dz_0]\,K_{ii;0}\,(W_i-W_0)^xW_0^y(W_i-W_0)^z\,\mathrm{Tr}\big[F^xF^yF^zF^a\big]\frac{\delta}{\delta W_i^a} \\ & + \frac{\alpha_s^2}{6\pi}\int [dz_i][dz_j][dz_0]\,K_{ij;0}\,(F^xF^yF^zF^t)^{ab}\Big[(W_i-W_0)^xW_0^yW_0^z(W_j-W_0)^t \\ & - W_i^x(W_i-W_0)^yW_0^z(W_j-W_0)^t - (W_i-W_0)^xW_0^y(W_j-W_0)^zW_j^t\Big]\frac{\delta^2}{\delta W_i^a\delta W_j^b}. \end{aligned} \tag{3.11}$$

We have included the second term for future reference only, since in this paper we will only need the $1\to 3$ transition, contained in the first line. (We observe, a posteriori, that the two terms are not completely independent: the first can be obtained from the second by moving $\delta/\delta W_j$ to the left and letting it act on $W_i$.)

Finally, let us explain the relationship between the Balitsky-JIMWLK power counting ($U\sim 1$) and the BFKL power-counting ($W\sim 1$), and how it justifies our extraction of the multi-Reggeon vertices. The key is to substitute eqs. (3.6) and (3.7) into (3.2), which show that an $m\to m+k$ transition taken from the $\ell$-loop Balitsky-JIMWLK equation is proportional to $g_s^{2\ell+k}$. Thus for $k\geq 0$, all the leading interactions can be extracted from just the leading-order equation. On the other hand, because of the symmetry of $H$ (2.45),

interactions with $k<0$ are suppressed by at least $g_s^{2+|k|}$, which means that they can first appear in the $(|k|+1)$-loop Balitsky-JIMWLK Hamiltonian. Thus to obtain the $m\to m-2$ transition by direct calculation of the Hamiltonian would require a rather formidable three-loop non-planar computation. However, this is unnecessary, since the symmetry of $H$ predicts the result; this is carried out explicitly in the following subsection (see eq. (3.18)).

### 3.1 Evolution in momentum space

Due to the simple form eq. (3.4) of the kernel in momentum space, the perturbative calculation will be easier in this space. Let us thus introduce the Fourier transform:

$$W^a(p)=\int [dz]\, e^{-ipz}\, W^a(z), \qquad W^a(z)=\int [đp]\, e^{ipz}\, W^a(p). \tag{3.12}$$

Substituting into eq. (3.10), and using the Fourier representation of the kernel eq. (3.5), one finds, after a bit of algebra again,

$$\begin{aligned} H_{k\to k} &= -\int [dp]\, C_A\, \alpha_g(p)\, W^a(p) \frac{\delta}{\delta W^a(p)} \\ &+\alpha_s \int [đq][dp_1][dp_2]\, H_{22}(q;p_1,p_2)\, W^x(p_1+q) W^y(p_2-q) (F^x F^y)^{ab} \frac{\delta}{\delta W^a(p_1)} \frac{\delta}{\delta W^b(p_2)}, \end{aligned} \tag{3.13}$$

where the gluon Regge trajectory and pairwise interactions come out as some specific combinations of the momentum space kernel $R$ of eq. (3.4) (see [16] for more details). Given that we consider here only the leading order contribution to the kernel $K_{ij;0}$ in eq. (3.2), the gluon Regge trajectory in eq. (3.13) is actually the leading-order trajectory defined in eq. (2.19), that we recall here for the reader's convenience:

$$\begin{aligned} \alpha_g(p) &= \frac{\alpha_s}{\pi}\, \alpha_g^{(1)}(p^2) + \mathcal{O}(\alpha_s^2) \\ &= -\alpha_s(\mu) S_\epsilon(\mu^2) \int [đq] \frac{p^2}{q^2(p-q)^2} + \mathcal{O}(\alpha_s^2) = \frac{\alpha_s(\mu)\, r_\Gamma}{2\pi\epsilon} \left(\frac{\mu^2}{p^2}\right)^\epsilon + \mathcal{O}(\alpha_s^2). \end{aligned} \tag{3.14}$$

The solution to the single-Reggeon part of the evolution equation above, in which one consider the LO Regge trajectory, is responsible for the leading-logarithmic behaviour of the amplitude. Below we will analyse the structure of the scattering amplitude up to NNLL accuracy, which means that we will need also the first two corrections to $\alpha_g(p^2)$, namely $\alpha_g^{(2)}(p^2)$ and $\alpha_g^{(3)}(p^2)$. The NLO Regge trajectory $\alpha_g^{(2)}(p^2)$ has been calculated in [58–61]; it can also be extracted from two-loop calculations of $2\to 2$ scattering amplitudes, see [44]. The NNLO correction to the Regge Trajectory $\alpha_g^{(3)}(p^2)$ is instead not yet known in full QCD, though it will be possible to extract it below at least in $\mathcal{N}=4$ SYM from a recent three-loop calculation [41]. As we will discuss below, it is not even possible to define it precisely, beyond the planar limit, without taking into account the mixing in the evolution between one- and three-Reggeon exchange given by $H_{1\to 3}$ and $H_{3\to 1}$. The other ingredient appearing in eq. (3.13) is then the leading-order momentum kernel for the evolution of two Reggeon states, [16], i.e.

$$H_{22}(q;p_1,p_2) = \frac{(p_1+p_2)^2}{p_1^2 p_2^2} - \frac{(p_1+q)^2}{p_1^2 q^2} - \frac{(p_2-q)^2}{q^2 p_2^2}. \tag{3.15}$$

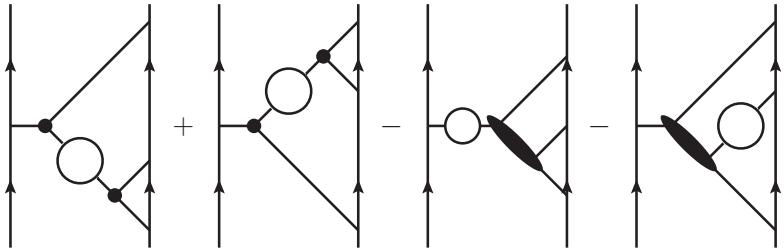

**Figure 5**. Diagrams representing the kinematical structure of the $1 \to 3$ and $3 \to 1$ evolution, i.e. the factor $H_{13}(p_1, p_2, p_3)$ in eq. (3.17). The hamiltonian $H_{13}(p_1, p_2, p_3)$ is derived in the context of an effective field theory in $2 - 2\epsilon$ dimensions, therefore the vertices indicated by black dots must be thought as effective vertices. The actual color structure associated to the $1 \to 3$ and $3 \to 1$ evolution is given by the diagrams in figure 7.

These ingredients are of course precisely as in the classic BFKL equation [1, 2], and eq. (3.13) encapsulates in a concise way its generalization to multi-Reggeon states [62–64]. Here they has been obtained in a systematic and straightforward way by linearizing the non-planar version of our starting point, the Balitsky-Kovchegov equation (3.1).

The less familiar ingredient we will need is the $1 \to 3$ transition, obtained again as the Fourier transform of eq. (3.11):

$$H_{1\to 3} = \alpha_s^2 \int [đp_1][đp_2][dp]\, \mathrm{Tr}[F^a F^b F^c F^d]\, W^b(p_1) W^c(p_2) W^d(p_3)\, H_{13}(p_1, p_2, p_3)\, \frac{\delta}{\delta W^a(p)}, \tag{3.16}$$

where $p_3 = p - p_1 - p_2$ and the kernel is

$$\begin{aligned} H_{13}(p_1, p_2, p_3) \;&=\; \frac{2\pi}{3} S_\epsilon(\mu^2) \int [đq] \left[ \frac{(p_1{+}p_2)^2}{q^2 (p_1{+}p_2{-}q)^2} + \frac{(p_2{+}p_3)^2}{q^2 (p_2{+}p_3 - q)^2} \right. \\ &\qquad \left. - \frac{(p_1{+}p_2{+}p_3)^2}{q^2 (p_1{+}p_2{+}p_3{-}q)^2} - \frac{p_2^2}{q^2 (p_2{-}q)^2} \right] \\ &=\; \frac{r_\Gamma}{3\epsilon} \left[ \left( \frac{\mu^2}{(p_1{+}p_2{+}p_3)^2} \right)^\epsilon + \left( \frac{\mu^2}{p_2^2} \right)^\epsilon - \left( \frac{\mu^2}{(p_1{+}p_2)^2} \right)^\epsilon - \left( \frac{\mu^2}{(p_2{+}p_3)^2} \right)^\epsilon \right]. \end{aligned} \tag{3.17}$$

Taking its transpose with respect to the inner product eq. (2.42) then gives the conjugate vertex:

$$\begin{aligned} H_{3\to 1} \;=\; \alpha_s^2 \int [dp_1][dp_2][dp_3]\, \mathrm{Tr}[F^a F^b F^c F^d]\, W^d(p_1{+}p_2{+}p_3)\, \frac{\delta}{\delta W^a(p_1)} \frac{\delta}{\delta W^b(p_2)} \frac{\delta}{\delta W^c(p_3)} \\ \times (-1) \frac{(p_1{+}p_2{+}p_3)^2}{p_1^2 p_2^2 p_3^2}\, H_{13}(p_1, p_2, p_3). \end{aligned} \tag{3.18}$$

This was obtained simply by equating the matrix elements

$$\big(\langle WWW|H\big)|W\rangle = \langle WWW|\big(H|W\rangle\big),$$

taking into account the mismatching propagators, $\frac{i}{(p_1+p_2+p_3)^2}$ compared with $\frac{i^3}{p_1^2 p_2^2 p_3^2}$.

Eq. (3.11) describes not only the $1 \to 3$, but also $2 \to 4$ transitions in position space. The latter are not necessary for the calculation of the odd contribution to the amplitude at three loops: $2 \to 4$ transitions start contributing only at four loops. It is however straightforward to derive their representation in momentum space, and we list it here for future reference. One has

$$H_{2\to4} = \frac{\pi\alpha_s^2}{3} S_\epsilon(\mu^2) \int [đp_1][đp_2][đp_3][đp_4][dp_a][dp_b](2\pi)^{2-2\epsilon}\delta^{2-2\epsilon}(p_1{+}p_2{+}p_3{+}p_4{-}p_a{-}p_b)$$
$$\times H_{24}(p_i)\,(F^xF^yF^zF^t)^{ab}\,W^x(p_1)W^y(p_2)W^z(p_3)W^t(p_4)\,\frac{\delta}{\delta W^a(p_a)}\frac{\delta}{\delta W^b(p_b)}, \tag{3.19}$$

where:

$$\begin{aligned} H_{24}(p_i) = {} & 2R(p_a, p_b{-}p_4) + 2R(p_a{-}p_1, p_b) - R(p_a, p_b) \\ & - 3R(p_a{-}p_1, p_b{-}p_4) + R(p_a{-}p_1, p_b{-}p_4{-}p_3) - R(p_a, p_b{-}p_4{-}p_3) \\ & + R(p_a{-}p_1{-}p_2, p_b{-}p_4) - R(p_a{-}p_1{-}p_2, p_b), \end{aligned} \tag{3.20}$$

and we recall that $R(p,q) = \frac{(p+q)^2}{p^2q^2}$ from eq. (3.4). Similarly, taking its transpose,

$$H_{4\to2} = \frac{\pi\alpha_s^2}{3} \int [đp_a][đp_b][dp_1][dp_2][dp_3][dp_4](2\pi)^{2-2\epsilon}\delta^{2-2\epsilon}(p_a{+}p_b{-}p_1{-}p_2{-}p_3{-}p_4)$$
$$\times (-1)\,\frac{p_a^2\,p_b^2}{p_1^2\,p_2^2\,p_3^2\,p_4^2}\,H_{24}(p_i)\,(F^xF^yF^zF^t)^{ab}\,W^a(p_a)W^b(p_b)$$
$$\times \frac{\delta}{\delta W^x(p_1)}\frac{\delta}{\delta W^y(p_2)}\frac{\delta}{\delta W^z(p_3)}\frac{\delta}{\delta W^t(p_4)}. \tag{3.21}$$

### 3.2 Impact factors

Given the Hamiltonian, all one needs to compute the amplitude are the target and projectile impact factors. At leading order these follow simply from the naive eikonal approximation:

$$|\psi_i\rangle^{(\mathrm{LO})} = \int [dz] e^{ip\cdot z} U_i(z), \tag{3.22}$$

where the Wilson line is in the representation of particle $i$, and $p$ in the transferred momentum, $p^2 = -t$. Expanding in powers of the Reggeon field according to eq. (3.6), and going to momentum space, this can also be written to NNLL accuracy as

$$|\psi_i\rangle^{(\mathrm{LO})} = ig\,\mathbf{T}_i^a W^a(p) - \frac{g^2}{2}\mathbf{T}_i^a\mathbf{T}_i^b \int [đq]\,W^a(q)W^b(p{-}q)$$
$$- \frac{ig^3}{6}\mathbf{T}_i^a\mathbf{T}_i^b\mathbf{T}_i^c \int [đq_1][đq_2]\,W^a(q_1)W^b(q_2)W^c(p{-}q_1{-}q_2) + \mathcal{O}(\mathrm{N^3LL}), \tag{3.23}$$

where we have dropped the coefficient of the unit operator.

At higher orders in the coupling, the color charge of the projectile is no longer concentrated in a single point, which leads to a nontrivial momentum dependence for multi-Reggeon impact factors. Restricting again to NNLL accuracy, the relevant corrections at relative order $\alpha_s$ reads

$$|\psi_i\rangle^{(\mathrm{NLO})} = \frac{\alpha_s}{\pi}\Big[ig\,\mathbf{T}_i^a W^a(p) D_i^{(1)}(p)$$

$$-\frac{g^2}{2}\mathbf{T}_i^a\mathbf{T}_i^b\int[đq]\,\psi_i^{(1)}(p,q)\,W^a(q)W^b(p-q)+\mathcal{O}(\mathrm{N^3LL})\Big], \tag{3.24}$$

and at the next order one has :

$$|\psi_i\rangle^{(\mathrm{NNLO})}=\left(\frac{\alpha_s}{\pi}\right)^2\left[ig\,\mathbf{T}_i^aW^a(p)D_i^{(2)}(p)+O(\mathrm{N^3LL})\right]. \tag{3.25}$$

### 3.3 Odd amplitude up to two loops

According to eq. (2.48), to get the signature-odd amplitude to two loops we need exchanges of one and three Reggeons, the latter first appearing at two loops. Let us consider first the single Reggeon exchange.

#### $W\to W$ amplitude

Concerning the reduced amplitude, the one-Reggeon exchange is rather simple, since the Regge trajectory is subtracted to all loop, see eq. (2.49). As a consequence, the $1\to 1$ transitions involves only the impact factors, and is given by a generalisation of eq. (2.27) to include NNLL effects. In terms of transitions between Wilson lines it is given by

$$\langle\psi_{j,1}|e^{-\hat{H}_{1\to 1}L}|\psi_{i,1}\rangle=D_i(t)\,D_j(t)\,\frac{i}{2s}\,4\pi\alpha_s\,\hat{\mathcal{M}}^{(0)}_{ij\to ij}, \tag{3.26}$$

where $\hat{\mathcal{M}}^{(0)}_{ij\to ij}=\mathcal{M}^{(0)}_{ij\to ij}$ has been defined in eq. (2.17). Effects up to NNLL are retained by considering impact factors $D_{i/j}$ up to NNLO. At tree level one trivially has

$$\langle\psi_{j,1}|\psi_{i,1}\rangle^{(\mathrm{LO})}=\frac{i}{2s}\,4\pi\alpha_s\,\hat{\mathcal{M}}^{(0)}_{ij\to ij}, \tag{3.27}$$

while at one and two loops one obtains

$$\langle\psi_{j,1}|\psi_{i,1}\rangle^{(\mathrm{NLO})}=\frac{\alpha_s}{\pi}\left(D_i^{(1)}(t)+D_j^{(1)}(t)\right)\frac{i}{2s}\,4\pi\alpha_s\,\hat{\mathcal{M}}^{(0)}_{ij\to ij}, \tag{3.28}$$

$$\langle\psi_{j,1}|\psi_{i,1}\rangle^{(\mathrm{NNLO})}=\left(\frac{\alpha_s}{\pi}\right)^2\left(D_i^{(2)}+D_j^{(2)}+D_i^{(1)}D_j^{(1)}\right)\frac{i}{2s}\,4\pi\alpha_s\,\hat{\mathcal{M}}^{(0)}_{ij\to ij}. \tag{3.29}$$

#### $3W\to 3W$ amplitude

The exchange of three Reggeons contributes to the amplitude starting at two-loops, and is given according to eq. (2.48c) by a simple Wick contraction of free propagators:

$$\langle\psi_{j,3}|\psi_{i,3}\rangle^{(\mathrm{LO})}=-i\pi^2\,(r_\Gamma)^2\,\mathcal{I}[1]\,\frac{g^2}{t}\left(\frac{\alpha_s}{\pi}\right)^2C_{33}^{(2)} \tag{3.30}$$

where $C_{33}^{(2)}$ represents the color factor, to be discussed below, and we have defined the basic two-loop integral

$$\mathcal{I}[N]\equiv\left(\frac{4\pi S_\epsilon(p^2)}{r_\Gamma}\right)^2\int[đp_1][đp_2]\,\frac{p^2}{p_1^2p_2^2(p-p_1-p_2)^2}\,N \tag{3.31}$$

where $N$ should be understood to be a function of the momenta $p_1$, $p_2$ and $p$. Integrals of the type $\mathcal{I}[N]$ are trivial to calculate, because they correspond to bubble integrals of the type

$$\int \frac{d^{2-2\epsilon}k}{(2\pi)^{2-2\epsilon}} \frac{1}{[k^2]^\alpha[(p-k)^2]^\beta} = \frac{B_{\alpha,\beta}(\epsilon)}{(4\pi)^{1-\epsilon}} (p^2)^{1-\epsilon-\alpha-\beta} \tag{3.32}$$

$$\text{with} \qquad B_{\alpha,\beta}(\epsilon) \equiv \frac{\Gamma(1-\alpha-\epsilon)\Gamma(1-\beta-\epsilon)\Gamma(\alpha+\beta-1+\epsilon)}{\Gamma(\alpha)\Gamma(\beta)\Gamma(2-2\epsilon-\alpha-\beta)} \,.$$

In particular, in case of eq. (3.30) we need the case $N = 1$, for which we get

$$\mathcal{I}[1] = \frac{4}{\epsilon^2} \frac{B_{1,1+\epsilon}(\epsilon)}{B_{1,1}(\epsilon)} = \frac{3}{\epsilon^2} - 18\epsilon\zeta_3 - 27\epsilon^2\zeta_4 + \ldots \tag{3.33}$$

This is a nice feature of the Regge limit: a two-loop amplitude has been reduced to essentially a free theory computation in the effective Reggeon theory. The more difficult aspect is to deal with the color factor:

$$C_{33}^{(2)} = \frac{1}{36} \sum_{\sigma\in\mathcal{S}_3} \left(\mathbf{T}_i^{\sigma(a)}\mathbf{T}_i^{\sigma(b)}\mathbf{T}_i^{\sigma(c)}\right)_{a_1a_4} \left(\mathbf{T}_j^a\mathbf{T}_j^b\mathbf{T}_j^c\right)_{a_2a_3} . \tag{3.34}$$

Our strategy, keeping in mind our goal to compare the infrared divergent part, is to express this as some kind of operator acting on the tree color factor. Fortunately, there is a systematic way to do so: we iteratively peel off contracted indices, starting from the outermost ones, and re-express them in terms of Casimirs, for example

$$\left[(\mathbf{T}_i^a\cdots)_{a_1a_4}\,(\mathbf{T}_j^a\cdots)_{a_2a_3}\right] = \frac{1}{2}(\mathbf{T}_s^2 - C_i - C_j)\left[(\cdots)_{a_1a_4}\,(\cdots)_{a_2a_3}\right]. \tag{3.35}$$

With the help of the identities used in eq. (2.32), the Casimirs can be further decomposed into signature even and odd combinations, which gives us the following two useful formulas:

$$\begin{aligned}\left[(\mathbf{T}_i^a\cdots)_{a_1a_4}\,(\mathbf{T}_j^a\cdots)_{a_2a_3}\right] &= \tfrac{1}{2}\left(\mathbf{T}_{s-u}^2 - \tfrac{1}{2}\mathbf{T}_t^2\right)\left[(\cdots)_{a_1a_4}\,(\cdots)_{a_2a_3}\right], \\ \left[(\mathbf{T}_i^a\cdots)_{a_1a_4}\,(\cdots\mathbf{T}_j^a)_{a_2a_3}\right] &= \tfrac{1}{2}\left(\mathbf{T}_{s-u}^2 + \tfrac{1}{2}\mathbf{T}_t^2\right)\left[(\cdots)_{a_1a_4}\,(\cdots)_{a_2a_3}\right].\end{aligned} \tag{3.36}$$

By repeatedly applying these formulas it is now a simple exercise to obtain that

$$C_{33}^{(2)} = \frac{1}{24}\left[(\mathbf{T}_{s-u}^2)^2 - \frac{1}{12}(C_A)^2\right](T_i^b)_{a_1a_4}(T_j^b)_{a_2a_3}, \tag{3.37}$$

and substituting into (3.30) gives the two-loop amplitude:

$$\langle\psi_{j,3}|\psi_{i,3}\rangle^{(\mathrm{LO})} = -\frac{\pi^2}{24}\left(\frac{\alpha_s}{\pi}\right)^2 (r_\Gamma)^2\,\mathcal{I}[1]\,\left[(\mathbf{T}_{s-u}^2)^2 - \tfrac{1}{12}(C_A)^2\right]\frac{i}{2s}\,4\pi\alpha_s\,\hat{\mathcal{M}}_{ij\to ij}^{(0)}. \tag{3.38}$$

**Total to two loops**

Adding the results of eqs. (3.27), (3.28), (3.29) and (3.38) as indicated in eq. (2.48) we get the total contribution to the odd amplitude at one and two loops. Explicitly, expanding the reduced amplitude in powers of $\alpha_s/\pi$ as defined for the complete amplitude in eq. (2.14), we have

$$\hat{\mathcal{M}}^{(-,1)}_{ij\to ij} = \left(D_i^{(1)} + D_j^{(1)}\right)\hat{\mathcal{M}}^{(0)}_{ij\to ij}, \tag{3.39a}$$

$$\hat{\mathcal{M}}^{(-,2)}_{ij\to ij} = \left[D_i^{(2)} + D_j^{(2)} + D_i^{(1)}D_j^{(1)} + \pi^2 R^{(2)}\left((\mathbf{T}^2_{s-u})^2 - \tfrac{1}{12}(C_A)^2\right)\right]\hat{\mathcal{M}}^{(0)}_{ij\to ij}, \tag{3.39b}$$

where we have introduced the function

$$R^{(2)} \equiv -\frac{1}{24}(r_\Gamma)^2\,\mathcal{I}[1] \;=\; -\frac{(r_\Gamma)^2}{6\epsilon^2}\,\frac{B_{1,1+\epsilon}(\epsilon)}{B_{1,1}(\epsilon)} = (r_\Gamma)^2\left(-\frac{1}{8\epsilon^2} + \frac{3}{4}\epsilon\zeta_3 + \frac{9}{8}\epsilon^2\zeta_4 + \dots\right), \tag{3.40}$$

where $B_{\alpha,\beta}(\epsilon)$ is given in eq. (3.32). Here we have factored out $\pi^2$ to emphasize that this term originates as a Regge cut proportional to $(i\pi)^2$. This formula, in particular the fact that $R^{(2)}$ multiplies the nontrivial color factor $(\mathbf{T}^2_{s-u})^2$, is responsible for the breakdown of Regge pole factorization as will be discussed in section 4. The fact that with two unknown impact factors $D_g^{(2)}$, $D_q^{(2)}$, this formula can describe the three processes of gluon-gluon, gluon-quark and quark-quark scattering is highly nontrivial.

### 3.4 Odd amplitude at three loops

The calculation of the three-loop amplitude through NNLL requires the evaluation of the triple, double and single $L$ coefficients in eq. (2.48d).

**$W \to W$ amplitude**

Once again, given eq. (2.49), the contribution of the $1 \to 1$ transition to the reduced amplitude is given by the higher-orders corrections to the impact factors, according to eq. (3.26). This equation does not involve evolution, and therefore at three loops it contributes only at N$^3$LO:

$$\langle\psi_{j,1}|\psi_{i,1}\rangle^{(\mathrm{N^3LO})} = \left(\frac{\alpha_s}{\pi}\right)^3\left(D_i^{(3)} + D_j^{(3)} + D_i^{(2)}D_j^{(1)} + D_i^{(1)}D_j^{(2)}\right)\frac{i}{2s}\,4\pi\alpha_s\,\hat{\mathcal{M}}^{(0)}_{ij\to ij}. \tag{3.41}$$

This is beyond the logarithmic accuracy which is the target of this paper, and therefore we will not consider this contribution further.

**$3W \to 3W$ amplitude**

We start by considering the single logarithmic term originating by applying the diagonal term $H_{k\to k}$ given in (3.13) to the wavefunction $|\psi_{i,3}\rangle$. A major simplification is that only the leading order wavefunction eq. (3.23) is required, whose momentum and color dependence are separately permutation invariant. This allows the sum over pairwise color factors in the Hamiltonian (3.13) to be simplified in terms of the total Casimir in the $t$-channel (a typical graph is shown in fig. 6). After a computation we find

$$\hat{H}_{3\to 3}\,W^a(p_1)W^b(p_2)W^c(p_3)\Big|_{\mathcal{S}^3}$$

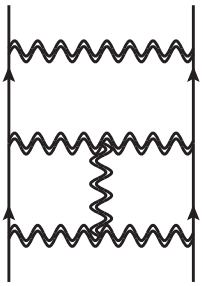

**Figure 6**. Example of a diagram involved in the calculation of the three-Reggeon cut at three loops. This diagram, together with all the other diagrams obtained by inserting a rung in all possible ways between the three Reggeons, and considering all possible permutation of the three Reggeons themselves, arises from the insertion of a single factor of $\hat{H}_{3\to 3}$, as discussed below eq. (3.42).

$$\simeq \frac{\alpha_s r_\Gamma}{2\pi\epsilon}\left[\mathbf{T}_t^2 - 3C_A\left(\frac{p^2}{p_1^2}\right)^\epsilon\right] W^a(p_1)W^b(p_2)W^c(p_3)$$
$$-\alpha_s\left(\mathbf{T}_t^2 - 3C_A\right) S_\epsilon \int [đq] H_{22}(q;p_1,p_2)\, W^a(p_1+q)W^b(p_2-q)W^c(p_3), \qquad (3.42)$$

where $H_{22}$ is the BFKL kernel in eq. (3.15). We emphasize that the simplification of the Hamiltonian is only valid for permutation invariant momentum dependence. Contracting the $W$'s against the target then gives the color factor derived in eq. (3.37), times three propagators, which produce simple two-dimensional integral:

$$\langle\psi_{j,3}|\hat{H}_{3\to 3}|\psi_{i,3}\rangle = \frac{\pi^2}{48}\left(\frac{\alpha_s}{\pi}\right)^3 (r_\Gamma)^3\Big[\mathbf{T}_t^2\,(2\mathcal{I}_b - \mathcal{I}_a - \mathcal{I}_c) + 3C_A\,(\mathcal{I}_c - \mathcal{I}_b)\Big]$$
$$\cdot\left[(\mathbf{T}_{s-u}^2)^2 - \tfrac{1}{12}(C_A)^2\right]\frac{i}{2s}\,4\pi\alpha_s\,\hat{\mathcal{M}}^{(0)}_{ij\to ij}. \qquad (3.43)$$

Here, using the elementary bubble integral in eq. (3.31), we have expressed all integrals in terms of three basic ones:

$$\mathcal{I}_a \equiv \mathcal{I}\left[\frac{1}{\epsilon}\right] = \frac{4}{\epsilon^3}\frac{B_{1,1+\epsilon}(\epsilon)}{B_{1,1}(\epsilon)} = \frac{3}{\epsilon^3} - 18\zeta_3 - 27\epsilon\zeta_4 + \ldots \qquad (3.44a)$$

$$\mathcal{I}_b \equiv \mathcal{I}\left[\frac{1}{\epsilon}\left(\frac{p^2}{p_1^2}\right)^\epsilon\right] = \frac{4}{\epsilon^3}\frac{B_{1+\epsilon,1+\epsilon}(\epsilon)}{B_{1,1}(\epsilon)} = \frac{2}{\epsilon^3} - 44\zeta_3 - 66\epsilon\zeta_4 + \ldots \qquad (3.44b)$$

$$\mathcal{I}_c \equiv \mathcal{I}\left[\frac{1}{\epsilon}\left(\frac{p^2}{(p_1+p_2)^2}\right)^\epsilon\right] = \frac{4}{\epsilon^3}\frac{B_{1,1+2\epsilon}(\epsilon)}{B_{1,1}(\epsilon)} = \frac{8}{3\epsilon^3} - \frac{128}{3}\zeta_3 - 64\epsilon\zeta_4 + \ldots. \qquad (3.44c)$$

While the integrals $\mathcal{I}_{a,b,c}$ are readily available in terms of $B_{\alpha,\beta}(\epsilon)$ of eq. (3.32) to all orders in $\epsilon$, here we chose to display the first few orders in their expansion, which will be used below.

### $3W \to W$ and $W \to 3W$ amplitudes: transition vertices

The next contribution comes from the off-diagonal $1 \to 3$ and $3 \to 1$ terms in the Hamiltonian, given in eqs. (3.16) and (3.18). These produce the color factor (represented by the

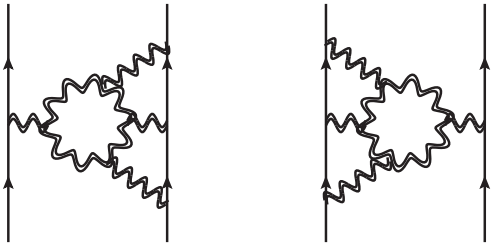

**Figure 7**. Diagrams representing the color structure of the $1 \to 3$ and $3 \to 1$ transitions. Notice that these diagrams are different from the ones representing the kinematical structure of the $1 \to 3$ and $3 \to 1$ transitions, i.e. $H_{13}(p_1, p_2, p_3)$ in eq. (3.17). This is a consequence of the fact that the BFKL evolution derived in section 3.1 represents an effective field theory in $2 - 2\epsilon$ dimensions, in which the longitudinal degrees of freedom have been integrated out.

graphs in fig. 7):

$$C^{(3)}_{13+31} \equiv \frac{1}{6} \sum_{\sigma \in \mathcal{S}^3} \mathrm{Tr}\big[F^a F^{\sigma(b)} F^{\sigma(c)} F^{\sigma(d)}\big] \Big[(T^a_i)_{a_1 a_4} (T^b_j T^c_j T^d_j)_{a_2 a_3} + (T^b_i T^c_i T^d_i)_{a_1 a_4} (T^a_j)_{a_2 a_3}\Big] . \tag{3.45}$$

Multiplying with the propagators according to our master equation (2.48d), and collecting the integrals, this contribution to the reduced amplitude is again written in terms of the same elementary integrals:

$$\langle \psi_{j,3} | \hat{H}_{1\to 3} | \psi_{i,1} \rangle + \langle \psi_{j,1} | \hat{H}_{3\to 1} | \psi_{i,3} \rangle = \frac{i}{12} \left(\frac{\alpha_s}{\pi}\right)^3 \pi^2 \, (r_\Gamma)^3 \Big[2\mathcal{I}_c - \mathcal{I}_a - \mathcal{I}_b\Big] \frac{g^2}{t} \, C^{(3)}_{13+31}. \tag{3.46}$$

The main nontrivial task is to simplify the color factor. Again we would like to obtain a color operator acting on the tree amplitude. This can be achieved by a simple systematic algorithm: move all $f^{abc}$'s onto the external states by using the Jacobi identity:

$$f^{abc} T^c_i = -i[T^a_i, T^b_i]. \tag{3.47}$$

In fact this can be done in multiple distinct ways, since one can applies this on the $i$ or $j$ leg. This makes it possible to arrange to get 4 color generators to act on each of the $i$ and $j$ legs, which then enable to use eq. (3.36) to read off the result in terms of quadratic Casimirs. In fact, we find that for the $1 \to 3$ and $3 \to 1$ transitions separately, the quadratic Casimir operators do not provide a sufficient basis since the nesting for some terms does not allow to extract any generator acting from the outside. However, the obstruction is odd under interchange of $i$ and $j$, and upon adding the two diagrams we do find a compact expression:

$$\begin{aligned} C^{(3)}_{13+31} = \frac{1}{4}\Big(&2\mathbf{T}^2_{s-u}[\mathbf{T}^2_t, \mathbf{T}^2_{s-u}] - [\mathbf{T}^2_t, \mathbf{T}^2_{s-u}]\mathbf{T}^2_{s-u} \\ &- (\mathbf{T}^2_{s-u})^2 C_A - \tfrac{1}{12}(C_A)^3\Big)(T^b_i)_{a_1 a_4} (T^b_j)_{a_2 a_3}, \end{aligned} \tag{3.48}$$

thus leading to

$$\langle \psi_{j,3} | \hat{H}_{1\to 3} | \psi_{i,1} \rangle + \langle \psi_{j,1} | \hat{H}_{3\to 1} | \psi_{i,3} \rangle$$

$$= \frac{\pi^2}{48}\left(\frac{\alpha_s}{\pi}\right)^3 (r_\Gamma)^3\,(2\mathcal{I}_c{-}\mathcal{I}_a{-}\mathcal{I}_b)\Big(2\mathbf{T}^2_{s-u}[\mathbf{T}^2_t,\mathbf{T}^2_{s-u}] - [\mathbf{T}^2_t,\mathbf{T}^2_{s-u}]\mathbf{T}^2_{s-u} - (\mathbf{T}^2_{s-u})^2 C_A - \tfrac{1}{12}(C_A)^3\Big)\frac{i}{2s}\,4\pi\alpha_s\,\hat{\mathcal{M}}^{(0)}_{ij\to ij}. \tag{3.49}$$

Adding the results in eqs. (3.43) and (3.49), and expressing the color operators in a common basis, we get:

$$\begin{aligned}\langle\psi_{j,3}|\hat{H}_{3\to3}|\psi_{i,3}\rangle + \langle\psi_{j,3}|\hat{H}_{1\to3}|\psi_{i,1}\rangle + \langle\psi_{j,1}|\hat{H}_{3\to1}|\psi_{i,3}\rangle \\ = \frac{\pi^2}{48}\left(\frac{\alpha_s}{\pi}\right)^3 (r_\Gamma)^3\Big[3(\mathcal{I}_c{-}\mathcal{I}_a)\,\mathbf{T}^2_{s-u}[\mathbf{T}^2_t,\mathbf{T}^2_{s-u}] + 3(\mathcal{I}_b{-}\mathcal{I}_c)\,[\mathbf{T}^2_t,\mathbf{T}^2_{s-u}]\mathbf{T}^2_{s-u} \\ - \tfrac{1}{6}(2\mathcal{I}_c{-}\mathcal{I}_a{-}\mathcal{I}_b)\,(C_A)^3\Big]\frac{i}{2s}\,4\pi\alpha_s\,\hat{\mathcal{M}}^{(0)}_{ij\to ij}.\end{aligned} \tag{3.50}$$

### 3.5 Result: the three-loop reduced amplitude to NNLL accuracy

To summarize, in this section we used BFKL theory to calculate the signature odd part of the $2 \to 2$ amplitude to NNLL accuracy. The result at one- and two-loop is recorded in eq. (3.39), while the three-loop result is obtained by multiplying the preceding equation with the appropriate minus sign and factor from eq. (2.48):

$$\hat{\mathcal{M}}^{(-,3,1)}_{ij\to ij} = \pi^2\Big(R^{(3)}_A\,\mathbf{T}^2_{s-u}[\mathbf{T}^2_t,\mathbf{T}^2_{s-u}] + R^{(3)}_B\,[\mathbf{T}^2_t,\mathbf{T}^2_{s-u}]\mathbf{T}^2_{s-u} + R^{(3)}_C\,(C_A)^3\Big)\hat{\mathcal{M}}^{(0)}_{ij\to ij}\,, \tag{3.51}$$

where we have introduced the functions

$$\begin{aligned} R^{(3)}_A &= \frac{1}{16}\,(r_\Gamma)^3(\mathcal{I}_a{-}\mathcal{I}_c) = (r_\Gamma)^3\left(\frac{1}{48\epsilon^3} + \frac{37}{24}\zeta_3 + \dots\right), \\ R^{(3)}_B &= \frac{1}{16}\,(r_\Gamma)^3(\mathcal{I}_c{-}\mathcal{I}_b) = (r_\Gamma)^3\left(\frac{1}{24\epsilon^3} + \frac{1}{12}\zeta_3 + \dots\right), \\ R^{(3)}_C &= \frac{1}{288}\,(r_\Gamma)^3(2\mathcal{I}_c{-}\mathcal{I}_a{-}\mathcal{I}_b) = (r_\Gamma)^3\left(\frac{1}{864\epsilon^3} - \frac{35}{432}\zeta_3 + \dots\right). \end{aligned} \tag{3.52}$$

This equation is the main result of this section. The integrals $\mathcal{I}_{a,b,c}$ are defined in eq. (3.44) where they are evaluated, using the bubble integral (3.32), to all orders in $\epsilon$ in terms of $\Gamma$ functions. Here we will be interested in particular in their $\epsilon \to 0$ limit, hence we quote their expansion through finite terms.

We note that all the integrals entering $\hat{\mathcal{M}}^{(-,3,1)}_{ij\to ij}$ in eq. (3.51) are of uniform polylogarithmic weight 3 (as usual in this context, $\epsilon$ is assigned weight $-1$). Given that $\hat{\mathcal{M}}^{(-,3,1)}_{ij\to ij}$ is itself the coefficient of a single (high-energy) logarithm, and taking into account the overall factor of $\pi^2$ in eq. (3.51), we see that the weight adds up to 6, which is the maximal weight at three loops. Such a uniform maximal weight structure is expected in $\mathcal{N} = 4$ SYM theory, while in general not in QCD. However, as we have seen, $\hat{\mathcal{M}}^{(-,3,1)}_{ij\to ij}$ is fully determined by gluon interactions, and therefore entirely independent of the matter contents of the theory. Thus, it is indeed expected that the result, which is valid for any gauge theory, should retain the uniform maximal weight nature characteristic of $\mathcal{N} = 4$ SYM.

We further emphasise that these results are valid for arbitrary projectiles (quarks or gluons) in arbitrary representation of the gauge group; only the impact factors $D_i^{(1)}$ and $D_i^{(2)}$ in eq. (3.39) depend upon this choice. In the next section we discuss our predictions for the amplitude itself, and discuss its nontrivial consistency with infrared exponentiation theorems.

Finally note that the gluon Regge trajectory does not enter the above formulae, because it is subtracted in the definition of the reduced amplitude, eq. (2.26). This definition is also the reason why terms with more logarithms are absent: $\hat{\mathcal{M}}^{(-,1,1)}_{ij\to ij} = \hat{\mathcal{M}}^{(-,2,2)}_{ij\to ij} = \hat{\mathcal{M}}^{(-,3,3)}_{ij\to ij} = 0$ and well as $\hat{\mathcal{M}}^{(-,2,1)}_{ij\to ij} = \hat{\mathcal{M}}^{(-,3,2)}_{ij\to ij} = 0$. The logarithm-free term at three loops, $\hat{\mathcal{M}}^{(-,3,0)}_{ij\to ij}$, is beyond our current NNLL accuracy. The presently known results from BFKL theory in the even sector, which hold to NLL accuracy, have been reviewed in eq. (2.28).

## 4 Comparison between Regge and infrared factorisation

As mentioned in the introduction, the structure of infrared divergences in massless scattering amplitudes is known in full to three-loop order [35]. The prediction for the reduced amplitude presented in the previous section is based solely on evolution equations of the Regge limit, and has taken no input from the theory of infrared divergences. It is therefore a highly nontrivial consistency test that this prediction is consistent with the known exponentiation pattern and the anomalous dimensions governing infrared divergences. Conversely, the prediction of the previous section can also be seen as a constraint on the soft anomalous dimension: the high-energy limit of the latter has a very special structure, which may ultimately help in determining it beyond three loops.

The possibility of performing a systematic comparison between results obtained in the context of Regge theory and the infrared factorisation theorem has been considered in the past [16, 37–40]. Given our calculation of the reduced amplitude up to NNLL within the Regge theory, we are now able to extend this analysis systematically to this logarithmic accuracy. In the following section we exploit this possibility by performing a comparison up to three loops: this will allow us to check consistency with the structure of infrared divergences in the first place; moreover, we will be able to use our result obtained in the context of Regge theory to extract the infrared renormalised amplitudes, i.e. the so-called hard functions, up to three loops.

We start this discussion by reviewing the structure of infrared divergences in the high-energy limit. In particular, the expansion of the quadrupole correction at three loops in this limit has not been presented elsewhere.

### 4.1 Infrared renormalization and the soft anomalous dimension

The infrared divergences of scattering amplitudes are controlled by a renormalization group equation, whose integrated version takes the form

$$\mathcal{M}_n\left(\{p_i\},\mu,\alpha_s(\mu^2)\right) \;=\; \mathbf{Z}_n\left(\{p_i\},\mu,\alpha_s(\mu^2)\right)\mathcal{H}_n\left(\{p_i\},\mu,\alpha_s(\mu^2)\right), \tag{4.1}$$

where $\mathcal{M}_n$ represents now an $n$-point scattering amplitude, and $\mathbf{Z}_n$ is given as a path-ordered exponential of the soft-anomalous dimension:

$$\mathbf{Z}_n\left(\{p_i\},\mu,\alpha_s(\mu^2)\right) \;=\; \mathcal{P}\exp\left\{-\frac{1}{2}\int_0^{\mu^2}\frac{d\lambda^2}{\lambda^2}\,\mathbf{\Gamma}_n\left(\{p_i\},\lambda,\alpha_s(\lambda^2)\right)\right\}, \tag{4.2}$$

where the dependence on the scale is both explicit and via the $4-2\epsilon$ dimensional coupling, which obeys the renormalization group equation

$$\beta(\alpha_s,\epsilon)\equiv\frac{d\alpha_s}{d\ln\mu}=-2\epsilon\,\alpha_s-\frac{\alpha_s^2}{2\pi}\sum_{n=0}^{\infty}b_n\left(\frac{\alpha_s}{\pi}\right)^n, \tag{4.3}$$

with $b_0=\frac{11}{3}C_A-\frac{2}{3}n_f$. The soft anomalous dimension for scattering of massless partons ($p_i^2=0$) is an operator in color space given, through three loops, by [30–32, 35, 65]

$$\mathbf{\Gamma}_n\left(\{p_i\},\lambda,\alpha_s(\lambda^2)\right) \;=\; \mathbf{\Gamma}_n^{\text{dip.}}\left(\{p_i\},\lambda,\alpha_s(\lambda^2)\right)\;+\;\mathbf{\Delta}_n\left(\{\rho_{ijkl}\}\right) \tag{4.4}$$

$$\text{with}\qquad \mathbf{\Gamma}_n^{\text{dip.}}\left(\{p_i\},\lambda,\alpha_s(\lambda^2)\right)=-\frac{\gamma_K(\alpha_s)}{2}\sum_{i<j}\log\left(\frac{-s_{ij}}{\lambda^2}\right)\mathbf{T}_i\cdot\mathbf{T}_j\;+\;\sum_i\gamma_i(\alpha_s)\,,$$

where $\mathbf{\Gamma}_n^{\text{dip.}}$ involves only pairwise interactions amongst the hard partons, and is therefore referred to as the "dipole formula" [30–32, 65], while the term $\mathbf{\Delta}_n\left(\{\rho_{ijkl}\}\right)$ involves interactions of up to four partons, and is called the "quadrupole correction". In eq. (4.4) one defines the kinematic variables $-s_{ij}=2|p_i\cdot p_j|e^{-i\pi\lambda_{ij}}$ with $\lambda_{ij}=1$ if partons $i$ and $j$ both belong to either the initial or the final state and $\lambda_{ij}=0$ otherwise; $\mathbf{T}_i$ represent color change operators [28] in an arbitrary representation, according to the notation introduced in section 2.2. The function $\gamma_K(\alpha_s)$ in eq. (4.4) is the (lightlike) cusp anomalous dimension [19–21], *normalised* by the quadratic Casimir of the corresponding Wilson lines. The universality of $\gamma_K$ (so-called *Casimir scaling*) may be broken at four loops and beyond. Corresponding corrections may be induced in $\mathbf{\Gamma}_n$ in eq. (4.4), but these will not be discussed here, since we restrict explicit computations to three loops. In turn, $\gamma_i(\alpha_s)$ represent the field anomalous dimension corresponding to the parton $i$, which governs hard collinear singularities. The coefficients of both $\gamma_K$ and $\gamma_i$ are known through three loops and are summarized in Appendix A.

The quadrupole correction $\mathbf{\Delta}_n\left(\{\rho_{ijkl}\}\right)$, which appears first at three loops, depends on the cross ratios $\rho_{ijkl}=\frac{(-s_{ij})(-s_{kl})}{(-s_{ik})(-s_{jl})}$, which are invariant under rescaling of any of the momenta. The quadrupole correction is expanded in powers of $\alpha_s/\pi$ as follows:

$$\mathbf{\Delta}_n(\{\rho_{ijkl}\})=\sum_{i=3}^{\infty}\left(\frac{\alpha_s}{\pi}\right)^i\mathbf{\Delta}_n^{(i)}(\{\rho_{ijkl}\}). \tag{4.5}$$

The leading contribution has been computed for the first time only recently [35], and is given by

$$\mathbf{\Delta}_n^{(3)}(\{\rho_{ijkl}\})=\frac{1}{4}f^{abe}f^{cde}\sum_{1\le i<j<k<l\le n}\Big[\mathbf{T}_i^a\mathbf{T}_j^b\mathbf{T}_k^c\mathbf{T}_l^d\,\mathcal{F}(\rho_{ikjl},\rho_{iljk})$$

$$+\mathbf{T}_i^a\mathbf{T}_k^b\mathbf{T}_j^c\mathbf{T}_l^d\,\mathcal{F}(\rho_{ijkl},\rho_{ilkj})+\mathbf{T}_i^a\mathbf{T}_l^b\mathbf{T}_j^c\mathbf{T}_k^d\,\mathcal{F}(\rho_{ijlk},\rho_{iklj})\Big]$$
$$-\frac{C}{4}f^{abe}f^{cde}\sum_{i=1}^{n}\sum_{\substack{1\le j<k\le n,\\ j,k\neq i}}\{\mathbf{T}_i^a,\mathbf{T}_i^d\}\mathbf{T}_j^b\mathbf{T}_k^c, \tag{4.6}$$

where $\mathcal{F}$ is a function of two cross-ratios and $C$ is a constant:

$$\begin{aligned}\mathcal{F}(\rho_{ikjl},\rho_{ilkj}) &= F(1-z_{ijkl})-F(z_{ijkl}),\\ C &= \zeta_5+2\zeta_2\zeta_3,\end{aligned} \tag{4.7}$$

with $z_{ijkl}\,\bar{z}_{ijkl}=\rho_{ijkl}$ and $(1-z_{ijkl})(1-\bar{z}_{ijkl})=\rho_{ilkj}$. In turn one has

$$F(z)=\mathcal{L}_{10101}(z)+2\zeta_2\Big(\mathcal{L}_{001}(z)+\mathcal{L}_{100}(z)\Big), \tag{4.8}$$

where the functions $\mathcal{L}_w(z)$ are Brown's single-valued harmonic polylogarithms [66] (see also [67]) in which $w$ is a word made out of 0's and 1's. The function $F$ implicitly depends on $\bar{z}$ as well, but it is initially defined in the part of the Euclidean region where $\bar{z}=z^*$, where it is single valued. One may then analytically continue the function beyond this region, treating $z$ and $\bar{z}$ as independent variables. It can then be seen that $F$ develops discontinuities, with three branch points for $z$ and $\bar{z}$ equals $\{0,1,\infty\}$ corresponding to forward or backward scattering.

Focusing now on the case of 2 to 2 scattering amplitudes, we restrict the index $n$ in eq. (4.1) above to $n=4$, and drop the index $n$ from now on. The dipole contributions to the anomalous dimension for $2\to 2$ scattering with timelike $s=s_{12}>0$ and spacelike $t=s_{14}<0$ and $u=s_{13}<0$, is

$$\begin{aligned}\mathbf{\Gamma}^{\text{dip.}}\left(\{p\},\lambda,\alpha_s(\lambda^2)\right) = -\frac{\gamma_K(\alpha_s)}{2}\Bigg[&(\mathbf{T}_1\cdot\mathbf{T}_2+\mathbf{T}_3\cdot\mathbf{T}_4)\log\frac{s\,e^{-i\pi}}{\lambda^2}\\ &+(\mathbf{T}_1\cdot\mathbf{T}_3+\mathbf{T}_2\cdot\mathbf{T}_4)\log\frac{-u}{\lambda^2}+(\mathbf{T}_1\cdot\mathbf{T}_4+\mathbf{T}_2\cdot\mathbf{T}_3)\log\frac{-t}{\lambda^2}\Bigg]+\sum_{i=1}^{4}\gamma_i(\alpha_s)\,.\end{aligned} \tag{4.9}$$

In the high-energy limit $u\approx -s$ this expression simplifies significantly. In particular, by expressing it in terms of the color operators introduced in eq. (2.30) one obtains

$$\begin{aligned}\Gamma^{\text{dip.}}\left(\{p_i\},\lambda,\alpha_s(\lambda^2)\right) \xrightarrow{\text{Regge}} \frac{\gamma_K(\alpha_s)}{2}\left[L\,\mathbf{T}_t^2+i\pi\,\mathbf{T}_{s-u}^2+\frac{C_{\text{tot}}}{2}\log\frac{-t}{\lambda^2}\right]\\ +\sum_{i=1}^{4}\gamma_i(\alpha_s)+\mathcal{O}\left(\frac{t}{s}\right),\end{aligned} \tag{4.10}$$

where $L=\log\left|\frac{s}{t}\right|-i\frac{\pi}{2}$ is the natural signature-even combination of logarithms introduced in eq. (2.7).

Obtaining $\mathbf{\Delta}^{(3)}$ in the high-energy limit requires some more work [35, 68]. This function is initially defined in Euclidean kinematics where the invariants are all spacelike, and the momenta of the colored partons $p_i$ are not required to admit momentum conservation. One

therefore needs to first analytically continue the functions $\mathcal{F}$ in eq. (4.6) across the cut to the region where $p_1$ and $p_2$ are incoming while $p_3$ and $p_4$ outgoing. Once this is done, one imposes the momentum conserving limit where one identifies $s = s_{12} = s_{34} > 0$ and $t = s_{14} = s_{23} < 0$, and the variables $z$ and $\bar{z}$ approach the real axis from opposite sides and coincide, such that $z, \bar{z} \to s/(s+t)$. At the final stage one takes the high-energy limit where $s \gg -t$. Details of these calculations will be presented elsewhere. One obtains

$$\begin{aligned}\mathbf{\Delta}^{(3)} = i\pi\,[\mathbf{T}_t^2,[\mathbf{T}_t^2,\mathbf{T}_{s-u}^2]]\frac{1}{4}\Big[\zeta_3 L + 11\zeta_4\Big] + \frac{1}{4}[\mathbf{T}_{s-u}^2,[\mathbf{T}_t^2,\mathbf{T}_{s-u}^2]]\Big[\zeta_5 - 4\zeta_2\zeta_3\Big] \\ -\frac{\zeta_5+2\zeta_2\zeta_3}{8}\Big\{f^{abe}f^{cde}\Big[\{\mathbf{T}_t^a,\mathbf{T}_t^d\}\Big(\{\mathbf{T}_{s-u}^b,\mathbf{T}_{s-u}^c\}+\{\mathbf{T}_{s+u}^b,\mathbf{T}_{s+u}^c\}\Big) \\ +\{\mathbf{T}_{s-u}^a,\mathbf{T}_{s-u}^d\}\{\mathbf{T}_{s+u}^b,\mathbf{T}_{s+u}^c\}\Big] - \frac{5}{8}C_A^2\mathbf{T}_t^2\Big\},\end{aligned} \tag{4.11}$$

where we introduced the color operators

$$\mathbf{T}_{s-u}^a \equiv \tfrac{1}{\sqrt{2}}\left(\mathbf{T}_s^a - \mathbf{T}_u^a\right), \qquad \mathbf{T}_{s+u}^a \equiv \tfrac{1}{\sqrt{2}}\left(\mathbf{T}_s^a + \mathbf{T}_u^a\right). \tag{4.12}$$

Note that the second and third lines in (4.11) correspond to the kinematics-independent term $C$ in the quadrupole correction of eq. (4.6); it appears that it cannot be written in terms of quadratic invariants. The symmetry properties of (4.11) under $s$ to $u$ exchange, are nevertheless clear, and as expected (recall that the hard function on which this operator will act is color odd) the imaginary part is color odd while the real part is color even. We observe that this expression contains only a single factor of $L$, with an imaginary coefficient. Therefore the quadrupole contribution to the even amplitude $\mathcal{M}^{(+)}$ starts at NNLL while for the odd amplitude $\mathcal{M}^{(-)}$ it starts only at N$^3$LL. The evaluation of the color operator in the second and third line of eq. (4.11) in an explicit color basis is provided in the appendices. More specifically, in appendix B we provide it in an orthonormal color basis in the $t$-channel, while in appendix C we give it in a "trace" color basis.

The anomalous dimension would be straightforward to exponentiate according to eq. (4.2), were it not for the fact that $\mathbf{T}_t^2$, $\mathbf{T}_{s-u}^2$ and the color operators in $\mathbf{\Delta}^{(3)}$ do not commute. This non-commutativity by itself implies that the amplitude projected on the tree-level color factor cannot be written as a simple power law, that is, it cannot be interpreted as exchange of a single Reggeized gluon [16, 38], as discussed in section 2.2.

The last two terms in the dipole formula Eq. (4.10) do not depend on colors nor or the total energy $s$, which suggests to attribute them to the projectile and target separately and write $Z$ factor in eq. (4.2) in the following factorized form:

$$\mathbf{Z}\left(\{p_i\},\mu,\alpha_s(\mu^2)\right) = \tilde{\mathbf{Z}}\left(\frac{s}{t},\mu,\alpha_s(\mu^2)\right) Z_i\left(t,\mu,\alpha_s(\mu^2)\right) Z_j\left(t,\mu,\alpha_s(\mu^2)\right), \tag{4.13}$$

where the $Z_{i/j}$ are just scalar factors that depend only on either the projectile or target:

$$Z_i = \exp\left\{-\int_0^{\mu^2}\frac{d\lambda^2}{\lambda^2}\left[\frac{\gamma_K\left(\alpha_s(\lambda^2)\right)}{4}C_i\,\log\frac{-t}{\lambda^2} + \gamma_i\left(\alpha_s(\lambda^2)\right)\right]\right\}. \tag{4.14}$$

The more interesting factor is $\tilde{\mathbf{Z}}$ which is a color operator given to three-loop accuracy as:

$$\tilde{\mathbf{Z}}\left(\frac{s}{t},\mu,\alpha_s(\mu^2)\right)=\exp\left\{K\left(\alpha_s(\mu^2)\right)\left[L\,\mathbf{T}_t^2+i\pi\,\mathbf{T}_{s-u}^2\right]+Q_{\mathbf{\Delta}}^{(3)}\right\} \tag{4.15}$$

with $K\left(\alpha_s(\mu^2)\right)$ defined as the integral over the cusp anomalous dimension:

$$K\left(\alpha_s(\mu^2)\right)=-\frac{1}{4}\int_0^{\mu^2}\frac{d\lambda^2}{\lambda^2}\,\gamma_K\left(\alpha_s(\lambda^2)\right)\;=\;\frac{1}{2\epsilon}\,\frac{\alpha_s(\mu^2)}{\pi}+\dots, \tag{4.16}$$

while $Q_{\mathbf{\Delta}}^{(3)}$ represent the contribution of the quadrupole correction at three loops,

$$Q_{\mathbf{\Delta}}^{(3)}=-\frac{\mathbf{\Delta}^{(3)}}{2}\int_0^{\mu^2}\frac{d\lambda^2}{\lambda^2}\left(\frac{\alpha_s(\lambda^2)}{\pi}\right)^3=\frac{\mathbf{\Delta}^{(3)}}{6\epsilon}\left(\frac{\alpha_s(\mu^2)}{\pi}\right)^3. \tag{4.17}$$

The extra logarithm of $\lambda$ in the integration in eq. (4.14) is responsible for double poles combining infrared and collinear singularities. Thus we see that all double poles are included in the factors $Z_{i/j}$, while the factor $K$ (and consequently $\tilde{\mathbf{Z}}$) contains at most a single infrared pole per loop order. To three loops one has

$$\begin{aligned}K(\alpha_s)=\frac{\alpha_s}{\pi}\,\frac{\gamma_K^{(1)}}{4\epsilon}+\left(\frac{\alpha_s}{\pi}\right)^2\left(\frac{\gamma_K^{(2)}}{8\epsilon}-\frac{b_0\,\gamma_K^{(1)}}{32\epsilon^2}\right),\\ +\left(\frac{\alpha_s}{\pi}\right)^3\left(\frac{\gamma_K^{(3)}}{12\epsilon}-\frac{b_0\,\gamma_K^{(2)}+b_1\,\gamma_K^{(1)}}{48\epsilon^2}+\frac{b_0^2\,\gamma_K^{(1)}}{192\epsilon^3}\right)+\mathcal{O}(\alpha_s^4)\end{aligned} \tag{4.18}$$

where explicit expressions for the $\alpha_s$ expansion of the cusp anomalous dimensions $\gamma_K$, as well as the quark and gluon anomalous dimension $\gamma_i$ and the scalar factor $Z_{i/j}$ are provided in appendix A.

The scalar factors $Z_i$ removed in eq. (4.13) are the same as those we removed from the reduced amplitude eq. (2.26) in the BFKL context, and in fact, at leading log accuracy the exponent of eq. (4.15) is also very similar to the gluon Regge trajectory subtracted in the reduced amplitude. This makes the relation between the "infrared-renormalized" amplitude (hard function) $\mathcal{H}_{ij\to ij}$ and reduced matrix element particularly simple. Comparing eq. (4.1) with eq. (2.26) and using eqs. (4.13) and (4.15), we indeed find

$$\begin{aligned}\mathcal{H}_{ij\to ij}\left(\{p_i\},\mu,\alpha_s(\mu^2)\right)\;=\;&\exp^{-1}\left\{K\left(\alpha_s(\mu^2)\right)\left[L\,\mathbf{T}_t^2+i\pi\,\mathbf{T}_{s-u}^2\right]+Q_{\mathbf{\Delta}}^{(3)}\right\}\\ &\cdot\exp\left\{\alpha_g(t)L\,\mathbf{T}_t^2\right\}\hat{\mathcal{M}}_{ij\to ij}\left(\{p_i\},\mu,\alpha_s(\mu^2)\right).\end{aligned} \tag{4.19}$$

This equation allows us to pass from directly from the reduced amplitude $\hat{\mathcal{M}}_{ij\to ij}$, predicted in the previous section using BFKL theory, to the more conventional scattering amplitude or hard function. In particular, the statement that the left-hand-side $\mathcal{H}_{ij\to ij}$ is finite, which is equivalent to the exponentiation of infrared divergences, is a highly nontrivial constraint on our result.

### 4.2 Expansion of the hard amplitude

Similarly to eq. (2.14), we introduce a power expansion for the hard function:

$$\mathcal{H}_{ij\to ij}\left(\{p_i\},\mu,\alpha_s(\mu^2)\right) = 4\pi\alpha_s \sum_{n=0}^{\infty}\sum_{k=0}^{n}\left(\frac{\alpha_s}{\pi}\right)^n L^k\,\mathcal{H}^{(n,k)}\left(\frac{-t}{\mu^2}\right). \tag{4.20}$$

In the rest of this section we derive the coefficients $\mathcal{H}^{(n,k)}$ order by order in perturbation theory, applying eq. (4.19) to the results of the preceding section. The color factors in the exponent do not commute, but the formula can be expanded in perturbation theory by repeatedly applying the Baker-Campbell-Hausdorff formula. Up to three loops we find explicitly:

$$\begin{aligned}\mathcal{H}_{ij\to ij}\left(\{p_i\},\mu,\alpha_s(\mu^2)\right) = &\left(1+\tfrac{K^3(\alpha_s)}{3!}\Big(2\pi^2\,L\,[\mathbf{T}^2_{s-u},[\mathbf{T}^2_t,\mathbf{T}^2_{s-u}]] - i\,\pi L^2\,[\mathbf{T}^2_t,[\mathbf{T}^2_t,\mathbf{T}^2_{s-u}]]\Big)\right.\\ &\left.+i\pi\tfrac{K^2(\alpha_s)}{2}L\,[\mathbf{T}^2_t,\mathbf{T}^2_{s-u}] - Q^{(3)}_{\mathbf{\Delta}}\right)\cdot\exp\Big\{-i\pi\,K(\alpha_s)\,\mathbf{T}^2_{s-u}\Big\}\\ &\cdot\exp\Big\{\Big(\alpha_g(t)-K(\alpha_s)\Big)\,L\,\mathbf{T}^2_t\Big\}\,\hat{\mathcal{M}}_{ij\to ij}\left(\{p_i\},\mu,\alpha_s(\mu^2)\right).\end{aligned} \tag{4.21}$$

Notice that we have combined the exponent containing the Regge trajectory with the $\mathbf{T}^2_t$ term in the infrared factorisation formula, since they have the same color structure. Because of the structure of this exponent, the combination $\alpha_g(t)-K(\alpha_s)$ frequently appears in the following. For this reason, it proves useful to introduce the short-hand notation

$$\hat{\alpha}_g(t) = \alpha_g(t) - K(\alpha_s), \tag{4.22}$$

to indicate the "finite" Regge trajectory divided by $N_c$. Expanding in the coupling, we write

$$\hat{\alpha}_g(t) = \hat{\alpha}_g^{(n)}\left(\frac{\alpha_s(-t)}{\pi}\right)^n. \tag{4.23}$$

The fact that the combination entering the hard function is the difference between the Regge trajectory and $K(\alpha_s)$ is a manifestation of the relation between the divergent part of the gluon Regge trajectory and the cusp anomalous dimension discovered in Refs. [9, 10]. Below we will see that this relation breaks down by the Regge cut, and in our scheme $\hat{\alpha}_g(t)$ will not be finite at three loops.

At one- and two-loops, using the known trajectory in eq. (A.6) and cusp anomalous dimension in eq. (A.2) we get $\hat{\alpha}_g(t)$ with

$$\hat{\alpha}_g^{(1)} = \frac{1}{2\epsilon}(r_\Gamma - 1) = -\frac{1}{4}\zeta_2\,\epsilon - \frac{7}{6}\zeta_3\,\epsilon^2 + \mathcal{O}(\epsilon^3), \tag{4.24a}$$

$$\hat{\alpha}_g^{(2)} = C_A\left(\frac{101}{108} - \frac{\zeta_3}{8}\right) - \frac{7n_f}{54} + O(\epsilon)\,. \tag{4.24b}$$

This is nicely infrared finite. The first term would in fact vanish if we worked in a scheme where the coupling is $\alpha_s r_\Gamma$ instead of $\alpha_s$, which would simplify many of our predictions.

However, to simplify comparisons with the literature, we will stick with the standard $\overline{\text{MS}}$ coupling $\alpha_s$.

At leading logarithmic accuracy, and to any order in the coupling, only the rightmost exponential factor in (4.21) is relevant, and we obtain

$$\mathcal{H}^{(n,n)}_{ij\to ij} = \frac{1}{n!}\left(\hat{\alpha}_g^{(1)}\right)^n \left(\mathbf{T}_t^2\right)^n \hat{\mathcal{M}}^{(0)}_{ij\to ij}, \tag{4.25}$$

which is of course finite. At NLL accuracy and beyond the expansion of (4.21) requires input with regards to the coefficients of $\hat{\mathcal{M}}_{ij\to ij}$. The computation is significantly simplified here by working with the reduced amplitude, whose leading logarithms $\hat{\mathcal{M}}^{(n,n)}_{ij\to ij}$ vanish, and whose next-to-leading logarithms beyond one loop are purely imaginary and are given by eq. (2.28) above (the real part of $\hat{\mathcal{M}}^{(n,n-1)}_{ij\to ij}$ for $n \geq 2$ vanishes by construction). Next-to-next-to-leading logarithms in the real part of $\hat{\mathcal{M}}_{ij\to ij}$ are determined by the BFKL analysis of the previous section.

An important feature visible in eq. (4.21) is that the conversion to hard function does not commute with the projection onto even and odd signatures. Specifically, the odd part of the hard function at NNLL receives some contamination from the even reduced amplitude at NLL, multiplied by $i\pi K(\alpha_s)\mathbf{T}^2_{s-u}$ or $i\pi\frac{K^2(\alpha_s)}{2}[\mathbf{T}_t^2, \mathbf{T}^2_{s-u}]$. This is not going to pose a problem, because these ingredients are already known.

Our comparison between Regge and infrared factorization below follows closely the analysis in [40] (see also [16]). Nevertheless, there are several new elements allowing us to make a significant step forward: first, our present analysis makes a clear and transparent separation between signature odd and even, corresponding respectively to real and imaginary parts of the amplitude expressed in terms of $L \equiv \log\left|\frac{s}{t}\right| - i\frac{\pi}{2}$; second is the possibility to compare the infrared factorisation formula with the contribution originating from three Reggeon exchange at two and three loops, which we have calculated here for the first time; third is the availability of the complete infrared structure at three loops, i.e. eq. (4.11) based on [35, 68], which implies, in particular, that the odd amplitude receives no new NNLL high-energy corrections beyond the dipole formula through three loops, while the even amplitude does; a final new ingredient is the availability of the $\mathcal{N} = 4$ SYM result for $2 \to 2$ gluon-gluon scattering amplitude [41], which beyond consistency checks, also provides new information on the odd amplitude at NNLL: together with the computation of the three-Reggeon cut performed here, it allows us to fix the three-loop gluon Regge trajectory in this theory.

### 4.3 Comparison at one loop

At tree level one has $\mathcal{H}^{(0)} = \hat{\mathcal{M}}^{(0)} = \mathcal{M}^{(0)}$. Comparison at one loop is simple, and completely equivalent to the discussion in [16, 40]. We repeat it here in order to adapt it to the conventions used in this paper, in particular, the fact that we expand the amplitude in powers of $L = \log|s/t| - i\pi/2$ instead of powers of $\log|s/t|$.

Expanding eq. (4.21) to one loop, and suppressing the indices $ij \to ij$ for brevity, we get

$$\mathcal{H}^{(1,1)} = \hat{\alpha}_g^{(1)}\,\mathbf{T}_t^2\,\hat{\mathcal{M}}^{(0)}, \tag{4.26a}$$

$$\mathcal{H}^{(1,0)} = \hat{\mathcal{M}}^{(1,0)} - i\pi\, K^{(1)}\, \mathbf{T}^2_{s-u}\, \hat{\mathcal{M}}^{(0)}. \tag{4.26b}$$

As anticipated (see the discussion regarding eq. (4.22)) the fact that the hard function must be finite relates to the connection between the divergent part of $\alpha_g^{(1)}$ and the cusp anomalous dimension [9, 10]. The vanishing of $\hat{\alpha}_g^{(1)}$ in the four-dimensional limit, as shown in eq. (4.24a), reflects the fact that gluon Reggeisation at this order is determined entirely by soft corrections, hence no high-energy logarithms arise in the hard function at one loop in the $\epsilon \to 0$ limit.

The finite part in eq. (4.26b) contains informations both its in real and imaginary parts. Using the direct correspondence between the real and imaginary parts of the amplitude, respectively, and its odd and even signature parts, we get

$$\mathrm{Re}[\mathcal{H}^{(1,0)}] = \hat{\mathcal{M}}^{(-,1,0)}, \tag{4.27a}$$

$$i\,\mathrm{Im}[\mathcal{H}^{(1,0)}] = \hat{\mathcal{M}}^{(+,1,0)} - i\pi\, K^{(1)}\, \mathbf{T}^2_{s-u}\, \hat{\mathcal{M}}^{(0)}. \tag{4.27b}$$

Using the results for $\hat{\mathcal{M}}^{(-,1,0)}$ and $\hat{\mathcal{M}}^{(+,1,0)}$ in eqs. (3.39a) and (2.28) one explicitly gets

$$\mathrm{Re}[\mathcal{H}^{(1,0)}] = \left(D_i^{(1)} + D_j^{(1)}\right) \hat{\mathcal{M}}^{(0)}, \tag{4.28a}$$

$$i\,\mathrm{Im}[\mathcal{H}^{(1,0)}] = i\pi \left(\mathbb{d}_1 - K^{(1)}\right) \mathbf{T}^2_{s-u}\, \hat{\mathcal{M}}^{(0)} \;=\; i\pi\, \hat{\alpha}_g^{(1)}\, \mathbf{T}^2_{s-u}\, \hat{\mathcal{M}}^{(0)}\,, \tag{4.28b}$$

where $\mathbb{d}_1 = \frac{r_\Gamma}{2\epsilon}$ is the one-loop coefficient in eq. (2.29); in the last expression in eq. (4.28b) we used (4.24) to replace the difference of divergent coefficients $\mathbb{d}_1 - K^{(1)}$ by the $\mathcal{O}(\epsilon)$ coefficient $\hat{\alpha}_g^{(1)}$. This replacement will be used in what follows to obtain simpler expressions at higher orders.

Infrared factorization tells us that both of the equations in eq. (4.28) are finite as $\epsilon \to 0$. This is evidently satisfied for the imaginary part, eq. (4.28b). Finiteness of the real part in eq. (4.28a) in turn implies that the impact factors $D_i$ must also be finite – indeed they are, as we have already extracted the divergences into the factors $Z_i$ of eq. (4.14) (see eq. (2.21)). A systematic way to extract these, which will work to higher orders as well, is to consider the fixed-order hard functions projected onto the color octet (see e.g. eq. (2.24)). Then we have simply

$$D_i^{(1)} = \frac{1}{2}\, \frac{\mathrm{Re}[\mathcal{H}^{(1,0)[8_a]}_{ii\to ii}]}{\mathcal{H}^{(0)[8_a]}_{ii\to ii}}. \tag{4.29}$$

Explicitly, using the one-loop gluon-gluon and quark-quark octet hard function from Ref. [40], converting to the convention where the amplitude is expanded in powers of $L = \log|s/t| - i\pi/2$ instead of powers of $\log|s/t|$, we extract the results for the one-loop impact factors, which are indeed finite:

$$\begin{aligned} D_g^{(1)} = &-N_c\left(\frac{67}{72} - \zeta_2\right) + \frac{5}{36} n_f + \epsilon\left[N_c\left(-\frac{101}{54} + \frac{11}{48}\zeta_2 + \frac{17}{12}\zeta_3\right) + n_f\left(\frac{7}{27} - \frac{\zeta_2}{24}\right)\right] \\ &+ \epsilon^2\left[N_c\left(-\frac{607}{162} + \frac{67}{144}\zeta_2 + \frac{77}{72}\zeta_3 + \frac{41}{32}\zeta_4\right) + n_f\left(\frac{41}{81} - \frac{5}{72}\zeta_2 - \frac{7}{36}\zeta_3\right)\right] + \mathcal{O}(\epsilon^3)\,, \end{aligned} \tag{4.30a}$$

$$D_q^{(1)} = N_c\left(\frac{13}{72}+\frac{7}{8}\zeta_2\right)+\frac{1}{N_c}\left(1-\frac{1}{8}\zeta_2\right)-\frac{5}{36}n_f+\epsilon\Bigg[N_c\left(\frac{10}{27}-\frac{\zeta_2}{24}+\frac{5}{6}\zeta_3\right)$$
$$+\frac{1}{N_c}\left(2-\frac{3}{16}\zeta_2-\frac{7}{12}\zeta_3\right)+n_f\left(-\frac{7}{27}+\frac{\zeta_2}{24}\right)\Bigg]+\epsilon^2\Bigg[N_c\left(\frac{121}{162}-\frac{13}{144}\zeta_2-\frac{7}{36}\zeta_3+\frac{35}{64}\zeta_4\right)$$
$$+\frac{1}{N_c}\left(4-\frac{\zeta_2}{2}-\frac{7}{8}\zeta_3-\frac{47}{64}\zeta_4\right)+n_f\left(-\frac{41}{81}+\frac{5}{72}\zeta_2+\frac{7}{36}\zeta_3\right)\Bigg]+\mathcal{O}(\epsilon^3)\,. \tag{4.30b}$$

Note that, with these two coefficients extracted, the quark-gluon amplitude is then predicted unambiguously and correctly, as explicitly shown in Ref. [40] (see eq. (4.17) there).

### 4.4 Comparison at two loops

At two-loops, the expansion of eq. (4.21) gives

$$\mathcal{H}^{(2,2)} = \frac{1}{2}(\hat{\alpha}_g^{(1)})^2(\mathbf{T}_t^2)^2\,\hat{\mathcal{M}}^{(0)}, \tag{4.31a}$$
$$\mathcal{H}^{(2,1)} = \hat{\mathcal{M}}^{(2,1)}+\hat{\alpha}_g^{(1)}\mathbf{T}_t^2\,\hat{\mathcal{M}}^{(1,0)}+\hat{\alpha}_g^{(2)}\mathbf{T}_t^2\,\hat{\mathcal{M}}^{(0)}$$
$$+\,i\pi K^{(1)}\Big[\tfrac{1}{2}K^{(1)}[\mathbf{T}_t^2,\mathbf{T}_{s-u}^2]-\hat{\alpha}_g^{(1)}\mathbf{T}_{s-u}^2\mathbf{T}_t^2\Big]\hat{\mathcal{M}}^{(0)}, \tag{4.31b}$$
$$\mathcal{H}^{(2,0)} = \hat{\mathcal{M}}^{(2,0)}-\frac{\pi^2}{2}(K^{(1)})^2(\mathbf{T}_{s-u}^2)^2\hat{\mathcal{M}}^{(0)}-i\pi\left[K^{(2)}\mathbf{T}_{s-u}^2\hat{\mathcal{M}}^{(0)}+K^{(1)}\mathbf{T}_{s-u}^2\hat{\mathcal{M}}^{(1,0)}\right]. \tag{4.31c}$$

Note that the leading-log term of eq. (4.31a) is a simple exponentiation of eq. (4.26a). More interesting are the lower-logarithmic terms of the amplitude. Using explicitly the information for $\hat{\mathcal{M}}^{(1,0)}$ and $\hat{\mathcal{M}}^{(2,1)}$ in eq. (2.27), (2.28) and (3.39b) we obtain

$$\mathrm{Re}[\mathcal{H}^{(2,1)}] = \left[\hat{\alpha}_g^{(2)}+\hat{\alpha}_g^{(1)}\left(D_i^{(1)}+D_j^{(1)}\right)\right]\mathbf{T}_t^2\,\hat{\mathcal{M}}^{(0)}, \tag{4.32a}$$
$$i\,\mathrm{Im}[\mathcal{H}^{(2,1)}] = i\pi\left[\left(\tfrac{1}{2}\mathbb{d}_2+\tfrac{1}{2}(K^{(1)})^2+K^{(1)}\hat{\alpha}_g^{(1)}\right)[\mathbf{T}_t^2,\mathbf{T}_{s-u}^2]+\left(\hat{\alpha}_g^{(1)}\right)^2\mathbf{T}_t^2\mathbf{T}_{s-u}^2\right]\hat{\mathcal{M}}^{(0)}. \tag{4.32b}$$

Finiteness of the first line is manifest, and finiteness of the second line is a constraint on the divergent part of $\mathbb{d}_2$, which again is satisfied by the explicit expression in eq. (2.29) (with $K^{(1)}=1/(2\epsilon)$, see eq. (4.18)); this was also verified in Ref. [16].

Considering finally the coefficient of the zero-th order logarithm, i.e. eq. (4.31c), the operator $\left(\mathbf{T}_{s-u}^2\right)^2$ makes its first appearance. We focus on the odd component, i.e. $\hat{\mathcal{M}}^{(-,2,0)}$, which we have calculated in eq. (3.39b). Inserting this result along with the previous result for the one-loop even amplitude we obtain

$$\mathrm{Re}[\mathcal{H}^{(2,0)}] = \Big[D_i^{(2)}+D_j^{(2)}+D_i^{(1)}D_j^{(1)}-\pi^2R^{(2)}\tfrac{1}{12}(C_A)^2$$
$$+\pi^2\left(R^{(2)}+\tfrac{1}{2}(K^{(1)})^2+K^{(1)}\hat{\alpha}_g^{(1)}\right)(\mathbf{T}_{s-u}^2)^2\Big]\hat{\mathcal{M}}^{(0)}. \tag{4.33}$$

It is clear at this point that the term proportional to $(\mathbf{T}_{s-u}^2)^2$ in the infrared factorisation formula can be attributed to multi-Reggeon exchange, and this is confirmed by the fact

that the quantity in squared brackets in eq. (4.33) proportional to $(\mathbf{T}^2_{s-u})^2$ is finite. Upon explicit substitution of $R^{(2)}$ in eq. (3.40), we get

$$\hat{R}^{(2)} \equiv R^{(2)} + \tfrac{1}{2}(K^{(1)})^2 + K^{(1)}\hat{\alpha}_g^{(1)} = \frac{3}{4}\epsilon\zeta_3 + \frac{67}{64}\epsilon^2\zeta_4 + \dots \tag{4.34}$$

which is indeed finite, as required for the infrared renormalized amplitude $\mathrm{Re}[\mathcal{H}^{(2,0)}]$.

This equation can thus be used to extract the impact factors at two loops from the known two-loop fixed-order amplitudes. As before, it suffices to consider the projection of the amplitude onto the adjoint channel, but the projection of the color factor $(\mathbf{T}^2_{s-u})^2$ needs to be carried out on a case-by-case basis. This can be done using the matrices given in appendix B. For gluon-gluon scattering with $\mathrm{SU}(N_c)$ gauge group, we get:

$$2D_g^{(2)} = \frac{\mathcal{H}^{(2,0)[8_a]}_{gg\to gg}}{\mathcal{H}^{(0)[8_a]}_{gg\to gg}} - (D_g^{(1)})^2 + \pi^2 R^{(2)}\frac{N_c^2}{12} - \pi^2\hat{R}^{(2)}\frac{N_c^2+24}{4}, \tag{4.35}$$

where in turn $D_g^{(1)}$ can be found in eq. (4.30a). The impact factor $D_g^{(2)}$ would be finite, were it not for the double pole originating from the $R^{(2)} \approx -\frac{1}{8\epsilon^2}$ term. For quark-gluon scattering we find:

$$D_q^{(2)} + D_g^{(2)} = \frac{\mathcal{H}^{(2,0)[8_a]}_{qg\to qg}}{\mathcal{H}^{(0)[8_a]}_{qg\to qg}} - D_q^{(1)}D_g^{(1)} + \pi^2 R^{(2)}\frac{N_c^2}{12} - \pi^2\hat{R}^{(2)}\frac{N_c^2+4}{4}\,. \tag{4.36}$$

Finally, for quark-quark scattering, we find instead:

$$2D_q^{(2)} = \frac{\mathrm{Re}[\mathcal{H}^{(2,0)[8_a]}_{qq\to qq}]}{\mathcal{H}^{(0)[8_a]}_{qq\to qq}} - (D_q^{(1)})^2 + \pi^2 R^{(2)}\frac{N_c^2}{12} - \pi^2\hat{R}^{(2)}\frac{N_c^4-4N_c^2+12}{4N_c^2}. \tag{4.37}$$

The important thing to notice is that the coefficient of the $\hat{R}^{(2)}$ term, which represents the color structure $(\mathbf{T}^2_{s-u})^2$ attributed to three-Reggeon exchange, is different in each case. This contribution (in addition to the extra factors of $(\mathbf{T}^2_{s-u})^2$ coming from the infrared renormalization) explains why the amplitude does not take a simple factorized form, as was first observed in ref. [44] based on explicit computations of two-loop amplitudes for gluon-gluon, quark-gluon and quark-quark scattering (for the departure from simple Regge-pole factorization see also [16, 37–40]). Quantitatively, it is a highly nontrivial check on the BFKL formalism that the three equations (4.35) through (4.37) can be solved for the two unknowns $D_g^{(2)}$ and $D_q^{(2)}$. By using the explicit result for the two-loop gluon-gluon and quark-quark hard functions $\mathcal{H}^{(2,0)[8_a]}_{ij\to ij}$ provided in Ref. [40], and expanding them in powers of $L = \log|s/t| - i\pi/2$ we find:

$$\begin{aligned} D_g^{(2)} = &-\frac{\zeta_2}{32\epsilon^2}N_c^2 + N_c^2\left(-\frac{26675}{10368} + \frac{335}{288}\zeta_2 + \frac{11}{18}\zeta_3 - \frac{\zeta_4}{64}\right) \\ &+ N_c n_f\left(\frac{2063}{3456} - \frac{25}{144}\zeta_2 + \frac{\zeta_3}{72}\right) + \frac{n_f}{N_c}\left(-\frac{55}{384} + \frac{\zeta_3}{8}\right) - \frac{25}{2592}n_f^2 + \mathcal{O}(\epsilon)\,, \end{aligned} \tag{4.38a}$$

$$D_q^{(2)} = -\frac{\zeta_2}{32\epsilon^2}N_c^2 + N_c^2\left(\frac{22537}{41472} + \frac{87}{64}\zeta_2 + \frac{41}{144}\zeta_3 - \frac{15}{256}\zeta_4\right) + \frac{28787}{10368} + \frac{19}{32}\zeta_2$$
$$- \frac{205}{288}\zeta_3 - \frac{47}{128}\zeta_4 + \frac{1}{N_c^2}\left(\frac{255}{512} + \frac{21}{64}\zeta_2 - \frac{15}{32}\zeta_3 - \frac{83}{256}\zeta_4\right)$$
$$+ N_c n_f\left(-\frac{325}{648} - \frac{\zeta_2}{4} - \frac{23}{144}\zeta_3\right) + \frac{n_f}{N_c}\left(-\frac{505}{1296} - \frac{\zeta_2}{16} - \frac{19}{144}\zeta_3\right) + \frac{25}{864}n_f^2 + \mathcal{O}(\epsilon)\,. \tag{4.38b}$$

Remarkably, these impact factors then correctly predict the quark-gluon amplitude according to eq. (4.36), as it should!

Finally, we comment on the infrared divergences in $D_i^{(2)}$, which contrast with the finite $D_i^{(1)}$. We believe one should not be overly concerned about this, because of the arbitrary basis choice in eq. (2.44) which has forced the physics into a very specific basis, where one- and three-Reggeon states are orthogonal to each other, therefore removing $1 \to 3$ and $3 \to 1$ correlators of Wilson lines. In practice, the color factors $\sim (C_A)^2$ of such correlators would not be distinguishable from single-Reggeon exchange at this order. It seems plausible that, in a more natural basis, the infrared divergences would appear only in these off-diagonal contributions rather than being pushed into the $1 \to 1$ single-Reggeon transition, thus leaving finite impact factors which may be closer to the ones defined empirically in Ref. [40]. We leave this for future investigation: since the choice used in this paper corresponds to a well-defined basis, it should always be possible to convert the result to other schemes.

### 4.5 Comparison at three loops

Let us now turn to the comparison between the BFKL results and infrared factorization at three loops. Because the expressions are rather lengthy, we will discuss the various logarithmic orders in turn. At leading logarithmic accuracy the expansion of the infrared factorisation formula in eq. (4.21) gives

$$\mathcal{H}^{(3,3)} = \frac{1}{6}\left(\hat{\alpha}_g^{(1)}\right)^3 \left(\mathbf{T}_t^2\right)^3 \hat{\mathcal{M}}^{(0)}, \tag{4.39}$$

as anticipated in eq. (4.25). At next-to-leading logarithmic accuracy, the infrared factorisation in formula in eq. (4.21) gives

$$\begin{aligned}\mathcal{H}^{(3,2)} = {} & \hat{\mathcal{M}}^{(3,2)} + \hat{\alpha}_g^{(1)}\,\mathbf{T}_t^2\,\hat{\mathcal{M}}^{(2,1)} + \tfrac{1}{2}(\hat{\alpha}_g^{(1)})^2(\mathbf{T}_t^2)^2\hat{\mathcal{M}}^{(1,0)} + \hat{\alpha}_g^{(1)}\hat{\alpha}_g^{(2)}\,(\mathbf{T}_t^2)^2\,\hat{\mathcal{M}}^{(0)} \\ & + i\pi\Big(-\tfrac{1}{2}(\hat{\alpha}_g^{(1)})^2 K^{(1)}\mathbf{T}_{s-u}^2(\mathbf{T}_t^2)^2 + \tfrac{1}{2}\hat{\alpha}_g^{(1)}(K^{(1)})^2[\mathbf{T}_t^2,\mathbf{T}_{s-u}^2]\mathbf{T}_t^2 \\ & \qquad - \tfrac{1}{6}(K^{(1)})^3[\mathbf{T}_t^2,[\mathbf{T}_t^2,\mathbf{T}_{s-u}^2]]\Big)\hat{\mathcal{M}}^{(0)}.\end{aligned} \tag{4.40}$$

Inserting the explicit results for the $\hat{\mathcal{M}}^{(n,n-1)}$ terms as given in eqs. (3.39) and (2.28) the hard function can be brought into the form

$$\mathrm{Re}[\mathcal{H}^{(3,2)}] = \hat{\alpha}_g^{(1)}\left[\hat{\alpha}_g^{(2)} + \tfrac{1}{2}\hat{\alpha}_g^{(1)}\left(D_i^{(1)} + D_j^{(1)}\right)\right](\mathbf{T}_t^2)^2\,\hat{\mathcal{M}}^{(0)}, \tag{4.41a}$$

$$i\,\mathrm{Im}[\mathcal{H}^{(3,2)}] = i\pi\left[\tfrac{1}{6}\Big(\mathbb{d}_3 - (K^{(1)})^3 - 3K^{(1)}(\hat{\alpha}_g^{(1)})^2 - 3(K^{(1)})^2\hat{\alpha}_g^{(1)}\Big)[\mathbf{T}_t^2,[\mathbf{T}_t^2,\mathbf{T}_{s-u}^2]]\right.$$

$$+\ \tfrac{1}{2}\hat{\alpha}_g^{(1)}\Big(\mathbb{d}_2+(K^{(1)})^2+2K^{(1)}\hat{\alpha}_g^{(1)}\Big)\mathbf{T}_t^2[\mathbf{T}_t^2,\mathbf{T}_{s-u}^2]$$
$$+\ \tfrac{1}{2}(\hat{\alpha}_g^{(1)})^3(\mathbf{T}_t^2)^2\mathbf{T}_{s-u}^2\Big]\hat{\mathcal{M}}^{(0)}. \tag{4.41b}$$

It is easy to check by explicit substitution of the functions involved in eq. (4.41) that $\mathcal{H}^{(3,2)}$ is indeed finite. The only $\mathcal{O}(\epsilon^0)$ contribution is given by $\mathrm{Im}[\mathcal{H}^{(3,2)}]$, i.e. one has

$$\begin{aligned}\mathrm{Re}[\mathcal{H}^{(3,2)}] &= \mathcal{O}(\epsilon),\\ i\,\mathrm{Im}[\mathcal{H}^{(3,2)}] &= i\pi\left(-\frac{11}{24}\zeta_3+\mathcal{O}(\epsilon)\right)[\mathbf{T}_t^2,[\mathbf{T}_t^2,\mathbf{T}_{s-u}^2]]+\mathcal{O}(\epsilon).\end{aligned} \tag{4.42}$$

More interesting is the amplitude at NNLL, since at this logarithmic accuracy we can confront our new predictions concerning the three-Reggeon exchange to the infrared factorisation formula. Starting from the latter, eq. (4.21) gives

$$\begin{aligned}\mathcal{H}^{(3,1)} &= \hat{\mathcal{M}}^{(3,1)}+\hat{\alpha}_g^{(1)}\mathbf{T}_t^2\hat{\mathcal{M}}^{(2,0)}+\hat{\alpha}_g^{(2)}\mathbf{T}_t^2\hat{\mathcal{M}}^{(1,0)}+\hat{\alpha}_g^{(3)}\mathbf{T}_t^2\hat{\mathcal{M}}^{(0)}\\
&+\frac{\pi^2}{6}\Big[-3\hat{\alpha}_g^{(1)}(K^{(1)})^2(\mathbf{T}_{s-u}^2)^2\mathbf{T}_t^2+(K^{(1)})^3\Big(2\mathbf{T}_{s-u}^2[\mathbf{T}_t^2,\mathbf{T}_{s-u}^2]+[\mathbf{T}_t^2,\mathbf{T}_{s-u}^2]\mathbf{T}_{s-u}^2\Big)\Big]\hat{\mathcal{M}}^{(0)}\\
&+i\pi\Big[-K^{(1)}\mathbf{T}_{s-u}^2\hat{\mathcal{M}}^{(2,1)}+\Big(\tfrac{1}{2}(K^{(1)})^2[\mathbf{T}_t^2,\mathbf{T}_{s-u}^2]-K^{(1)}\hat{\alpha}_g^{(1)}\mathbf{T}_{s-u}^2\mathbf{T}_t^2\Big)\hat{\mathcal{M}}^{(1,0)}\\
&\quad+\Big(K^{(1)}K^{(2)}[\mathbf{T}_t^2,\mathbf{T}_{s-u}^2]-K^{(2)}\hat{\alpha}_g^{(1)}\mathbf{T}_{s-u}^2\mathbf{T}_t^2-K^{(1)}\hat{\alpha}_g^{(2)}\mathbf{T}_{s-u}^2\mathbf{T}_t^2\\
&\qquad-\frac{\zeta_3}{24\epsilon}[\mathbf{T}_t^2,[\mathbf{T}_t^2,\mathbf{T}_{s-u}^2]]\Big)\hat{\mathcal{M}}^{(0)}\Big].\end{aligned} \tag{4.43}$$

Note that the last term this equation, proportional to $\zeta_3/\epsilon$, originates from the recently-computed quadrupole correction [35], as shown in section 4.1 (see eqs. (4.11) and (4.17) above), while all other terms in eq. (4.43), which involve $K^{(n)}$, originate in the dipole formula $\Gamma^{\mathrm{dip.}}$. Eq. (4.43) shows explicitly that, in the high-energy limit, the quadrupole correction contributes first at NNLL, and it only contributes at this logarithmic order to the *even part* of the amplitude.

Our prediction from BFKL theory concerns the odd amplitude, hence we focus now on the real part of eq. (4.43). Inserting results for the amplitude coefficients $\hat{\mathcal{M}}^{(n,k)}$ determined in the previous section, we get

$$\begin{aligned}\mathrm{Re}[\mathcal{H}^{(3,1)}] =\ &\Big[\hat{\alpha}_g^{(3)}+\hat{\alpha}_g^{(2)}\Big(D_i^{(1)}+D_j^{(1)}\Big)+\hat{\alpha}_g^{(1)}\Big(D_i^{(2)}+D_j^{(2)}+D_i^{(1)}D_j^{(1)}\Big)\Big]\mathbf{T}_t^2\,\hat{\mathcal{M}}^{(0)}\\
&+\pi^2\Big[R_C^{(3)}-\tfrac{1}{12}\hat{\alpha}_g^{(1)}R^{(2)}\Big](\mathbf{T}_t^2)^3\,\hat{\mathcal{M}}^{(0)}+\pi^2\,\hat{\alpha}_g^{(1)}\,\hat{R}^{(2)}\,\mathbf{T}_t^2(\mathbf{T}_{s-u}^2)^2\,\hat{\mathcal{M}}^{(0)}\\
&+\pi^2\Big[R_A^{(3)}+\tfrac{1}{6}\,K^{(1)}\Big(2(K^{(1)})^2+3\hat{\alpha}_g^{(1)}K^{(1)}+3\mathbb{d}_2\Big)\Big]\mathbf{T}_{s-u}^2[\mathbf{T}_t^2,\mathbf{T}_{s-u}^2]\,\hat{\mathcal{M}}^{(0)}\\
&+\pi^2\Big[R_B^{(3)}-\tfrac{1}{3}\,K^{(1)}\Big((K^{(1)})^2+3\hat{\alpha}_g^{(1)}K^{(1)}+3(\hat{\alpha}_g^{(1)})^2\Big)\Big][\mathbf{T}_t^2,\mathbf{T}_{s-u}^2]\mathbf{T}_{s-u}^2\,\hat{\mathcal{M}}^{(0)}.\end{aligned} \tag{4.44}$$

In this equation, the parameters $\hat{\alpha}_g^{(i)}$ are related to the perturbative expansion of the Regge trajectory, representing the one-Reggeon evolution, according to the definition in eq. (4.22). As already discussed, these parameters are unknown in our formulation of the Regge theory, beyond $\hat{\alpha}_g^{(1)}$. However, $\hat{\alpha}_g^{(2)}$ can be determined from the two loop analysis, see eq. (4.24b), which means that only $\alpha_g^{(3)}$ is unknown in eq. (4.44). We discuss below how this parameter

can be extracted from a three-loop calculation. Similarly, the impact factors $D_{i/j}^{(n)}$ represent corrections to the one-Reggeon wavefunction, and can be determined by matching with explicit calculations. Eq. (4.44) depends on the impact factors up to two loops, and these have all been determined through the one- and two-loop analysis, see eqs. (4.29) and (4.35) through (4.37). The two terms proportional to $\mathbf{T}^2_{s-u}[\mathbf{T}^2_t, \mathbf{T}^2_{s-u}]$ and $[\mathbf{T}^2_t, \mathbf{T}^2_{s-u}]\mathbf{T}^2_{s-u}$ depend only on quantities which have been calculatated explicitly: the loop functions $R^{(3)}_{A,B,C}$ originating from the BFKL evolution of the $1 \to 3$, $3 \to 1$ and $3 \to 3$ Reggeon exchange, terms from the one-loop soft anomalous dimension cubed, plus the signature-odd log part of the quadrupole correction eq. (4.11) (which turns out to be zero). The fact that these terms add up to something finite is therefore a highly non-trivial check of both BFKL theory and of the specific form of the quadrupole correction. Indeed, expanding explicitly to $\mathcal{O}(\epsilon^0)$ one finds

$$\begin{aligned}\mathrm{Re}[\mathcal{H}^{(3,1)}] = &\left[\hat{\alpha}_g^{(3)} + \hat{\alpha}_g^{(2)}\left(D_i^{(1)} + D_j^{(1)}\right) + \hat{\alpha}_g^{(1)}\left(D_i^{(2)} + D_j^{(2)} + D_i^{(1)} D_j^{(1)}\right)\right.\\ &\left. + C_A^2 \frac{\pi^2}{864}\left(\frac{1}{\epsilon^3} - \frac{15\zeta_2}{4\epsilon} - \frac{175\zeta_3}{2}\right)\right] C_A\, \hat{\mathcal{M}}^{(0)}\\ &+ \pi^2 \frac{5\zeta_3}{12}\mathbf{T}^2_{s-u}[\mathbf{T}^2_t, \mathbf{T}^2_{s-u}]\, \hat{\mathcal{M}}^{(0)} + \pi^2 \frac{\zeta_3}{12}[\mathbf{T}^2_t, \mathbf{T}^2_{s-u}]\mathbf{T}^2_{s-u}\, \hat{\mathcal{M}}^{(0)} + \mathcal{O}(\epsilon).\end{aligned} \tag{4.45}$$

where the term proportional to $C_A^2$ originates in the combination $\pi^2\left[R_C^{(3)} - \frac{1}{12}\hat{\alpha}_g^{(1)} R^{(2)}\right]$ in eq. (4.44).

We stress that the color operators $\mathbf{T}^2_{s-u}[\mathbf{T}^2_t, \mathbf{T}^2_{s-u}]$ and $[\mathbf{T}^2_t, \mathbf{T}^2_{s-u}]\mathbf{T}^2_{s-u}$ originate, within the infrared factorisation approach, only from the expansion of the "dipole term" in eq. (4.10), since, as discussed after eq. (4.43), the quadrupole correction turns out to contribute at NNLL only to the even amplitude. The fact that the calculation of the odd amplitude at NNLL within the Regge theory matches exactly the poles originating from the dipole contribution can be seen as an indirect confirmation of the result in Ref. [35]; in the computation of the previous section, the fact that the quadrupole contribution to the odd amplitude vanishes can be seen to be a reflection of the absence of $1/\epsilon$ single poles in the bubble integrals of eq. (3.44). Finiteness of the left-hand-side also predicts the infrared poles of the presently unknown "trajectory" $\hat{\alpha}_3$.

Eq. (4.44) represents not only a check of the infrared factorisation formula, but also a prediction for the real part of the infrared-finite amplitude, in the high-energy limit, up to three loops. In order to show what parts of the amplitude are predicted, we focus now on gluon-gluon scattering. Recalling our discussion in section 2.2, in particular eq. (2.24), we see that the real part of the hard function corresponds to the antisymmetric octet $8_a$ and the $10 + \overline{10}$ components of the amplitude. Evaluating the color operators in eq. (4.45) in the orthonormal color basis in the $t$-channel defined in appendix B we find

$$\begin{aligned}\mathrm{Re}[\mathcal{H}^{(3,1),[8_a]}] = &\left\{C_A\left[\hat{\alpha}_g^{(3)} + \hat{\alpha}_g^{(2)}\left(D_i^{(1)} + D_j^{(1)}\right) + \hat{\alpha}_g^{(1)}\left(D_i^{(2)} + D_j^{(2)} + D_i^{(1)} D_j^{(1)}\right)\right]\right.\\ &\left. + C_A^3 \frac{\pi^2}{864}\left(\frac{1}{\epsilon^3} - \frac{15\zeta_2}{4\epsilon} - \frac{175\zeta_3}{2}\right) - C_A \pi^2 \frac{2\zeta_3}{3} + \mathcal{O}(\epsilon)\right\}\hat{\mathcal{M}}^{(0),[8_a]},\end{aligned} \tag{4.46a}$$

$$\mathrm{Re}[\mathcal{H}^{(3,1),[10+\overline{10}]}] = \sqrt{2}C_A\sqrt{C_A^2-4}\left\{\frac{11\pi^2\zeta_3}{24}+\mathcal{O}(\epsilon)\right\}\hat{\mathcal{M}}^{(0),[8_a]}. \tag{4.46b}$$

Concerning the antisymmetric octet component, we see that it involves the Regge trajectory at three loops, $\hat{\alpha}_g^{(3)}$, which is unknown within our formalism. Given that the impact factors up to two loops are known from our previous analysis, see in particular eq. (4.35), this means that, knowing $\mathrm{Re}[\mathcal{H}^{(3,1),[8_a]}]$, eq. (4.46a) can be used to extract $\hat{\alpha}_g^{(3)}$. We will take this point of view below. Before, however, we note that $\hat{\alpha}_g^{(3)}$ does not contribute to the $10+\overline{10}$ component of the amplitude. Therefore, in our formalism we are able to predict this term unambiguously, and in eq. (4.46b) we have provided the explicit result up to three loops. As already mentioned, this result does not depend on the matter contents of the theory. Indeed, we find that our prediction agrees perfectly with a recent calculation [41] of $2\to 2$ gluon-gluon scattering amplitude at three loops in $\mathcal{N}=4$ SYM!

In appendix B we provide an explicit prediction for the gluon-gluon hard amplitude up to three loops in perturbation theory, which is based on the combination of the BFKL theory developed in section 3 and the comparison with the infrared factorisation formula discussed in this section. The hard function is provided in appendix B in an orthonormal color basis in the $t$-channel, while in appendix C we provide the same quantity in the "trace" basis commonly used in literature, see Ref. [69].

For completeness, we end this section by quoting the infrared factorisation result for the N$^3$LL coefficient of the hard function, namely, $\mathcal{H}^{(3,0)}$. This result relies on the 3-loop soft anomalous dimension described in eq. (4.11) but not on BFKL theory. One has

$$\begin{aligned}
\mathcal{H}^{(3,0)} &= \hat{\mathcal{M}}^{(3,0)} - \frac{\pi^2}{2}(K^{(1)})^2(\mathbf{T}^2_{s-u})^2\hat{\mathcal{M}}^{(1,0)} - \pi^2 K^{(1)}K^{(2)}(\mathbf{T}^2_{s-u})^2\hat{\mathcal{M}}^{(0)} \\
&\quad - \frac{1}{6\epsilon}\Bigg[[\mathbf{T}^2_{s-u},[\mathbf{T}^2_t,\mathbf{T}^2_{s-u}]]\frac{\zeta_5-4\zeta_2\zeta_3}{4} \\
&\qquad -\frac{\zeta_5+2\zeta_2\zeta_3}{8}\Big\{f^{abe}f^{cde}\Big[\{\mathbf{T}^a_t,\mathbf{T}^d_t\}\Big(\{\mathbf{T}^b_{s-u},\mathbf{T}^c_{s-u}\}+\{\mathbf{T}^b_{s+u},\mathbf{T}^c_{s+u}\}\Big) \\
&\qquad\qquad +\{\mathbf{T}^b_{s-u},\mathbf{T}^c_{s-u}\}\{\mathbf{T}^b_{s+u},\mathbf{T}^c_{s+u}\}\Big]-\frac{5}{8}C_A^2\mathbf{T}_t^2\Big\}\Bigg]\hat{\mathcal{M}}^{(0)} \\
&\quad -i\pi\Big\{K^{(1)}\mathbf{T}^2_{s-u}\hat{\mathcal{M}}^{(2,0)}+K^{(2)}\mathbf{T}^2_{s-u}\hat{\mathcal{M}}^{(1,0)}+6K^{(3)}\mathbf{T}^2_{s-u}\hat{\mathcal{M}}^{(0)} \\
&\qquad -\pi^2(K^{(1)})^3(\mathbf{T}^2_{s-u})^3\,\hat{\mathcal{M}}^{(0)}-\frac{11\zeta_4}{24\epsilon}[\mathbf{T}^2_t,[\mathbf{T}^2_t,\mathbf{T}^2_{s-u}]]\,\hat{\mathcal{M}}^{(0)}\Big\}.
\end{aligned} \tag{4.47}$$

This result is interesting on its own, because it provides the structure of infrared divergences at three loops, for a $2\to 2$ scattering amplitude in the high energy limit, including the quadrupole correction calculated in [35]. The explicit structure can be obtained in the orthonormal color basis in the $t$-channel defined in eq. (B.1), or in the "trace" basis defined in eq. (C.1), by substituting the color operators with their explicit matrix representations in that basis, which are also provided in the appendices B and C. The structure of infrared singularities in eq. (4.47) agrees with the calculation of gluon gluon scattering at three loops in $\mathcal{N}=4$ SYM presented in [41]. Eq. (4.47) is however more general, as it predicts the infrared structure for any $2\to 2$ scattering amplitude in QCD, thus including also quark-quark and quark-gluon scattering.

### Three-loop gluon Regge trajectory

Finally, let us state the precise relation between the three-loop "gluon Regge trajectory" and the logarithmic terms in the three-loop amplitude. Starting from three loops the "gluon Regge trajectory" is scheme-dependent. In this paper we pragmatically defined it to be the one-to-one matrix element of the Hamiltonian, $\alpha_g(t) = -H_{1\to1}/C_A$, in the scheme defined by eq. (2.44) where states corresponding to a different number of Reggeon are orthogonal, as discussed following eq. (2.48). This can be related to fixed-order amplitudes by taking the logarithm of the reduced amplitude projected onto the signature-odd adjoint channel. When projected onto that channel, the full amplitude and reduced amplitude defined in eq. (2.26) differ by a simple multiplicative factor whose logarithm is linear in $L$. Therefore, evaluating the prediction eq. (3.51) in the adjoint representation using the matrices given appendix B, we find

$$\log \frac{\mathcal{M}^{[8_a]}_{gg\to gg}}{\mathcal{M}^{(0)[8_a]}_{gg\to gg}} = L\Big\{ - H_{1\to1}(t) + \Big(\frac{\alpha_s}{\pi}\Big)^3 \pi^2 \Big[ N_c\Big( -2R^{(3)}_A + 2R^{(3)}_B\Big) + N_c^3 R^{(3)}_C\Big]\Big\} + \mathcal{O}(L^0, \alpha_s^4), \tag{4.48}$$

where the constants $R^{(3)}_A$, $R^{(3)}_B$, $R^{(3)}_C$ are given in eq. (3.52).

While this paper was in preparation, a remarkable calculation of the non-planar three-loop gluon-gluon amplitude in $\mathcal{N}=4$ SYM appeared [41], which yields, in terms of the $\overline{\text{MS}}$ coupling at scale $-t$,

$$\log \frac{\mathcal{M}^{[8_a],\mathcal{N}=4}_{gg\to gg}}{\mathcal{M}^{(0)[8_a]}_{gg\to gg}}\bigg|_L = N_c \left[\frac{\alpha_s}{\pi} k_1 + \Big(\frac{\alpha_s}{\pi}\Big)^2 k_2 + \Big(\frac{\alpha_s}{\pi}\Big)^3 k_3 + \cdots\right] \tag{4.49}$$

with

$$\begin{aligned}
k_1 &= \frac{1}{2\epsilon} - \epsilon\frac{\zeta_2}{4} - \epsilon^2\frac{7}{6}\zeta_3 - \epsilon^3\frac{47}{32}\zeta_4 + \epsilon^4\left(\frac{7}{12}\zeta_2\zeta_3 - \frac{31}{10}\zeta_5\right) + \mathcal{O}(\epsilon^5) \\
k_2 &= N_c\left[-\frac{\zeta_2}{8}\frac{1}{\epsilon} - \frac{\zeta_3}{8} - \epsilon\frac{3}{16}\zeta_4 + \epsilon^2\left(\frac{71}{24}\zeta_2\zeta_3 + \frac{41}{8}\zeta_5\right) + \mathcal{O}(\epsilon^3)\right] \\
k_3 &= N_c^2\left[\frac{11\zeta_4}{48}\frac{1}{\epsilon} + \frac{5}{24}\zeta_2\zeta_3 + \frac{1}{4}\zeta_5 + \mathcal{O}(\epsilon)\right] + \left[\frac{\zeta_2}{4}\frac{1}{\epsilon^3} - \frac{15\zeta_4}{16}\frac{1}{\epsilon} - \frac{77}{4}\zeta_2\zeta_3 + \mathcal{O}(\epsilon)\right].
\end{aligned} \tag{4.50}$$

Using (4.48) we are therefore able to obtain, in this theory, the "trajectory" $\alpha_g(t)N_c = -H_{1\to1}$ to three loop:

$$-H^{\mathcal{N}=4\,\text{SYM}}_{1\to1} = N_c\left[\frac{\alpha_s}{\pi}\alpha_g^{(1)}|_{\mathcal{N}=4\,\text{SYM}} + \Big(\frac{\alpha_s}{\pi}\Big)^2 \alpha_g^{(2)}|_{\mathcal{N}=4\,\text{SYM}} + \Big(\frac{\alpha_s}{\pi}\Big)^3 \alpha_g^{(3)}|_{\mathcal{N}=4\,\text{SYM}} + \cdots\right] \tag{4.51}$$

with the first two coefficients, $\alpha_g^{(1)}|_{\mathcal{N}=4\,\text{SYM}} = k_1$ and $\alpha_g^{(2)}|_{\mathcal{N}=4\,\text{SYM}} = k_2$ given in eq. (4.50), while the three-loop one given instead by

$$\alpha_g^{(3)}|_{\mathcal{N}=4\,\text{SYM}} = N_c^2\left[-\frac{\zeta_2}{144}\frac{1}{\epsilon^3} + \frac{49\zeta_4}{192}\frac{1}{\epsilon} + \frac{107}{144}\zeta_2\zeta_3 + \frac{\zeta_5}{4} + \mathcal{O}(\epsilon)\right] + N_c^0\left[0 + \mathcal{O}(\epsilon)\right]. \tag{4.52}$$

It is important to stress that, even though to three loop accuracy the adjoint amplitude may *look* like a Regge pole, e.g. a pure power-law, it is actually not: starting from two-loops it is really a sum of multiple powers. Simply exponentiating the exponent defined by

eq. (4.49) would predict a definitely incorrect four-loop amplitude. The correct, predictive, procedure is to exponentiate the action of the Hamiltonian following eq. (2.39). With the "trajectory" eq. (4.51) now fixed, this procedure will not require any new parameter for the odd amplitude at NNLL to all loop orders.

Finally, we comment on the fact that the trajectory of eq. (4.51), minus single-poles from the cusp anomalous dimension, is not finite. Superficially, this would seem to contradict the prediction of Ref. [10]. However, it is important to stress that $\alpha_g^{(3)}$ is not physically observable by itself and in the present BFKL framework, it depends on an arbitrary choice of scheme used to separate one- and three-Reggeon contributions. As explained below eq. (4.38), it is likely that our (arbitrary) choice to force the physics into a somewhat peculiar basis, in which multi-Reggeon states are orthogonal, is causing these spurious divergences in the intermediate quantity $H_{1\to1}$. In fact this can be seen clearly in the planar limit, where general arguments show that in the $U$-basis the evolution is trivial and the amplitude is a pure Regge pole [16], whereas in the present $W$-basis this pole is split between $1 \to 1$, $1 \to 3$ and $3 \to 3$ transitions. Thus our $H_{1\to1}$, even in the planar limit, is *not* equal to the position of this pure Regge pole.

Despite the not entirely satisfactory properties of the basis we used with regards to the simplicity of the large-$N_c$ limit, nor the relation between the singularities of the trajectory and the cusp anomalous dimension, it is important to stress that the basis is well-defined and sufficient to provide a fully predictive framework to all loop orders. A non-trivial confirmation is the fact that the $10 + \overline{10}$ amplitude component eq. (4.46b) is predicted correctly. Furthermore, one would expect the ambiguities from the choice of basis described below in eq. (2.44) to be proportional to $C_A^3$, which is completely consistent with the fact that the $N_c^0$ part of eq. (4.52) is finite. In fact, we see that the subleading color term proportional to $N_c^0$ is zero, up to $\mathcal{O}(\epsilon)$. This is an interesting result, which would be important to understand further, especially in light of the integrability properties of the planar amplitude [7, 8].

## 5 Conclusions

In this paper we have analyzed parton-parton scattering in gauge theories in the high-energy limit (Regge limit), pushing the accuracy to the next-to-next-to-leading logarithmic order. Our main tool has been BFKL theory, or more precisely its modern formulation as an effective theory of Wilson lines reviewed in section 2. An important observation is that many terms at this order can be fully predicted using only leading-order ingredients. These terms are distinguished, for example, by their color factors, and this paper has focused on such terms. Our predictions provide stringent constraints that the Regge limit of three-loop $2 \to 2$ QCD amplitudes must satisfy. Specifically, the odd reduced amplitude is predicted in eq. (3.51) to all order in $\epsilon$.

An interesting feature of the Regge limit is the reduction to a two-dimensional effective theory. Technically, this dramatically simplifies the loop integrals, and indeed the most complicated integral we needed in this paper is the standard bubble integral in eq. (3.32). The main work is reduced to the bookkeeping of color factors.

The NNLL amplitude is conceptually interesting from the BFKL perspective because it exhibits a new phenomenon: the mixing between one- and three- Reggeon states, both contributing to the odd part of the amplitude. To deal with this we used the symmetry property of the Hamiltonian, eq. (2.45), also known as target-projective duality, to obtain the $3 \to 1$ terms in the Hamiltonian from the $1 \to 3$ terms. This is the first time that this symmetry property is tested quantitatively. The tests described below can therefore be viewed as a nontrivial check of this symmetry.

As a consequence of the mixing between one- and three- Reggeon states, starting at NNLL the gluon Regge pole is not physically distinct from the Regge cut. In particular, in the $t$-channel colour flow basis, the antisymmetric octet color component receives contributions from both the pole corresponding to $1 \to 1$ Reggeon transition and the $3 \to 3$ as well as the $1 \to 3$ and $3 \to 1$ cut components. In general, using this formalism one may compute the signature odd NNLL $2 \to 2$ amplitude in QCD to all loop orders up to a single presently unknown parameter, the three-loop gluon Regge trajectory. The other color component of the odd amplitude, $10 + \overline{10}$, is entirely determined by the cut contributions, and hence it is fully predicted already, see eq. (4.46b). Because of the mentioned mixing, the result in either channel does *not* take the form of a single exponential (except in the planar limit), rather what exponentiates is the Hamiltonian in eq. (2.46).

Our results have been tested in two ways. First, the infrared divergent part of the result is in agreement with predictions from the general theory, including the recently computed three-loop soft anomalous dimension [35, 36]. Conversely, our results provide a valuable test of the latter. Second, our predictions, which are general and valid in any theory, turn out to agree with a recent explicit three-loop calculation in $\mathcal{N} = 4$ super Yang-Mills. This comparison also allows us to fix in this theory the one free parameter we have left, the three-loop gluon Regge trajectory in eq. (4.51), thereby making the formalism fully predictive at higher loop orders. Our predictions for the odd part of the three-loop amplitude are summarised in appendices B and C in a $t-$channel orthonormal basis and in a trace basis, respectively. These explicit results may be used as a stringent test of future multiloop amplitude computations.

To complete the NNLL description of $2 \to 2$ amplitudes, the only missing ingredient is in the even sector, namely the NLO impact factor to two gluons, which would thus be interesting to compute in the future. More generally, we have seen that the BFKL theory is consistent with infrared exponentiation, such that the hard function $\mathcal{H}$ (see eq. (4.1)) is finite; it would thus be interesting to understand how to setup the BFKL calculation of $\mathcal{H}$ in a manifestly finite way, which would alleviate the need to $\epsilon$-expand all intermediate quantities. This would make it possible to exploit the integrability of the Hamiltonian in two dimensions [7, 8].

**Note Added:** While this paper was being completed, partially overlapping results were announced in Ref. [70].

## Acknowledgments

SCH's research in its early stages was partly funded by the Danish National Research Foundation (DNRF91). EG's research is supported by the STFC Consolidated Grant "Particle Physics at the Higgs Centre." LV's research is supported by the People Programme (Marie Curie Actions) of the European Union's Horizon 2020 Framework Programme H2020-MSCA-IF-2014 under REA grant No. 656463 – "Soft Gluons". SCH thanks the Higgs Centre for Theoretical Physics for hospitality in the early stages this work. LV thanks the Niels Bohr Institute, Copenhagen, for hospitality during the completion of this work. In addition, EG and LV would like to thank the Erwin Schrödinger International Institute for Mathematics and Physics (ESI) in Vienna for hospitality during the program "Challenges and Concepts for Field Theory and Applications in the Era of LHC Run-2", during which part of this work was done.

## A Anomalous dimensions, renormalization group factors and Regge trajectory

We write the $\alpha_s$ expansion of the anomalous dimension (in the $\overline{\text{MS}}$ scheme) as

$$\gamma_i(\alpha_s) = \sum_{k=1}^{\infty} \gamma_i^{(k)} \left(\frac{\alpha_s}{\pi}\right)^k. \tag{A.1}$$

With this notation, the coefficients of the cusp anomalous dimension (with the quadratic Casimir factor $C_i$ removed) read [19, 71, 72]

$$\begin{aligned}
\gamma_K^{(1)} &= 2, \\
\gamma_K^{(2)} &= \left(\frac{67}{18} - \zeta_2\right) C_A - \frac{10}{9} T_R n_f, \\
\gamma_K^{(3)} &= \frac{C_A^2}{96}\left(490 - \frac{1072}{3}\zeta_2 + 88\zeta_3 + 264\zeta_4\right) + \frac{C_F T_R n_f}{32}\left(-\frac{220}{3} + 64\zeta_3\right) \\
&\quad + \frac{C_A T_R n_f}{96}\left(-\frac{1672}{9} + \frac{320}{3}\zeta_2 - 224\zeta_3\right) - \frac{2T_R^2 n_f^2}{27},
\end{aligned} \tag{A.2}$$

where $T_R = 1/2$. The coefficients of the quark and gluon anomalous dimension are given by [73, 74]

$$\begin{aligned}
\gamma_q^{(1)} &= -\frac{3}{4} C_F, \\
\gamma_q^{(2)} &= \frac{C_F^2}{16}\left(-\frac{3}{2} + 12\zeta_2 - 24\zeta_3\right) \\
&\quad + \frac{C_A C_F}{16}\left(-\frac{961}{54} - 11\zeta_2 + 26\zeta_3\right) + \frac{C_F T_R n_f}{16}\left(\frac{130}{27} + 4\zeta_2\right),
\end{aligned} \tag{A.3}$$

and

$$\gamma_g^{(1)} = -\frac{b_0}{4},$$

$$\gamma_g^{(2)} = \frac{C_A^2}{16}\left(-\frac{692}{27}+\frac{11}{3}\zeta_2+2\zeta_3\right)+\frac{C_A T_R n_f}{16}\left(\frac{256}{27}-\frac{4}{3}\zeta_2\right)+\frac{C_F T_R n_f}{4}. \tag{A.4}$$

The scalar factors in eq. (4.14) start at $\mathcal{O}\left(\alpha_s^0\right)$. In terms of the coefficients in eqs. (A.3) and (A.4), and setting $\mu^2 = -t$, they are:

$$\begin{aligned}
Z_i^{(0)} &= 1, \\
Z_i^{(1)} &= -C_i\,\gamma_K^{(1)}\frac{1}{4\epsilon^2}+\frac{\gamma_i^{(1)}}{\epsilon}, \\
Z_i^{(2)} &= C_i^2\left(\gamma_K^{(1)}\right)^2\frac{1}{32\epsilon^4}+C_i\left[\frac{1}{\epsilon^3}\frac{\gamma_K^{(1)}}{4}\left(\frac{3b_0}{16}-\gamma_i^{(1)}\right)-\frac{1}{\epsilon^2}\frac{\gamma_K^{(2)}}{16}\right] \\
&\quad+\frac{1}{\epsilon^2}\frac{\gamma_i^{(1)}}{2}\left(\gamma_i^{(1)}-\frac{b_0}{4}\right)+\frac{\gamma_i^{(2)}}{2\epsilon}.
\end{aligned} \tag{A.5}$$

Finally, we quote the one- and two-loop gluon Regge trajectory (divided by $C_A$) in terms of the coupling at scale $\mu^2 = -t$ [58–61]:

$$\begin{aligned}
\alpha_g^{(1)}(t) &= \frac{r_\Gamma}{2\epsilon}, \\
\alpha_g^{(2)}(t) &= -\frac{b_0}{16\epsilon^2}+\frac{1}{8\epsilon}\left[\left(\frac{67}{18}-\zeta_2\right)C_A-\frac{10T_R n_f}{9}\right] \\
&\quad+C_A\left(\frac{101}{108}-\frac{\zeta_3}{8}\right)-\frac{7\,T_R n_f}{27}+\mathcal{O}(\epsilon)\,.
\end{aligned} \tag{A.6}$$

## B The hard function for gluon-gluon scattering in an orthonormal $t$-channel color basis

Predictions for the infrared renormalised amplitude (hard function) based on the Regge theory developed in this paper have been presented in section 4. These predictions have been given in color space notation, i.e., writing the amplitude in terms of color operators acting on a vector amplitude. Predictions for the single components can be obtained by choosing a specific color basis. In this appendix and the next we provide explicit results within two color basis widely considered in literature. Here we focus on the orthonormal color basis in the $t$-channel, which, as discussed in the main text, is particularly useful to highlight the factorisation properties of the amplitude in the high-energy limit. In the next appendix we will focus on a "trace" basis, which has been typically used in the context of multi-loop calculations.

Before proceeding, we stress once more that the calculations performed on this paper are based solely on the BFKL evolution at leading order. The corrections $D_i$ to the impact factors, defined in eqs. (3.24) and (3.25), as well as the higher-loop corrections to the gluon Regge trajectory $\alpha_g$ (more precisely $H_{1\to1}$ in the scheme eq. (2.44)) are therefore kept in this appendix as free parameters. Their values can be obtained by matching with fixed-order amplitudes and are listed in appendix D.

### Definition of the $t$-channel color basis

We consider gluon-gluon scattering with external legs labelled as in figure 2. Within SU($N_c$), an orthonormal color basis in the $t$-channel can be obtained decomposing the color representations $8 \otimes 8$ of legs one and four into the direct sum $1 \oplus 8_s \oplus 8_a \oplus 10 + \overline{10} \oplus 27 \oplus 0$. Such basis has been provided in [40], and we repeat it here for the reader convenience:

$$
\begin{aligned}
c^{[1]} &= \frac{1}{N_c^2-1}\,\delta^{a_4}{}_{a_1}\,\delta^{a_3}{}_{a_2}\,, \\
c^{[8_s]} &= \frac{N_c}{N_c^2-4}\,\frac{1}{\sqrt{N_c^2-1}}\,d^{a_1a_4b}\,d^{a_2a_3}{}_{b}\,, \\
c^{[8_a]} &= \frac{1}{N_c}\,\frac{1}{\sqrt{N_c^2-1}}\,f^{a_1a_4b}\,f^{a_2a_3}{}_{b}\,, \\
c^{[10+\overline{10}]} &= \sqrt{\frac{2}{(N_c^2-4)(N_c^2-1)}}\left[\frac{1}{2}\left(\delta^{a_1}{}_{a_2}\,\delta^{a_3}{}_{a_4}-\delta^{a_3}{}_{a_1}\,\delta^{a_4}{}_{a_2}\right)-\frac{1}{N_c}f^{a_1a_4b}\,f^{a_2a_3}{}_{b}\right], \\
c^{[27]} &= \frac{2}{N_c\sqrt{(N_c+3)(N_c-1)}}\left[-\frac{N_c+2}{2N_c(N_c+1)}\,\delta^{a_4}{}_{a_1}\,\delta^{a_3}{}_{a_2}\right. \\
&\quad +\frac{N_c+2}{4N_c}\left(\delta^{a_1}{}_{a_2}\,\delta^{a_3}{}_{a_4}+\delta^{a_3}{}_{a_1}\,\delta^{a_4}{}_{a_2}\right)-\frac{N_c+4}{4(N_c+2)}\,d^{a_1a_4b}\,d^{a_2a_3}{}_{b} \\
&\quad \left.+\frac{1}{4}\left(d^{a_1a_2b}\,d^{a_3a_4}{}_{b}+d^{a_1a_3b}\,d^{a_2a_4}{}_{b}\right)\right], \\
c^{[0]} &= \frac{2}{N_c\sqrt{(N_c-3)(N_c+1)}}\left[\frac{N_c-2}{2N_c(N_c-1)}\,\delta^{a_4}{}_{a_1}\,\delta^{a_3}{}_{a_2}\right. \\
&\quad +\frac{N_c-2}{4N_c}\left(\delta^{a_1}{}_{a_2}\,\delta^{a_3}{}_{a_4}+\delta^{a_3}{}_{a_1}\,\delta^{a_4}{}_{a_2}\right)+\frac{N_c-4}{4(N_c-2)}\,d^{a_1a_4b}\,d^{a_2a_3}{}_{b} \\
&\quad \left.-\frac{1}{4}\left(d^{a_1a_2b}\,d^{a_3a_4}{}_{b}+d^{a_1a_3b}\,d^{a_2a_4}{}_{b}\right)\right].
\end{aligned}
\tag{B.1}
$$

We treat the two decuplet representations together, since they always contribute to the amplitude with the same coefficients. The tensors $c^{[8_a]}$ and $c^{[10+\overline{10}]}$ are odd under the exchanges $a_1 \leftrightarrow a_4$ and $a_2 \leftrightarrow a_3$, while $c^{[1]}$, $c^{[8_s]}$, $c^{[27]}$ and $c^{[0]}$ are even. The last representation does not contribute for $N_c = 3$, since its dimensionality is given by

$$
\dim\left[\,\mathbf{0}\,\right] \;=\; \frac{N_c^2(N_c-3)(N_c+1)}{4}\,, \tag{B.2}
$$

and it vanishes for SU(3). In the orthormal basis defined by eq. (B.1) (in that order), the diagonal matrix $\mathbf{T}_t^2$ evaluates to

$$
(\mathbf{T}_t^2)_{gg} \;=\; \mathrm{diag}\Big[0,\, N_c,\, N_c,\, 2N_c,\, 2(N_c+1),\, 2(N_c-1)\Big]\,, \tag{B.3}
$$

while $\mathbf{T}_{s-u}$ can be calculated starting from $\mathbf{T}_s$ provided in [40], by exploiting the relation $\mathbf{T}_t^2+\mathbf{T}_s^2+\mathbf{T}_u^2=C_{\rm tot}$. $\mathbf{T}_{s-u}$ is symmetric and traceless, and reads

$$(\mathbf{T}^2_{s-u})_{gg} = \begin{bmatrix} 0 & 0 & \mathcal{T}_{1,8_a} & 0 & 0 & 0 \\ 0 & 0 & \mathcal{T}_{8_s,8_a} & \mathcal{T}_{8_s,10} & 0 & 0 \\ \mathcal{T}_{1,8_a} & \mathcal{T}_{8_s,8_a} & 0 & 0 & \mathcal{T}_{8_a,27} & \mathcal{T}_{8_a,0} \\ 0 & \mathcal{T}_{8_s,10} & 0 & 0 & \mathcal{T}_{10,27} & \mathcal{T}_{10,0} \\ 0 & 0 & \mathcal{T}_{8_a,27} & \mathcal{T}_{10,27} & 0 & 0 \\ 0 & 0 & \mathcal{T}_{8_a,0} & \mathcal{T}_{10,0} & 0 & 0 \end{bmatrix}, \tag{B.4}$$

where

$$\begin{aligned} \mathcal{T}_{1,8_a} &= -\frac{2N_c}{\sqrt{N_c^2-1}}, \qquad \mathcal{T}_{8_s,8_a} = -\frac{N_c}{2}, \qquad \mathcal{T}_{8_s,10} = -N_c\sqrt{\frac{2}{N_c^2-4}}, \\ \mathcal{T}_{8_a,27} &= -\sqrt{\frac{N_c+3}{N_c+1}}, \qquad \mathcal{T}_{8_a,0} = -\sqrt{\frac{N_c-3}{N_c-1}}, \\ \mathcal{T}_{10,27} &= -\sqrt{\frac{(N_c+3)(N_c+1)(N_c-2)}{2(N_c+2)}}, \qquad \mathcal{T}_{10,0} = -\sqrt{\frac{(N_c-3)(N_c-1)(N_c+2)}{2(N_c-2)}}. \end{aligned} \tag{B.5}$$

Similarly, for the gluon-gluon amplitude we obtain also the color matrix representing the color operator associated to the constant term $\zeta_5+2\zeta_2\zeta_3$ in eq. (4.11):

$$\begin{aligned} &\frac{1}{2}\Big\{ f^{abe}f^{cde}\Big[\{\mathbf{T}_t^a,\mathbf{T}_t^d\}\Big(\{\mathbf{T}_{s-u}^b,\mathbf{T}_{s-u}^c\}+\{\mathbf{T}_{s+u}^b,\mathbf{T}_{s+u}^c\}\Big) \\ &\qquad\qquad +\{\mathbf{T}_{s-u}^a,\mathbf{T}_{s-u}^d\}\{\mathbf{T}_{s+u}^b,\mathbf{T}_{s+u}^c\}\Big]-\frac{5}{8}C_A^2\mathbf{T}_t^2\Big\}_{gg} \end{aligned} \tag{B.6}$$

$$= \begin{bmatrix} 2N_c\mathcal{T}_{1,8_a}^2 & N_c\mathcal{T}_{1,8_a}\mathcal{T}_{8_s,8_a} & 0 & 0 & -2\mathcal{T}_{1,8_a}\mathcal{T}_{8_a,27} & 2\mathcal{T}_{1,8_a}\mathcal{T}_{8_a,0} \\ N_c\mathcal{T}_{1,8_a}\mathcal{T}_{8_s,8_a} & 2N_c\mathcal{T}_{8_s,10}^2 & 0 & 0 & \mathcal{T}_{8_a,27}\mathcal{T}_A & \mathcal{T}_{8_a,0}\mathcal{T}_B \\ 0 & 0 & 14N_c & -\frac{N_c^2}{\mathcal{T}_{8_s,10}} & 0 & 0 \\ 0 & 0 & -\frac{N_c^2}{\mathcal{T}_{8_s,10}} & 5N_c & 0 & 0 \\ -2\mathcal{T}_{1,8_a}\mathcal{T}_{8_a,27} & \mathcal{T}_{8_a,27}\mathcal{T}_A & 0 & 0 & \mathcal{T}_C & -2N_c\mathcal{T}_{8_a,27}\mathcal{T}_{8_a,0} \\ 2\mathcal{T}_{1,8_a}\mathcal{T}_{8_a,0} & \mathcal{T}_{8_a,0}\mathcal{T}_B & 0 & 0 & -2N_c\mathcal{T}_{8_a,27}\mathcal{T}_{8_a,0} & \mathcal{T}_D \end{bmatrix},$$

where we have introduced the color factors

$$\begin{aligned} \mathcal{T}_A &= \frac{8N_c+6N_c^2-N_c^3}{2(2+N_c)} \qquad \mathcal{T}_B = \frac{8N_c-6N_c^2-N_c^3}{2(2+N_c)}, \\ \mathcal{T}_C &= \frac{26N_c+31N_c^2+10N_c^3+N_c^4}{(1+N_c)(2+N_c)} \qquad \mathcal{T}_D = \frac{26N_c-31N_c^2+10N_c^3-N_c^4}{(1+N_c)(2+N_c)}. \end{aligned} \tag{B.7}$$

For quark-quark scattering, the representations are more limited and we let similarly [40]

$$c_{qq}^{[1]} = \frac{1}{N_c}\delta^{a_4}{}_{a_1}\delta^{a_3}{}_{a_2}\,, \qquad c_{qq}^{[8_a]} = \frac{2}{\sqrt{N_c^2-1}}(\mathbf{T}^b)^{a_4}{}_{a_1}(\mathbf{T}^b)^{a_3}{}_{a_2}\,, \tag{B.8}$$

and one finds

$$(\mathbf{T}_t^2)_{qq} = \mathrm{diag}\Big[0,\, N_c\Big]\,, \qquad (\mathbf{T}_{s-u}^2)_{qq} = \begin{bmatrix} 0 & \frac{\sqrt{N_c^2-1}}{N_c} \\ \frac{\sqrt{N_c^2-1}}{N_c} & \frac{N_c^2-4}{2N_c} \end{bmatrix}. \tag{B.9}$$

Finally for quark-gluon scattering we have

$$\begin{aligned} c_{qg}^{[1]} &= \frac{1}{\sqrt{N_c(N_c^2-1)}}\delta^{a_4}{}_{a_1}\,\delta^{a_3}{}_{a_2}\,, \qquad c_{qg}^{[8_s]} = \sqrt{\frac{2N_c}{(N_c^2-4)(N_c^2-1)}}(T^b)^{a_4}{}_{a_1}\,d^{\,a_2a_3b}\,, \\ c_{qg}^{[8_a]} &= \sqrt{\frac{2}{N_c(N_c^2-1)}}(T^b)^{a_4}{}_{a_1}\,i f^{\,a_2a_3b}\,, \end{aligned} \tag{B.10}$$

with

$$(\mathbf{T}_t^2)_{qg} = \mathrm{diag}\Big[0,\, N_c,\, N_c\Big]\,, \qquad (\mathbf{T}_{s-u}^2)_{qg} = \begin{bmatrix} 0 & 0 & -\sqrt{2} \\ 0 & 0 & -\frac{1}{2}\sqrt{N_c^2-4} \\ -\sqrt{2} & -\frac{1}{2}\sqrt{N_c^2-4} & 0 \end{bmatrix}. \tag{B.11}$$

For antiquark scattering we define the same color structures. Note that in the quark-quark case the signature in the adjoint channel is not determined by the color projection and can only be determined by comparing the quark and antiquark amplitudes. In the quark-gluon case the structures have definite signatures (respectively even, even, odd) due to Bose symmetry on the gluon side.

### The hard function for gluon-gluon scattering

Let us now present explicit results for the hard function components in the orthonormal $t$-channel basis defined above. We restrict the discussion here to the gluon-gluon amplitude, since it should hopefully be clear how the formulas presented below are obtained from the formulas in section 4 by evaluating the color operators. We decompose the hard function according to eq. (2.23), namely

$$\mathcal{H}_{gg\to gg}(s,t) = \sum_i c^{[i]}\,\mathcal{H}^{[i]}(s,t). \tag{B.12}$$

Within the orthonormal basis eq. (B.1) the tree-level hard function in eq. (2.17) reads

$$\begin{aligned} \mathcal{H}^{(0),[1]} &= \mathcal{H}^{(0),[8_s]} = \mathcal{H}^{(0),[10+\overline{10}]} = \mathcal{H}^{(0),[27]} = \mathcal{H}^{(0),[0]} = 0, \\ \mathcal{H}^{(0),[8_a]} &= -2\frac{s}{t}N_c\sqrt{N_c^2-1}. \end{aligned} \tag{B.13}$$

In section 4 we have presented results up to three loops, but the Regge theory develop in section 3 allows one to calculate higher orders, too. For feature reference, therefore, we expand here the amplitude in powers of $\epsilon$, consistently as it would be needed for a four loop calculation. Namely, we expand the one loop functions up to power $\epsilon^6$, the two loop ones up to $\epsilon^4$, and the three loops functions up to power $\epsilon^2$.

The one loop amplitude, and more in general the leading logarithmic contribution can be expressed entirely in terms of the one-loop function defined in eq. (4.24a). Up to $\epsilon^6$ one has

$$\begin{aligned}\hat{\alpha}_g^{(1)} &= \frac{1}{2\epsilon}(r_\Gamma - 1) = -\frac{1}{4}\zeta_2\,\epsilon - \frac{7}{6}\zeta_3\,\epsilon^2 - \frac{47}{32}\zeta_4\epsilon^3 + \left(\frac{7}{12}\zeta_z\zeta_3 - \frac{31}{10}\zeta_5\right)\epsilon^4 \\ &\quad + \left(\frac{49}{36}\zeta_3^2 - \frac{949}{256}\zeta_6\right)\epsilon^5 + \left(\frac{31}{20}\zeta_2\zeta_5 + \frac{329}{96}\zeta_3\zeta_4 - \frac{127}{14}\zeta_7\right)\epsilon^6 + \mathcal{O}(\epsilon^7). \end{aligned} \tag{B.14}$$

In term of this function, the leading-logarithmic amplitude in components reads:

$$\begin{aligned}&\mathcal{H}^{(n,n),[1]} = \mathcal{H}^{(n,n),[8_s]} = \mathcal{H}^{(n,n),[10+\overline{10}]} = \mathcal{H}^{(n,n),[27]} = \mathcal{H}^{(n,n),[0]} = 0, \\ &\mathcal{H}^{(n,n),[8_a]} = -\frac{2}{n!}\,N_c^{n+1}\,\sqrt{N_c^2-1}\,(\hat{\alpha}_g^{(1)}(t))^n\,\frac{s}{t}.\end{aligned} \tag{B.15}$$

Next, we consider $\mathcal{H}^{(1,0)}$, whose result has been obtained in eq. (4.28). In components one obtains

$$\begin{aligned}\mathcal{H}^{(1,0),[1]} &= i\pi\,4N_c^2\,\hat{\alpha}_g^{(1)}\frac{s}{t}, \\ \mathcal{H}^{(1,0),[8_s]} &= i\pi\,N_c^2\sqrt{N_c^2-1}\,\hat{\alpha}_g^{(1)}\frac{s}{t}, \\ \mathcal{H}^{(1,0),[8_a]} &= -2N_c\sqrt{N_c^2-1}(D_i^{(1)} + D_j^{(1)})\frac{s}{t} \\ \mathcal{H}^{(1,0),[10+\overline{10}]} &= 0, \\ \mathcal{H}^{(1,0),[27]} &= i\pi\,2N_c\sqrt{(N_c+3)(N_c-1)}\,\hat{\alpha}_g^{(1)}\frac{s}{t}, \\ \mathcal{H}^{(1,0),[0]} &= i\pi\,2N_c\sqrt{(N_c-3)(N_c+1)}\,\hat{\alpha}_g^{(1)}\frac{s}{t}.\end{aligned} \tag{B.16}$$

At two loops the NLL term reads

$$\begin{aligned}\mathcal{H}^{(2,1),[1]} &= -2i\pi\,N_c^3\,f_a^{(2,1)}\frac{s}{t}, \\ \mathcal{H}^{(2,1),[8_s]} &= i\pi\,N_c^3\sqrt{N_c^2-1}\,(\hat{\alpha}_g^{(1)}(t))^2\frac{s}{t}, \\ \mathcal{H}^{(2,1),[8_a]} &= -2N_c^2\sqrt{N_c^2-1}\left[\hat{\alpha}_g^{(2)} + \hat{\alpha}_g^{(1)}(D_i^{(1)} + D_j^{(1)})\right]\frac{s}{t} \\ \mathcal{H}^{(2,1),[10+\overline{10}]} &= 0, \\ \mathcal{H}^{(2,1),[27]} &= i\pi\,N_c\sqrt{(N_c+3)(N_c-1)}\left[(N_c+2)f_a^{(2,1)} + 4(N_c+1)(\hat{\alpha}_g^{(1)}(t))^2\right]\frac{s}{t}, \\ \mathcal{H}^{(2,1),[0]} &= i\pi\,N_c\sqrt{(N_c-3)(N_c+1)}\left[(N_c-2)f_a^{(2,1)} + 4(N_c-1)(\hat{\alpha}_g^{(1)}(t))^2\right]\frac{s}{t},\end{aligned} \tag{B.17}$$

where we have expressed the amplitude in terms of the functions

$$f_a^{(2,1)} = K^{(1)}(2\hat{\alpha}_g^{(1)} + K^{(1)}) + \text{¢}_2$$

$$= -\frac{9}{2}\zeta_3\epsilon - \frac{221}{32}\zeta_4\epsilon^2 + \left(\frac{47}{12}\zeta_2\zeta_3 - \frac{63}{2}\zeta_5\right)\epsilon^3 + \left(\frac{1193}{36}\zeta_3^2 - \frac{14585}{256}\zeta_6\right)\epsilon^4 + \mathcal{O}(\epsilon^5). \tag{B.18}$$

At NNLL accuracy we are able to make predictions for the real component of the hard function only. Given that this contribution corresponds to the odd amplitude, it implies that this correction affects only the $8_a$ and $10 + \overline{10}$ representation:

$$\begin{aligned}
\mathrm{Re}[\mathcal{H}^{(2,0),[1]}] &= 0,\\
\mathrm{Re}[\mathcal{H}^{(2,0),[8_s]}] &= 0,\\
\mathrm{Re}[\mathcal{H}^{(2,0),[8_a]}] &= -2N_c\sqrt{(N_c^2-1)}\Big\{D_i^{(1)}D_j^{(1)} + D_i^{(2)} + D_j^{(2)}\\
&\qquad - \pi^2\left(\frac{N_c^2}{12}R^{(2)} - \frac{N_c^2+24}{4}\hat{R}^{(2)}\right)\Big\}\frac{s}{t},\\
\mathrm{Re}[\mathcal{H}^{(2,0),[10+\overline{10}]}] &= -3\pi^2 N_c\sqrt{2(N_c^2-4)(N_c^2-1)}\hat{R}^{(2)}\frac{s}{t},\\
\mathrm{Re}[\mathcal{H}^{(2,0),[27]}] &= 0,\\
\mathrm{Re}[\mathcal{H}^{(2,0),[0]}] &= 0.
\end{aligned} \tag{B.19}$$

where the function $\hat{R}^{(2)}$ has been defined in eq. (4.34). Explicitly, up to $\mathcal{O}(\epsilon^5)$ one has

$$\hat{R}^{(2)} = \frac{3}{4}\zeta_3\epsilon + \frac{67}{64}\zeta_4\epsilon^2 + \left(\frac{21}{4}\zeta_5 - \frac{25}{24}\zeta_2\zeta_3\right)\epsilon^3 + \left(\frac{4423}{512}\zeta_6 - \frac{463}{72}\zeta_3^2\right)\epsilon^4 + \mathcal{O}(\epsilon^5). \tag{B.20}$$

At three loops, the NLL component reads

$$\begin{aligned}
\mathcal{H}^{(3,2),[1]} &= i\pi\, N_c^4\, f_a^{(3,2)}\frac{s}{t},\\
\mathcal{H}^{(3,2),[8_s]} &= i\pi\, N_c^4\sqrt{N_c^2-1}\,(\hat{\alpha}_g^{(1)}(t))^3\,\frac{s}{t},\\
\mathcal{H}^{(3,2),[8_a]} &= -2N_c^3\sqrt{N_c^2-1}\,\hat{\alpha}_g^{(1)}\left[\hat{\alpha}_g^{(2)} + \frac{\hat{\alpha}_g^{(1)}}{2}\left(D_i^{(1)} + D_j^{(1)}\right)\right]\frac{s}{t},\\
\mathcal{H}^{(3,2),[10+\overline{10}]} &= 0,\\
\mathcal{H}^{(3,2),[27]} &= i\pi\,\frac{N_c}{2}\sqrt{(N_c-1)(N_c+3)}\left[(N_c+2)^2 f_a^{(3,2)} + 8(N_c+1)^2(\hat{\alpha}_g^{(1)}(t))^3\right.\\
&\qquad \left. + (N_c+1)(N_c+2)f_b^{(3,2)}\right]\frac{s}{t},\\
\mathcal{H}^{(3,2),[0]} &= i\pi\,\frac{N_c}{2}\sqrt{(N_c+1)(N_c-3)}\Big[(N_c-2)^2 f_a^{(3,2)} + 8(N_c-1)^2(\hat{\alpha}_g^{(1)}(t))^3\\
&\qquad + (N_c-1)(N_c-2)f_b^{(3,2)}\Big]\frac{s}{t},
\end{aligned} \tag{B.21}$$

where we have expressed the amplitude in terms of the functions

$$\begin{aligned}
f_a^{(3,2)} &= -\frac{2}{3}\left[K^{(1)}\left(3(\hat{\alpha}_g^{(1)})^2 + 3\hat{\alpha}_g^{(1)}K^{(1)} + (K^{(1)})^2\right) - \mathbb{d}_3\right]\\
&= -\frac{11}{6}\zeta_3 - \frac{11}{4}\zeta_4\epsilon + \left(\frac{11}{4}\zeta_2\zeta_3 - \frac{119}{2}\zeta_5\right)\epsilon^2 + \mathcal{O}(\epsilon^3),
\end{aligned}$$

$$f_b^{(3,2)} = 4\hat{\alpha}_g^{(1)}\Big[K^{(1)}\Big(2\hat{\alpha}_g^{(1)} + K^{(1)}\Big) + \mathbb{d}_2\Big] = \frac{9}{2}\zeta_2\zeta_3\epsilon^2 + \mathcal{O}(\epsilon^3).$$

Notice also that $(\hat{\alpha}_g^{(1)}(t))^3 = \mathcal{O}(\epsilon^3)$. Last, the real part of the NNLL term at three loops reads

$$\begin{aligned}
\mathrm{Re}[\mathcal{H}^{(3,1),[1]}] &= 0,\\
\mathrm{Re}[\mathcal{H}^{(3,1),[8_s]}] &= 0,\\
\mathrm{Re}[\mathcal{H}^{(3,1),[8_a]}] &= -2N_c^2\sqrt{N_c^2-1}\Big[\hat{\alpha}_g^{(3)} + \hat{\alpha}_g^{(2)}\Big(D_i^{(1)} + D_j^{(1)}\Big) + \hat{\alpha}_g^{(1)}\Big(D_i^{(2)} + D_j^{(2)}\Big)\\
&\quad + \hat{\alpha}_g^{(1)} D_i^{(1)} D_j^{(1)} - \pi^2\Big(\frac{N_c^2+24}{4} f_a^{(3,1)} + 2(f_b^{(3,1)} + f_c^{(3,1)}) - N_c^2 f_d^{(3,1)}\Big)\Big]\frac{s}{t},\\
\mathrm{Re}[\mathcal{H}^{(3,1),[10+\overline{10}]}] &= N_c^2\sqrt{\frac{(N_c^2-4)(N_c^2-1)}{2}}\Big[24 f_a^{(3,1)} - 2f_b^{(3,1)} + f_c^{(3,1)}\Big]\frac{s}{t},\\
\mathrm{Re}[\mathcal{H}^{(3,1),[27]}] &= 0,\\
\mathrm{Re}[\mathcal{H}^{(3,1),[0]}] &= 0,
\end{aligned} \tag{B.22}$$

where we have expressed the amplitude in terms of the functions

$$\begin{aligned}
f_a^{(3,1)} &= \frac{1}{2}\hat{\alpha}_g^{(1)}\Big[K^{(1)}\Big(K^{(1)} + 2\hat{\alpha}_g^{(1)}\Big) + 2R^{(2)}\Big]\\
&= -\frac{3}{16}\zeta_2\zeta_3\epsilon^2 + \mathcal{O}(\epsilon^3),\\
f_b^{(3,1)} &= \frac{1}{6}\Big[K^{(1)}\Big(K^{(1)}(3\hat{\alpha}_g^{(1)} + 2K^{(1)}) + 3\mathbb{d}_2\Big) + 6R_A^{(3)}\Big]\\
&= \frac{5}{12}\zeta_3 + \frac{5}{8}\zeta_4\epsilon + \Big(\frac{65}{4}\zeta_5 - \frac{19}{16}\zeta_2\zeta_3\Big)\epsilon^2 + \mathcal{O}(\epsilon^3),\\
f_c^{(3,1)} &= \frac{1}{3}\Big[K^{(1)}\Big(K^{(1)}(3\hat{\alpha}_g^{(1)} + 2K^{(1)}) + 3\hat{\alpha}_g^{(1)}(2\hat{\alpha}_g^{(1)} + K^{(1)})\Big) - 6R_B^{(3)}\Big]\\
&= -\frac{1}{6}\zeta_3 - \frac{1}{4}\zeta_4\epsilon + \Big(\frac{11}{2}\zeta_5 + \frac{1}{4}\zeta_2\zeta_3\Big)\epsilon^2 + \mathcal{O}(\epsilon^3),\\
f_d^{(3,1)} &= \frac{1}{12}\Big[-\hat{\alpha}_g^{(1)}R^{(2)} + 12R_c^{(3)}\Big]\\
&= \frac{1}{864\epsilon^3} - \frac{5}{1152\epsilon}\zeta_2 - \frac{175}{1728}\zeta_3 - \frac{425}{3072}\epsilon\zeta_4 + \Big(\frac{23}{128}\zeta_2\zeta_3 - \frac{99}{64}\zeta_5\Big)\epsilon^2 + \mathcal{O}(\epsilon^3).
\end{aligned} \tag{B.23}$$

## C Gluon-gluon hard function in a "trace" color basis

In SU($N_c$) gauge theory, the four-gluon amplitude can be written in a basis of single- and double-trace operators. We follow the definitions in [69] (with traces normalized as $\mathrm{Tr}\,[1] = N_c$ and $\mathrm{Tr}\,[T^a T^b] = \frac{1}{2}\delta^{ab}$):

$$\begin{aligned}
c^{[\mathrm{Tr1}]} &= \mathrm{Tr}\,[T^{a_1}T^{a_2}T^{a_3}T^{a_4}] + \mathrm{Tr}\,[T^{a_1}T^{a_4}T^{a_3}T^{a_2}]\,,\\
c^{[\mathrm{Tr2}]} &= \mathrm{Tr}\,[T^{a_1}T^{a_2}T^{a_4}T^{a_3}] + \mathrm{Tr}\,[T^{a_1}T^{a_3}T^{a_4}T^{a_2}]\,,\\
c^{[\mathrm{Tr3}]} &= \mathrm{Tr}\,[T^{a_1}T^{a_4}T^{a_2}T^{a_3}] + \mathrm{Tr}\,[T^{a_1}T^{a_3}T^{a_2}T^{a_4}]\,,
\end{aligned}$$

$$
\begin{aligned}
c^{[\mathrm{Tr4}]} &= \mathrm{Tr}\left[T^{a_1}T^{a_3}\right]\mathrm{Tr}\left[T^{a_2}T^{a_4}\right], \\
c^{[\mathrm{Tr5}]} &= \mathrm{Tr}\left[T^{a_1}T^{a_4}\right]\mathrm{Tr}\left[T^{a_2}T^{a_3}\right], \\
c^{[\mathrm{Tr6}]} &= \mathrm{Tr}\left[T^{a_1}T^{a_2}\right]\mathrm{Tr}\left[T^{a_3}T^{a_4}\right].
\end{aligned} \tag{C.1}
$$

Within this color basis the tree level amplitude is easily obtained by noting that

$$
f^{a_1a_4b}f^{a_2a_3b} = 2\left(c^{[\mathrm{Tr1}]} - c^{[\mathrm{Tr3}]}\right), \tag{C.2}
$$

and the amplitude reads (recall that $\mathcal{M}^{(0)} = \mathcal{H}^{(0)}$):

$$
\begin{aligned}
\mathcal{H}^{(0),[\mathrm{Tr1}]} &= -\frac{4s}{t}, \qquad \mathcal{H}^{(0),[\mathrm{Tr3}]} = \frac{4s}{t}, \\
\mathcal{H}^{(0),[\mathrm{Tr2}]} &= \mathcal{H}^{(0),[\mathrm{Tr4}]} = \mathcal{H}^{(0),[\mathrm{Tr5}]} = \mathcal{H}^{(0),[\mathrm{Tr6}]} = 0.
\end{aligned} \tag{C.3}
$$

Explicit result for the color amplitude components in the trace color basis can be obtained either by deriving a rotation matrix, which rotates from the orthonormal basis in eq. (B.1) to the trace basis in eq. (C.1), or by obtaining an explicit matrix representation for the operators $\mathbf{T}_t^2$ and $\mathbf{T}_{s-u}^2$ in the trace basis. We have performed the calculation in both ways, and here we report about the second method.

To represent the color Casimirs as matrices acting on this basis, the first step is to express the generators on the external color-adjoint gluons in terms of commutators inside the trace, which follow from the definition:

$$
\mathbf{T}_1^b T^{a_1} \equiv -if^{ba_1c}T^c = [T^{a_1}, T^b]. \tag{C.4}
$$

Color contractions inside the traces can then be simplified using the $\mathrm{SU}(N_c)$ identities

$$
\mathrm{Tr}\left[T^a X T^a Y\right] = \frac{1}{2}\mathrm{Tr}[X]\mathrm{Tr}[Y] - \frac{1}{2N_c}\mathrm{Tr}[XY]. \tag{C.5}
$$

Thus, for example,

$$
\begin{aligned}
\mathbf{T}_t^2 c^{[\mathrm{Tr1}]} &= \mathrm{Tr}\left[T^{a_1}\left(T^bT^bT^{a_2}T^{a_3} - 2T^bT^{a_2}T^{a_3}T^b + T^{a_2}T^{a_3}T^bT^b\right)T^{a_4}\right] \\
&= N_c\, c^{[\mathrm{Tr1}]} - 2\, c^{[\mathrm{Tr5}]}.
\end{aligned} \tag{C.6}
$$

Proceeding similarly for the other basis elements, we obtain the matrix representation:

$$
\mathbf{T}_t^2 = \begin{bmatrix}
N_c & 0 & 0 & 0 & 0 & -1 \\
0 & 2N_c & 0 & 1 & 0 & 1 \\
0 & 0 & N_c & -1 & 0 & 0 \\
0 & 2 & 0 & 2N_c & 0 & 0 \\
-2 & 0 & -2 & 0 & 0 & 0 \\
0 & 2 & 0 & 0 & 0 & 2N_c
\end{bmatrix}, \quad
\mathbf{T}_{s-u}^2 = \begin{bmatrix}
-\frac{N_c}{2} & 0 & 0 & 0 & -1 & -\frac{1}{2} \\
0 & 0 & 0 & -\frac{1}{2} & 0 & \frac{1}{2} \\
0 & 0 & \frac{N_c}{2} & \frac{1}{2} & 1 & 0 \\
0 & 1 & 2 & N_c & 0 & 0 \\
-1 & 0 & 1 & 0 & 0 & 0 \\
-2 & -1 & 0 & 0 & 0 & -N_c
\end{bmatrix}. \tag{C.7}
$$

Similarly, in the trace basis the the color operator defined in eq. (B.6), and associated to the constant term of the quadrupole correction reads

$$\frac{1}{2}\Big\{ f^{abe} f^{cde} \Big[ \{\mathbf{T}_t^a, \mathbf{T}_t^d\} \Big( \{\mathbf{T}_{s-u}^b, \mathbf{T}_{s-u}^c\} + \{\mathbf{T}_{s+u}^b, \mathbf{T}_{s+u}^c\} \Big) + \{\mathbf{T}_{s-u}^a, \mathbf{T}_{s-u}^d\} \{\mathbf{T}_{s+u}^b, \mathbf{T}_{s+u}^c\} \Big] - \frac{5}{8} C_A^2 \mathbf{T}_t^2 \Big\}_{gg}$$

$$= \begin{bmatrix} 9N_c & -4N_c & -4N_c & -4 & \frac{1}{2}(4+N_c^2) & \frac{1}{2}(4+N_c^2) \\ -4N_c & 9N_c & -4N_c & \frac{1}{2}(4+N_c^2) & -4 & \frac{1}{2}(4+N_c^2) \\ -4N_c & -4N_c & 9N_c & \frac{1}{2}(4+N_c^2) & \frac{1}{2}(4+N_c^2) & -4 \\ 2 & 2+N_c^2 & 2+N_c^2 & 6N_c & 0 & 0 \\ 2+N_c^2 & 2 & 2+N_c^2 & 0 & 6N_c & 0 \\ 2+N_c^2 & 2+N_c^2 & 2 & 0 & 0 & 6N_c \end{bmatrix}. \tag{C.8}$$

By using these result we obtain the following results: the LL hard function at all order reads

$$\begin{aligned} \mathcal{H}^{(n,n),[\mathrm{Tr1}]} &= -\frac{N_c^n}{n!} (\hat{\alpha}_g^{(1)})^n \frac{4s}{t}, \qquad \mathcal{H}^{(n,n),[\mathrm{Tr3}]} = \frac{N_c^n}{n!} (\hat{\alpha}_g^{(1)})^n \frac{4s}{t}, \\ \mathcal{H}^{(n,n),[\mathrm{Tr2}]} &= \mathcal{H}^{(n,n),[\mathrm{Tr4}]} = \mathcal{H}^{(n,n),[\mathrm{Tr5}]} = \mathcal{H}^{(n,n),[\mathrm{Tr6}]} = 0. \end{aligned} \tag{C.9}$$

Next, the we provide the NLL and the NNLL terms at each order of the perturbative expansion, starting at one loop. We obtain

$$\begin{aligned} \mathcal{H}^{(1,0),[\mathrm{Tr1}]} &= \Big[ 2\, i\pi\, N_c\, \hat{\alpha}_g^{(1)} - 4\Big( D_i^{(1)} + D_j^{(1)} \Big) \Big] \frac{s}{t}, \\ \mathcal{H}^{(1,0),[\mathrm{Tr2}]} &= 0, \\ \mathcal{H}^{(1,0),[\mathrm{Tr3}]} &= \Big[ 2\, i\pi\, N_c\, \hat{\alpha}_g^{(1)} + 4\Big( D_i^{(1)} + D_j^{(1)} \Big) \Big] \frac{s}{t} \\ \mathcal{H}^{(1,0),[\mathrm{Tr4}]} &= 8\, i\pi\, \hat{\alpha}_g^{(1)} \frac{s}{t}, \\ \mathcal{H}^{(1,0),[\mathrm{Tr5}]} &= 8\, i\pi\, \hat{\alpha}_g^{(1)} \frac{s}{t}, \\ \mathcal{H}^{(1,0),[\mathrm{Tr6}]} &= 8\, i\pi\, \hat{\alpha}_g^{(1)} \frac{s}{t}. \end{aligned} \tag{C.10}$$

At two loops the NLL term reads

$$\begin{aligned} \mathcal{H}^{(2,1),[\mathrm{Tr1}]} &= \Big\{ -4N_c \Big[ \hat{\alpha}_g^{(2)} + \hat{\alpha}_g^{(1)} \Big( D_i^{(1)} + D_i^{(1)} \Big) \Big] \\ &\qquad + 2i\pi \Big[ -2 f_a^{(2,1)} + (N_c^2 - 4)(\hat{\alpha}_g^{(1)})^2 \Big] \Big\} \frac{s}{t}, \\ \mathcal{H}^{(2,1),[\mathrm{Tr2}]} &= 8i\pi \Big[ f_a^{(2,1)} + 2(\hat{\alpha}_g^{(1)})^2 \Big] \frac{s}{t}, \\ \mathcal{H}^{(2,1),[\mathrm{Tr3}]} &= \Big\{ 4N_c \Big[ \hat{\alpha}_g^{(2)} + \hat{\alpha}_g^{(1)} \Big( D_i^{(1)} + D_j^{(1)} \Big) \Big] \\ &\qquad + 2i\pi \Big[ -2 f_a^{(2,1)} + (N_c^2 - 4)(\hat{\alpha}_g^{(1)})^2 \Big] \Big\} \frac{s}{t} \end{aligned}$$

$$
\begin{aligned}
\mathcal{H}^{(2,1),[\mathrm{Tr4}]} &= 4N_c i\pi\Big[f_a^{(2,1)} + 4(\hat{\alpha}_g^{(1)})^2\Big]\,\frac{s}{t},\\
\mathcal{H}^{(2,1),[\mathrm{Tr5}]} &= -8N_c i\pi\Big[f_a^{(2,1)} + (\hat{\alpha}_g^{(1)})^2\Big]\,\frac{s}{t},\\
\mathcal{H}^{(2,1),[\mathrm{Tr6}]} &= 4N_c i\pi\Big[f_a^{(2,1)} + 4(\hat{\alpha}_g^{(1)})^2\Big]\,\frac{s}{t},
\end{aligned}
\tag{C.11}
$$

where the function $f_a^{(2,1)}$ has been defined in eq. (B.18). At NNLL the real component of the amplitude reads

$$
\begin{aligned}
\mathrm{Re}[\mathcal{H}^{(2,0),[\mathrm{Tr1}]}] &= -\frac{1}{3}\Big[12\Big(D_i^{(1)}D_j^{(1)} + D_i^{(2)} + D_j^{(2)}\Big)\\
&\qquad + \pi^2\Big(3(N_c^2+12)\hat{R}^{(2)} - N_c^2 R^{(2)}\Big)\Big]\,\frac{s}{t},\\
\mathrm{Re}[\mathcal{H}^{(2,0),[\mathrm{Tr2}]}] &= 0,\\
\mathrm{Re}[\mathcal{H}^{(2,0),[\mathrm{Tr3}]}] &= \frac{1}{3}\Big[12\Big(D_i^{(1)}D_j^{(1)} + D_i^{(2)} + D_j^{(2)}\Big)\\
&\qquad + \pi^2\Big(3(N_c^2+12)\hat{R}^{(2)} - N_c^2 R^{(2)}\Big)\Big]\,\frac{s}{t},\\
\mathrm{Re}[\mathcal{H}^{(2,0),[\mathrm{Tr4}]}] &= 12\pi^2 N_c\,\hat{R}^{(2)}\,\frac{s}{t},\\
\mathrm{Re}[\mathcal{H}^{(2,0),[\mathrm{Tr5}]}] &= 0,\\
\mathrm{Re}[\mathcal{H}^{(2,0),[\mathrm{Tr6}]}] &= -12\pi^2 N_c\,\hat{R}^{(2)}\,\frac{s}{t},
\end{aligned}
\tag{C.12}
$$

At three loops, the NLL component reads

$$
\begin{aligned}
\mathcal{H}^{(3,2),[\mathrm{Tr1}]} &= \Big\{ -i\pi N_c\Big[2f_a^{(3,2)} + 2f_b^{(3,2)} - (N_c^2-12)(\hat{\alpha}_g^{(1)})^3\Big]\\
&\qquad - 4N_c^2\hat{\alpha}_g^{(1)}\Big[\hat{\alpha}_g^{(2)} + \tfrac{1}{2}\hat{\alpha}_g^{(1)}\Big(D_i^{(1)} + D_j^{(1)}\Big)\Big]\Big\}\,\frac{s}{t},\\
\mathcal{H}^{(3,2),[\mathrm{Tr2}]} &= 2\,i\pi\,N_c(4f_a^{(3,2)} + 16(\hat{\alpha}_g^{(1)})^3 + 3f_b^{(3,2)})\,\frac{s}{t},\\
\mathcal{H}^{(3,2),[\mathrm{Tr3}]} &= \Big\{ -i\pi N_c\Big[2f_a^{(3,2)} + 2f_b^{(3,2)} - (N_c^2-12)(\hat{\alpha}_g^{(1)})^3\Big]\\
&\qquad + 4N_c^2\hat{\alpha}_g^{(1)}\Big[\hat{\alpha}_g^{(2)} + \tfrac{1}{2}\hat{\alpha}_g^{(1)}\Big(D_i^{(1)} + D_j^{(1)}\Big)\Big]\Big\}\,\frac{s}{t},\\
\mathcal{H}^{(3,2),[\mathrm{Tr4}]} &= 2\,i\pi\Big[(N_c^2+4)f_a^{(3,2)} + (N_c^2+2)f_b^{(3,2)} + 8(N_c^2+1)(\hat{\alpha}_g^{(1)})^3\Big]\,\frac{s}{t},\\
\mathcal{H}^{(3,2),[\mathrm{Tr5}]} &= 4\,i\pi\Big[(N_c^2+2)f_a^{(3,2)} + f_b^{(3,2)} - (N_c^2-4)(\hat{\alpha}_g^{(1)})^3\Big]\,\frac{s}{t},\\
\mathcal{H}^{(3,2),[\mathrm{Tr6}]} &= 2\,i\pi\Big[(N_c^2+4)f_a^{(3,2)} + (N_c^2+2)f_b^{(3,2)} + 8(N_c^2+1)(\hat{\alpha}_g^{(1)})^3\Big]\,\frac{s}{t},
\end{aligned}
\tag{C.13}
$$

where the functions $f_a^{(3,2)}$, $f_b^{(3,2)}$ and $f_c^{(3,2)}$ have been defined in eq. (B.22). The real part of the NNLL term reads

$$
\begin{aligned}
\mathrm{Re}[\mathcal{H}^{(3,1),[\mathrm{Tr1}]}] &= -4N_c\Big[\hat{\alpha}_g^{(3)} + \hat{\alpha}_g^{(2)}\Big(D_i^{(1)} + D_j^{(1)}\Big) + \hat{\alpha}_g^{(1)}\Big(D_i^{(2)} + D_j^{(2)}\Big) + \hat{\alpha}_g^{(1)}D_i^{(1)}D_j^{(1)}\\
&\qquad + \pi^2\Big(N_c^2(4f_d^{(3,1)} - f_a^{(3,1)}) - 4(4f_b^{(3,1)} + f_c^{(3,1)})\Big)\Big]\,\frac{s}{t},\\
\mathrm{Re}[\mathcal{H}^{(3,1),[\mathrm{Tr2}]}] &= 0,\\
\mathrm{Re}[\mathcal{H}^{(3,1),[\mathrm{Tr3}]}] &= 4N_c\Big[\hat{\alpha}_g^{(3)} + \hat{\alpha}_g^{(2)}\Big(D_i^{(1)} + D_j^{(1)}\Big) + \hat{\alpha}_g^{(1)}\Big(D_i^{(2)} + D_j^{(2)}\Big) + \hat{\alpha}_g^{(1)}D_i^{(1)}D_j^{(1)}
\end{aligned}
$$

$$+\pi^2\Big(N_c^2(4f_d^{(3,1)}-f_a^{(3,1)})-4(4f_b^{(3,1)}+f_c^{(3,1)})\Big)\Big]\,\frac{s}{t},$$

$$\begin{aligned}
\mathrm{Re}[\mathcal{H}^{(3,1),[\mathrm{Tr4}]}] &= -4\pi^2 N_c^2\Big[6f_a^{(3,1)}-2f_b^{(3,1)}+f_c^{(3,1)}\Big]\,\frac{s}{t},\\
\mathrm{Re}[\mathcal{H}^{(3,1),[\mathrm{Tr5}]}] &= 0,\\
\mathrm{Re}[\mathcal{H}^{(3,1),[\mathrm{Tr6}]}] &= 4\pi^2 N_c^2\Big[6f_a^{(3,1)}-2f_b^{(3,1)}+f_c^{(3,1)}\Big]\,\frac{s}{t},
\end{aligned} \tag{C.14}$$

and the functions $f_a^{(3,1)}$, $f_b^{(3,1)}$, $f_c^{(3,1)}$ and $f_d^{(3,1)}$ have been defined in eq. (B.23).

## D Gluon Regge trajectory and impact factor in $\mathcal{N}=4$ SYM

In section 4 we have shown how to extract the impact factors and Regge trajectory from a given amplitude. These ingredients are necessary to obtain a complete description of the $1\to 1$ transition up to NNLL in the high-energy logarithm. As discussed in section 4, the recent calculation of the gluon-gluon amplitude up to three loops in $\mathcal{N}=4$ SYM [41] allows us to obtain the Gluon Regge trajectory at NNLO in this theory, which was previously unknown. According to eqs. (4.29) and (4.35), we are able to extract also the gluon impact factor in this theory. This information represents the last ingredient which is necessary in order to obtain a complete description of the $1\to 1$ transition up to NNLL in the high-energy logarithm, and we collect it in this appendix. We express the gluon Regge trajectory in terms of the coefficients $\hat{\alpha}_g^{(i)}$, which enters directly the fixed-order amplitude coefficients provided in appendix B and C.

At one loop the gluon Regge trajectory in $\mathcal{N}=4$ SYM is of course identical to the QCD case, i.e.

$$\hat{\alpha}_g^{(1)}|_{\mathcal{N}=4\,\mathrm{SYM}} = \frac{1}{2\epsilon}(r_\Gamma-1) = -\frac{1}{4}\zeta_2\,\epsilon-\frac{7}{6}\zeta_3\,\epsilon^2+\mathcal{O}(\epsilon^3). \tag{D.1}$$

The gluon impact factor at one loop reads

$$\begin{aligned}
D_g^{(1)}|_{\mathcal{N}=4\,\mathrm{SYM}} = N_c\Bigg[&\zeta_2+\epsilon\frac{17}{12}\zeta_3+\epsilon^2\frac{41}{32}\zeta_4+\epsilon^3\Big(-\frac{59}{24}\zeta_2\zeta_3+\frac{67}{20}\zeta_5\Big)\\
&+\epsilon^4\Big(-\frac{35}{18}\zeta_3^2-\frac{7}{6}\zeta_6\Big)+\mathcal{O}(\epsilon^5)\Bigg].
\end{aligned} \tag{D.2}$$

It is easy to check that the impact factor in $\mathcal{N}=4$ SYM correspond to the highest trascendental weight of the $N_c$ term of the correponsing QCD impact factor, see eq. (4.30a). At two loops the Regge trajectory reads

$$\hat{\alpha}_g^{(2)}|_{\mathcal{N}=4\,\mathrm{SYM}} = N_c\Big[-\frac{\zeta_3}{8}-\epsilon\frac{3}{16}\zeta_4+\epsilon^2\Big(\frac{71}{24}\zeta_2\zeta_3+\frac{41}{8}\zeta_5\Big)+\mathcal{O}(\epsilon^3)\Big], \tag{D.3}$$

which corresponds to the $\mathcal{O}(\alpha_s/\pi)^2$ coefficient of $-H_{1\to1}/C_A$ in eq. (4.51). Once again, it corresponds to the term with highest trascendental weight of the $N_c$ term of the QCD result, see eq. (4.24). The impact factor at two loops reads

$$D_g^{(2)} = N_c^2\Big[-\frac{\zeta_2}{32\epsilon^2}-\frac{\zeta_4}{64}+\epsilon\Big(\frac{17}{24}\zeta_2\zeta_3-\frac{39}{16}\zeta_5\Big)+\epsilon^2\Big(-\frac{659}{288}\zeta_3^2-\frac{5531}{512}\zeta_6\Big)+\mathcal{O}(\epsilon^3)\Big]. \tag{D.4}$$

Last, the Regge trajectory at three loops (with meaning explained below eq. (4.51)) reads

$$\hat{\alpha}_g^{(3)}|_{\mathcal{N}=4\,\mathrm{SYM}} = N_c^2\bigg[-\frac{\zeta_2}{144}\frac{1}{\epsilon^3}+\frac{5\zeta_4}{192}\frac{1}{\epsilon}+\frac{107}{144}\zeta_2\zeta_3+\frac{\zeta_5}{4}+\mathcal{O}(\epsilon)\bigg]. \tag{D.5}$$

Notice that the difference in the single pole compared to the $\mathcal{O}(\alpha_s/\pi)^3$ coefficient of $-H_{1\to1}/C_A$ in eq. (4.51) is due to the subtraction of $K^{(3)}$, see eq. (4.22).

## References


[1] E. A. Kuraev, L. N. Lipatov and V. S. Fadin, *The Pomeranchuk Singularity in Nonabelian Gauge Theories*, *Sov. Phys. JETP* **45** (1977) 199–204.

[2] I. I. Balitsky and L. N. Lipatov, *The Pomeranchuk Singularity in Quantum Chromodynamics*, *Sov. J. Nucl. Phys.* **28** (1978) 822–829.

[3] P. D. B. Collins, *An Introduction to Regge Theory and High-Energy Physics*. Cambridge Monographs on Mathematical Physics. Cambridge Univ. Press, Cambridge, UK, 2009.

[4] F. E. Low, *A Model of the Bare Pomeron*, *Phys. Rev.* **D12** (1975) 163–173.

[5] S. Nussinov, *Colored Quark Version of Some Hadronic Puzzles*, *Phys. Rev. Lett.* **34** (1975) 1286–1289.

[6] J. F. Gunion and D. E. Soper, *Quark Counting and Hadron Size Effects for Total Cross-Sections*, *Phys. Rev.* **D15** (1977) 2617–2621.

[7] L. N. Lipatov, *Asymptotic behavior of multicolor QCD at high energies in connection with exactly solvable spin models*, *JETP Lett.* **59** (1994) 596–599, [hep-th/9311037].

[8] L. D. Faddeev and G. P. Korchemsky, *High-energy QCD as a completely integrable model*, *Phys. Lett.* **B342** (1995) 311–322, [hep-th/9404173].

[9] I. A. Korchemskaya and G. P. Korchemsky, *High-energy scattering in QCD and cross singularities of Wilson loops*, *Nucl. Phys.* **B437** (1995) 127–162, [hep-ph/9409446].

[10] I. A. Korchemskaya and G. P. Korchemsky, *Evolution equation for gluon Regge trajectory*, *Phys. Lett.* **B387** (1996) 346–354, [hep-ph/9607229].

[11] I. Balitsky, *Operator expansion for high-energy scattering*, *Nucl. Phys.* **B463** (1996) 99–160, [hep-ph/9509348].

[12] Y. V. Kovchegov, *Small x F(2) structure function of a nucleus including multiple pomeron exchanges*, *Phys. Rev.* **D60** (1999) 034008, [hep-ph/9901281].

[13] J. Jalilian-Marian, A. Kovner, L. D. McLerran and H. Weigert, *The Intrinsic glue distribution at very small x*, *Phys. Rev.* **D55** (1997) 5414–5428, [hep-ph/9606337].

[14] J. Jalilian-Marian, A. Kovner, A. Leonidov and H. Weigert, *The Wilson renormalization group for low x physics: Towards the high density regime*, *Phys. Rev.* **D59** (1998) 014014, [hep-ph/9706377].

[15] E. Iancu, A. Leonidov and L. D. McLerran, *The Renormalization group equation for the color glass condensate*, *Phys. Lett.* **B510** (2001) 133–144, [hep-ph/0102009].

[16] S. Caron-Huot, *When does the gluon reggeize?*, *JHEP* **05** (2015) 093, [1309.6521].

[17] J. C. Collins, D. E. Soper and G. F. Sterman, *Factorization of Hard Processes in QCD*, *Adv. Ser. Direct. High Energy Phys.* **5** (1989) 1–91, [hep-ph/0409313].

[18] J. Botts and G. F. Sterman, *Hard Elastic Scattering in QCD: Leading Behavior*, *Nucl. Phys.* **B325** (1989) 62–100.

[19] G. P. Korchemsky and A. V. Radyushkin, *Loop Space Formalism and Renormalization Group for the Infrared Asymptotics of QCD*, *Phys. Lett.* **B171** (1986) 459–467.

[20] G. P. Korchemsky and A. V. Radyushkin, *Infrared asymptotics of perturbative QCD: renormalisation properties of the Wilson loops in higher orders of perturbation theory*, *Sov. J. Nucl. Phys.* **44** (1986) 877.

[21] G. P. Korchemsky and A. V. Radyushkin, *Renormalization of the Wilson Loops Beyond the Leading Order*, *Nucl. Phys.* **B283** (1987) 342–364.

[22] N. Kidonakis and G. F. Sterman, *Resummation for QCD hard scattering*, *Nucl. Phys.* **B505** (1997) 321–348, [hep-ph/9705234].

[23] N. Kidonakis, G. Oderda and G. F. Sterman, *Evolution of color exchange in QCD hard scattering*, *Nucl. Phys.* **B531** (1998) 365–402, [hep-ph/9803241].

[24] E. Gardi, J. M. Smillie and C. D. White, *The Non-Abelian Exponentiation theorem for multiple Wilson lines*, *JHEP* **06** (2013) 088, [1304.7040].

[25] E. Gardi, J. M. Smillie and C. D. White, *On the renormalization of multiparton webs*, *JHEP* **09** (2011) 114, [1108.1357].

[26] A. Mitov, G. F. Sterman and I. Sung, *The Massive Soft Anomalous Dimension Matrix at Two Loops*, *Phys. Rev.* **D79** (2009) 094015, [0903.3241].

[27] T. Becher and M. Neubert, *Infrared singularities of QCD amplitudes with massive partons*, *Phys. Rev.* **D79** (2009) 125004, [0904.1021].

[28] S. Catani, *The Singular behavior of QCD amplitudes at two loop order*, *Phys. Lett.* **B427** (1998) 161–171, [hep-ph/9802439].

[29] S. M. Aybat, L. J. Dixon and G. F. Sterman, *The Two-loop soft anomalous dimension matrix and resummation at next-to-next-to leading pole*, *Phys. Rev.* **D74** (2006) 074004, [hep-ph/0607309].

[30] E. Gardi and L. Magnea, *Factorization constraints for soft anomalous dimensions in QCD scattering amplitudes*, *JHEP* **03** (2009) 079, [0901.1091].

[31] E. Gardi and L. Magnea, *Infrared singularities in QCD amplitudes*, *Nuovo Cim.* **C32N5-6** (2009) 137–157, [0908.3273].

[32] T. Becher and M. Neubert, *On the Structure of Infrared Singularities of Gauge-Theory Amplitudes*, *JHEP* **06** (2009) 081, [0903.1126].

[33] L. J. Dixon, E. Gardi and L. Magnea, *On soft singularities at three loops and beyond*, *JHEP* **02** (2010) 081, [0910.3653].

[34] V. Ahrens, M. Neubert and L. Vernazza, *Structure of Infrared Singularities of Gauge-Theory Amplitudes at Three and Four Loops*, *JHEP* **09** (2012) 138, [1208.4847].

[35] Ø. Almelid, C. Duhr and E. Gardi, *Three-loop corrections to the soft anomalous dimension in multileg scattering*, *Phys. Rev. Lett.* **117** (2016) 172002, [1507.00047].

[36] E. Gardi, Ø. Almelid and C. Duhr, *Long-distance singularities in multi-leg scattering amplitudes*, *PoS* **LL2016** (2016) 058, [1606.05697].

[37] V. Del Duca, C. Duhr, E. Gardi, L. Magnea and C. D. White, *An infrared approach to Reggeization*, *Phys. Rev.* **D85** (2012) 071104, [1108.5947].

[38] V. Del Duca, C. Duhr, E. Gardi, L. Magnea and C. D. White, *The Infrared structure of gauge theory amplitudes in the high-energy limit*, *JHEP* **12** (2011) 021, [1109.3581].

[39] V. Del Duca, G. Falcioni, L. Magnea and L. Vernazza, *High-energy QCD amplitudes at two loops and beyond*, *Phys. Lett.* **B732** (2014) 233–240, [1311.0304].

[40] V. Del Duca, G. Falcioni, L. Magnea and L. Vernazza, *Analyzing high-energy factorization beyond next-to-leading logarithmic accuracy*, *JHEP* **02** (2015) 029, [1409.8330].

[41] J. M. Henn and B. Mistlberger, *Four-Gluon Scattering at Three Loops, Infrared Structure, and the Regge Limit*, *Phys. Rev. Lett.* **117** (2016) 171601, [1608.00850].

[42] M. Beneke, P. Falgari and C. Schwinn, *Soft radiation in heavy-particle pair production: All-order colour structure and two-loop anomalous dimension*, *Nucl. Phys.* **B828** (2010) 69–101, [0907.1443].

[43] S. Keppeler and M. Sjodahl, *Orthogonal multiplet bases in SU(Nc) color space*, *JHEP* **09** (2012) 124, [1207.0609].

[44] V. Del Duca and E. W. N. Glover, *The High-energy limit of QCD at two loops*, *JHEP* **10** (2001) 035, [hep-ph/0109028].

[45] S. Catani and M. H. Seymour, *The Dipole formalism for the calculation of QCD jet cross-sections at next-to-leading order*, *Phys. Lett.* **B378** (1996) 287–301, [hep-ph/9602277].

[46] S. Catani and M. H. Seymour, *A General algorithm for calculating jet cross-sections in NLO QCD*, *Nucl. Phys.* **B485** (1997) 291–419, [hep-ph/9605323].

[47] Yu. L. Dokshitzer and G. Marchesini, *Soft gluons at large angles in hadron collisions*, *JHEP* **01** (2006) 007, [hep-ph/0509078].

[48] A. Babansky and I. Balitsky, *Scattering of color dipoles: From low to high-energies*, *Phys. Rev.* **D67** (2003) 054026, [hep-ph/0212075].

[49] I. Balitsky, *Factorization for high-energy scattering*, *Phys. Rev. Lett.* **81** (1998) 2024–2027, [hep-ph/9807434].

[50] I. Balitsky, *Factorization and high-energy effective action*, *Phys. Rev.* **D60** (1999) 014020, [hep-ph/9812311].

[51] Y. V. Kovchegov, *Unitarization of the BFKL pomeron on a nucleus*, *Phys. Rev.* **D61** (2000) 074018, [hep-ph/9905214].

[52] I. Balitsky and G. A. Chirilli, *Rapidity evolution of Wilson lines at the next-to-leading order*, *Phys. Rev.* **D88** (2013) 111501, [1309.7644].

[53] A. Kovner, M. Lublinsky and Y. Mulian, *Jalilian-Marian, Iancu, McLerran, Weigert, Leonidov, Kovner evolution at next to leading order*, *Phys. Rev.* **D89** (2014) 061704, [1310.0378].

[54] A. Kovner, M. Lublinsky and Y. Mulian, *Conformal symmetry of JIMWLK Evolution at NLO*, *JHEP* **04** (2014) 030, [1401.0374].

[55] A. Kovner, M. Lublinsky and Y. Mulian, *NLO JIMWLK evolution unabridged*, *JHEP* **08** (2014) 114, [1405.0418].

[56] S. Caron-Huot, *Resummation of non-global logarithms and the BFKL equation*, 1501.03754.

[57] M. Lublinsky and Y. Mulian, *High Energy QCD at NLO: from light-cone wave function to JIMWLK evolution*, 1610.03453.

[58] V. S. Fadin, M. I. Kotsky and R. Fiore, *Gluon Reggeization in QCD in the next-to-leading order*, *Phys. Lett.* **B359** (1995) 181–188.

[59] V. S. Fadin, R. Fiore and M. I. Kotsky, *Gluon Regge trajectory in the two loop approximation*, *Phys. Lett.* **B387** (1996) 593–602, [hep-ph/9605357].

[60] V. S. Fadin, R. Fiore and A. Quartarolo, *Reggeization of quark quark scattering amplitude in QCD*, *Phys. Rev.* **D53** (1996) 2729–2741, [hep-ph/9506432].

[61] J. Blumlein, V. Ravindran and W. L. van Neerven, *On the gluon Regge trajectory in O alpha-s**2*, *Phys. Rev.* **D58** (1998) 091502, [hep-ph/9806357].

[62] J. Bartels, *High-Energy Behavior in a Nonabelian Gauge Theory (II)*, *Nucl. Phys.* **B175** (1980) 365–401.

[63] T. Jaroszewicz, *Infrared Divergences and Regge Behavior in QCD*, *Acta Phys. Polon.* **B11** (1980) 965.

[64] J. Kwiecinski and M. Praszalowicz, *Three Gluon Integral Equation and Odd c Singlet Regge Singularities in QCD*, *Phys. Lett.* **B94** (1980) 413–416.

[65] T. Becher and M. Neubert, *Infrared singularities of scattering amplitudes in perturbative QCD*, *Phys. Rev. Lett.* **102** (2009) 162001, [0901.0722].

[66] F. C. S. Brown, *Single-valued multiple polylogarithms in one variable*, *C. R. Acad. Sci. Paris* **Ser. I 338** (2004) 527.

[67] L. J. Dixon, C. Duhr and J. Pennington, *Single-valued harmonic polylogarithms and the multi-Regge limit*, *JHEP* **10** (2012) 074, [1207.0186].

[68] Ø. Almelid, C. Duhr and E. Gardi, *Computation of the three-loop soft anomalous dimension for massless scattering*, *in preparation* .

[69] S. G. Naculich, *All-loop group-theory constraints for color-ordered SU(N) gauge-theory amplitudes*, *Phys. Lett.* **B707** (2012) 191–197, [1110.1859].

[70] V. S. Fadin, *Particularities of the NNLLA BFKL*, in *9th International Workshop on Diffraction in High Energy Physics (Diffraction 2016) Santa Tecla di Acireale, Catania, Italy, September 2-8, 2016*, 2016. 1612.04481.

[71] S. Moch, J. A. M. Vermaseren and A. Vogt, *The Three loop splitting functions in QCD: The Nonsinglet case*, *Nucl. Phys.* **B688** (2004) 101–134, [hep-ph/0403192].

[72] A. Grozin, J. M. Henn, G. P. Korchemsky and P. Marquard, *Three Loop Cusp Anomalous Dimension in QCD*, *Phys. Rev. Lett.* **114** (2015) 062006, [1409.0023].

[73] S. Moch, J. A. M. Vermaseren and A. Vogt, *Three-loop results for quark and gluon form-factors*, *Phys. Lett.* **B625** (2005) 245–252, [hep-ph/0508055].

[74] T. Gehrmann, E. W. N. Glover, T. Huber, N. Ikizlerli and C. Studerus, *Calculation of the quark and gluon form factors to three loops in QCD*, *JHEP* **06** (2010) 094, [1004.3653].